Synthetic Studies towards New 22(S)-Hydroxycholesterol Analogues

Thesis for the degree of Master of Science/Pharmacy

Zeshan Iqbal

Department of Pharmaceutical Chemistry

Section for Medicinal Chemistry

School of Pharmacy

University of Oslo

May 15, 2012

Synthetic Studies towards New 22(S)-Hydroxycholesterol Analogues

Thesis for the degree of Master of Science/Pharmacy

Zeshan Iqbal

University Of Oslo
School of Pharmacy
Section for Medicinal Chemistry
Department of Pharmaceutical Chemistry

© Zeshan Iqbal

2012

Synthetic Studies towards New 22S-Hydroxycholesterol Analogues

Tutor(s): Associate Professor Pål Rongved (University of Oslo), Senior Research Scientist Marcel Sandberg (Synthetica AS)

This work is published through DUO – Digitale utgivelser ved UIO – http://www.duo.uio.no/
It is also catalogued in BIBSYS (http://www.bibsys.no/english)

Printed at Reprosentralen, University in Oslo

All rights reserved. No part of this publication may be reproduced or transmitted in any form, or by any means without any permission.

This thesis is dedicated to my parents, especially my father who has given me the opportunity and an education from the best institutions and support throughout his life. I would have never been here without him.

Acknowledgement

The work presented in this thesis was accomplished during 2011-2012, and could not have been completed without help and contribution from several people.

I wish to express my sincere gratitude to my supervisor Pål Rongved and my external tutor Marcel Sandberg for teaching me some things about chemistry and sciences, introducing me to the LXR field, letting me work so independently and still giving me support and feedback. You have been nothing less than fantastic! I am especially grateful for invaluable technical support within X-ray crystallography from chemistry professor Carl Henrik Gørbitz. A great thanks to Ove Alexander Åstrand for all help and good advices related to theoretical and practical chemistry, and teaching me that patience is a deed (I'm not so good at that).

All former and present friends and colleagues at the Institute of Pharmacy deserve thanks for creating a friendly and unique atmosphere. Finally, I would like to thank the employees and the other students at the department of pharmaceutical chemistry for supporting me with good ideas and experience in the field and for always being so positive, caring and enthusiastic!

Enjoy reading.

Oslo, May 2012

Zeshan Iqbal

Abstract

Liver X receptor is a transcription factor that is important for the metabolism of fat and cholesterol in the body. Known liver X receptor activators are endogenous oxysterols (cholesterol metabolites). 22S-hydroxycholesterol is a synthetic oxysterol which acts as an antagonist reducing production of fat but also increasing glucose uptake in skeletal muscle cells.

A variety of chiral and achiral compounds have been prepared in an effort to be utilized towards synthesis of new 22S-hydroxycholesterol analogues. The different syntheses have been optimized with yields ranging from 9- 91%.

Two stereogenic compounds generated are new which have not heretofore been described in the literature. The developed process described in this master thesis has given the desired stereochemistry, which has been confirmed by X-ray crystallography. In this context, it has been established a method of providing high-quality crystals of the *syn* aldol adduct.

Several attempts to synthesize two modulators of LXR have been investigated, but proven difficult and unsuccessful. Alkylation of the stereogenic diol with two naphatyl derivatives to obtain a new analogue has been studied at various temperatures and reaction conditions. Second, the synthesis of another analogue produced multiple products indicating a high reactivity of the stereogenic diol**.**

Graphical abstract

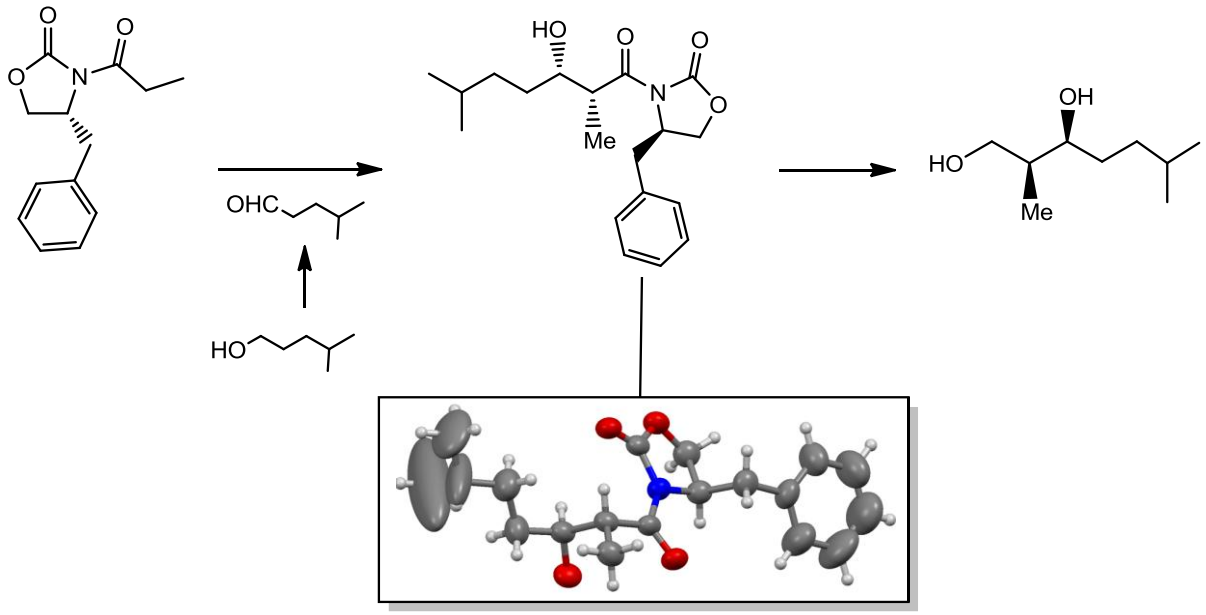

Scheme 1. Aldehyde and optically pure ligands to be utilized in synthesis of new 22S-hydroxycholesterol analogues.

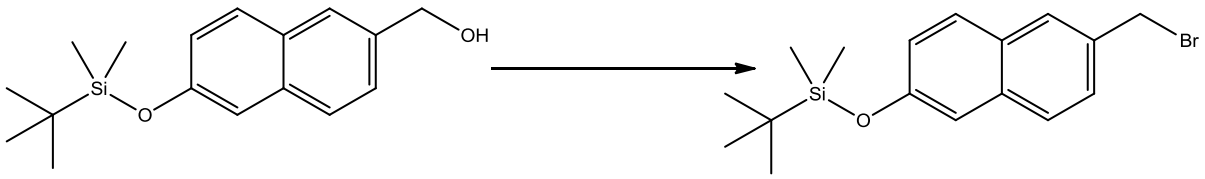

Scheme 2. Generation of naphatyl derivative**.**

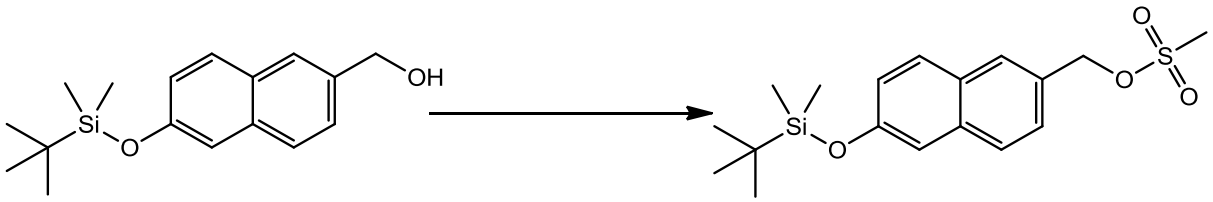

Scheme 3. Generation of naphatyl derivative**.**

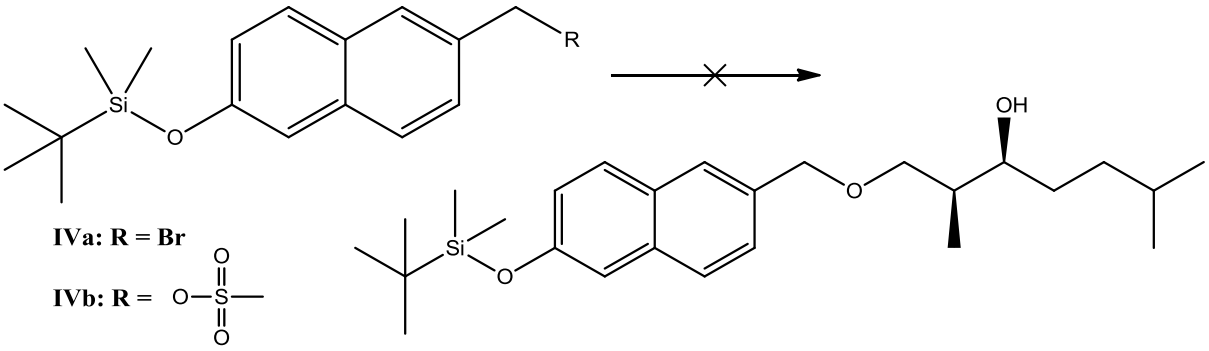

Scheme 4. Attempted synthesis of 22(S)-HC analogue using reaction conditions proposed by Marcel Sandberg and Pål Rongved.

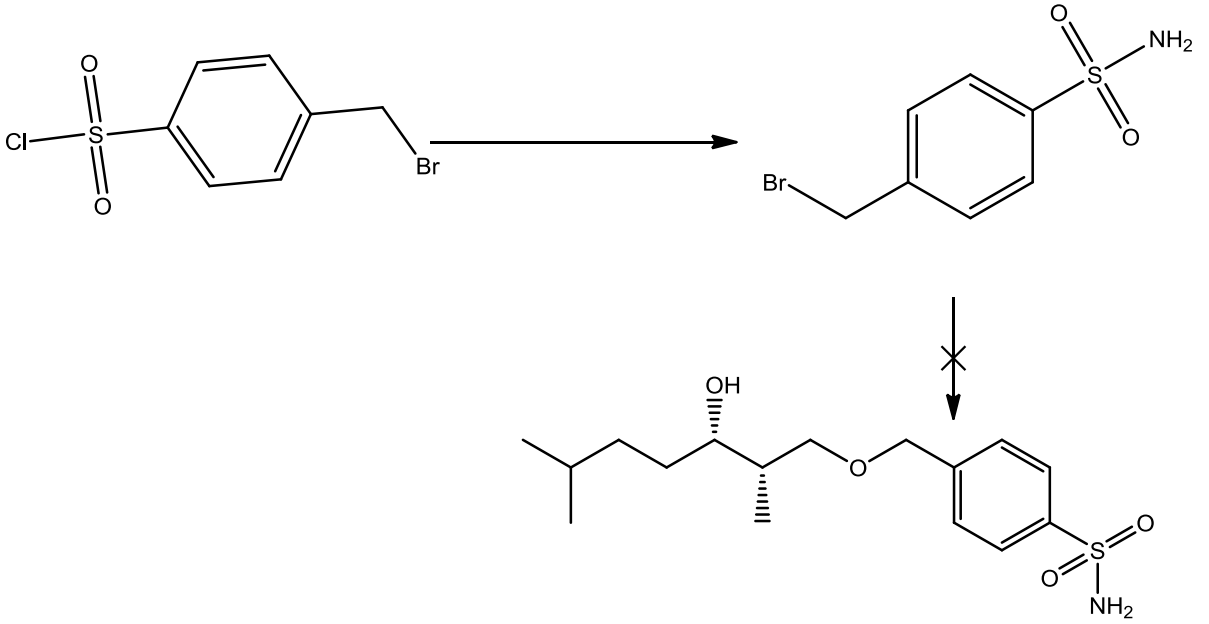

Scheme 5. General procedure based on work by Pål Rongved and Marcel Sandberg.

Abbreviations

$(COCl)_2$	Oxalyl chloride	$DMSO-d_6$	Deuterated dimethyl sulfoxide
22(R)-HC	22(R)-hydroxycholesterol	DNL	De novo lipogenesis
22(S)-HC	22(S)-hydroxycholesterol	FABPpm	Plasma membrane fatty acid-binding protein
24(S),25-EC	24(S),25-epoxycholesterol	FAS	Fatty acid synthase
24(S)-HC	24(S)-hydroxycholesterol	FAT/CD36	Fatty acid translocase
ABC	ATP-binding cassette transporters	FATP	Fatty acid-transport protein
ACC	Acetyl CoA carboxylase	FFA	Free fatty acids
APOA-I	Apolipoprotein A-I	G6-Pase	Glucose 6-phosphatase
BMI	Body Mass Index	GLUT	Glucose transporter
$CDCl_3$-d	Deuterated chloroform	hCETP	Human cholesteryl ester transport protein
ChREBP	Carbohydrate responsive element-binding protein	HCl	Hydrochloric acid
DBD	DNA binding domain	HDL	High density lipoprotein
DCM	Methylene chloride/Dichloromethane	HepG2	Human liver carcinoma cell line
DMF	Dimethylformamide	HMGC	3-hydroxy-3-methyl-glutaryl-CoA
DMSO	Dimethyl sulfoxide	HRE	Hormone response element

IGT	Insulin resistance	PEPCK	Phosphoenolpyruvate carboxykinase
IRS	Insulin receptor substrate	PI3	Phosphatidylinositol 3′
LBD	Ligand binding domain	PLTP	Phospholipid transfer protein
LCFA	Long-chain fatty acid	ppm	Parts per million
$LiBH_4$	Lithium borohydride	RAR	Retinoic receptor
LPL	Lipoprotein lipase	RXRα	Retinoic acid receptor alpha
LXR	Liver x receptor	SCD	Stearoyl CoA desaturase
LXRE	Liver x receptor response element	SEM	(Trimethylsilyl)ethoxymethyl
$MgSO_4$	Magnesium sulfate	SGBS	Simpson-Golabi-Behmel syndrome
MsCl	Mesyl chloride	SiO_2	Silicon dioxide/Silica
MTBE	Methyl-t-Butyl Ether	SREBP	Sterol regulatory element binding proteins
$NaBH_4$	Sodium borohydride	T2DM	Type 2 diabetes mellitus
NaH	Sodium hydride	TG	Triglycerids
NH3	Ammonia	THF	Tetrahydrofuran
NH_4Cl	Ammonium chloride	TLC	Thin layer chromatography
NMR	Nuclear magnetic Resonance	TR	Thyroid hormone receptor
NR	Nuclear Receptor	VDR	Vitamin D receptor
ob/ob	Leptin-deficient	VLDL	Triglycerids rich lipoproteins
PCC	Pyridinium chlorochromat	WHO	World Health Organization

Table of Contents

1 Theory

1.1 Obesity and Overweight

Obesity and overweight are increasingly important public health issues/threats (Figure 1a and 1b) contributing to serious health problems and extensive economic costs worldwide,[1] and since 1980 obesity has more than doubled.[2] In 2008, 1.5 billion adults, 20 and older, were overweight and of these over 200 million men and nearly 300 million women were obese. Furthermore, 65% of the world's population lives in countries where overweight and obesity kills more people than underweight. Once considered a high-income country problem, overweight and obesity are now growing trends in low- and middle-income countries. In 2010, around 43 million children under five were overweight where close to 35 million overweight children are living in developing countries, and 8 million in developed countries.[2]

Obesity and overweight are defined as abnormal or excessive fat accumulation that may impair health.[2] Body mass index (BMI) is a commonly used simple measure in classifying underweight, overweight and obesity in adult populations and individuals; it is defined as a person's weight in kilograms divided by the square of his height in meters (kg/m^2).

$$BMI = \frac{mass\ (kg)}{\left(height\ (m)\right)^2}$$

The World Health Organization (WHO) classification is: a BMI greater than or equal to 25 is overweight and a BMI greater than or equal to 30 is obesity. However, BMI should be considered a rough guide because it does not separate between men, women, nationality nor muscle mass when corresponding to the same degree of fatness.[2] There are several other ways of measuring body fat distribution in humans, but these methods are mainly used for research purposes.[3]

Globally, it is well known that essential cause of obesity and overweight is an energy imbalance between calories consumed and calories expended; food is more available to everyone, and the physical activity of workers is reduced with increasing urbanization.[2, 4] S. M. Grundy and others have further their work concluded that overweight and obesity are

results of a multifactorial syndrome, in which a decline in resting metabolic rate play a substantial role.[4-7]

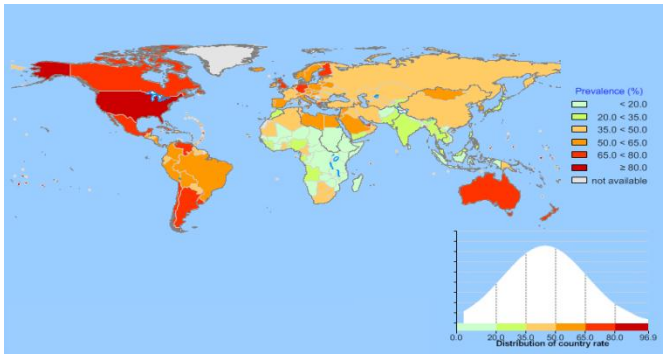

Figure 1a. Estimated overweight and obesity (BMI ≥ 25 kg/m^2) prevalence for males in age group 15+ in 2010.[8]

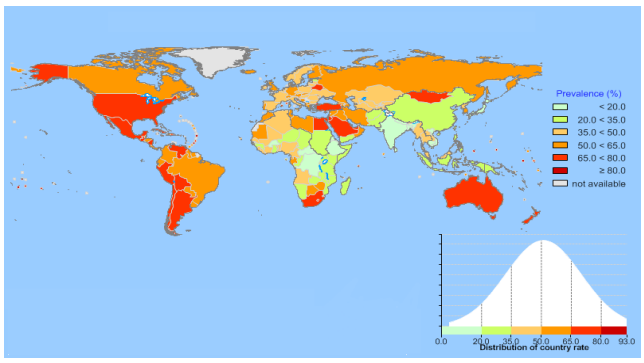

Figure 1b. Estimated overweight and obesity (BMI ≥ 25 kg/m^2) prevalence for females in age group 15+ in 2010.[9]

1.1.1 Diabetes and Skeletal muscle

Diabetes mellitus is a metabolic disorder resulting from a defect in insulin secretion, insulin action, or both. A consequence of this is chronic elevated levels of plasma glucose (hyperglycemia) with disturbances of carbohydrate, fat and protein metabolism.[10] Furthermore, untreated hyperglycemia contributes considerably to insulin resistance on the whole-body level (especially skeletal muscle).[11-12]

Type 2 Diabetes Mellitus (T2DM) and Insulin Resistance

Excessive body weight is associated with various diseases; it is therefore common that overweight and obese people often suffer from additional maladies such as heart disease, hypertension and osteoarthritis in addition to reduced life expectancy.[1] As well, excessive weight is major risk factor for stroke, some forms of cancer (endometrial, breast and colon) and the development and progression of type 2 diabetes mellitus (T2DM).[2]

In the literature obesity and diabetes are described as 'diabesity' because of such a strong relationship between these health issues. [11] The road from obesity to T2DM advances slowly over years and is preceded by defect in insulin secretion coupled with a progressive rise in insulin resistance (IGT).[11] Generally, IGT is recognized as an expression of abnormal glucose metabolism regulation, and can be considered as an intermediate stage between normal glucose tolerance and diabetes.[10] Events leading to the development of IGT is raised insulin plasma concentration in the presence of normal or increased glucose levels,[13] meaning that the basal plasma insulin level is proportional to the degree of insulin resistance.[14]

Metabolic Role of Skeletal Muscle

In humans, skeletal muscle is a major mass peripheral tissue that accounts ~40% of body weight in average man and rather less (30%) in average women. With such a large tissue mass, skeletal muscle has a major role in whole body energy homeostasis; it accounts for >30% of energy expenditure, is the primary tissue of insulin stimulated glucose uptake, disposal and storage, and in addition it influences metabolism via modulation of circulating and stored lipid/cholesterol flux.[15-16] Zurlo *et al.* have further in their article presented data emphasizing the relationship between skeletal muscle and energy expenditure and suggested that, because skeletal muscle is quantitatively the most important tissue of the body, energy expenditure and metabolic flux at rest may be greatly increased during exercise.[5]

Skeletal muscle is responsible for up to 75 % of whole insulin-dependent glucose disposal, whereas a small fraction also occurs in fat, cardiac muscle and splanchnic tissues.[17-18] These findings confirms earlier studies which presents that, in insulin-treated animals, ~25% of an intravenous glucose-dose enters the muscle cells within 1 min. Hence illustrating the quantitatively important regulatory role of skeletal muscle in limiting an exponential rise in circulating glucose.[19]

In skeletal muscle glucose uptake takes place by a system of diffusion-cascade involving glucose transporter (GLUT)-1 and GLUT-4. These two distinct transporter proteins coexist in insulin-responsive tissues. GLUT-1 being mostly in the plasma membrane mediating the basal rate of glucose transport in the not stimulated state. Whereas GLUT-4, predominantly stored intracellularly, is responsible for mediating, after the insulin-stimulated recruitment, the increased rate of glucose transport by translocation to plasma membrane.[20-21] Insulin-stimulated glucose uptake requires binding of insulin to its receptor which leads to

activation by phosphorylation of insulin receptor substrates (IRSs) 1-4, phosphatidylinositol 3′ (PI3) kinase and protein kinase B (PKB). Once GLUT-4 translocate to the cell membrane, it allows more glucose to enter the muscle fiber for phosphorylation to several branched glucose polymers and then shuttled into the synthesis of glycogen.[22] Glycogen is the major reservoir of carbohydrate stored in skeletal muscle where these assets are used as fuel to sustain contractile processes through glycogenolysis and glycolysis.[23-24]

In addition to carbohydrates, the second major fuel utilized by a healthy muscle is free fatty acids (FFA). All together, they are quantitatively the most important oxidisable substrates.[25] Transport of FFA across cellular membranes most likely occurs via both passive diffusion and a number of membrane-associated transporter-proteins. Important membrane-associated proteins involved in in the cellular fatty acid-uptake and the transport process are membrane proteins fatty acid translocase (FAT/CD36), plasma membrane fatty acid-binding protein ($FABP_{pm}$) and fatty acid-transport protein (FATP).Of these proteins $FABP_{pm}$ and FATP have been detected in virtually all tissues probably because such levels allow a rapid adaptation to changes in substrate flux as occurring, for instance, during the transition from a resting to contracting skeletal muscle. FAT/CD36 shows a more restricted expression, as in most species it is absent in liver and brain, but it is perhaps the one transporter-protein which can translocate to the plasma membrane within minutes by response to contraction and insulin to increase long-chain fatty acid (LCFA) uptake. Nevertheless, all these proteins are simultaneously expressed in heart and skeletal muscles.[26-28]

As previously mentioned, skeletal muscle has a significant role in insulin sensitivity, carbohydrate and lipid homeostasis. Therefore, there is crucial that skeletal muscle needs to be well adapted to survive the alternating periods of good and bad in both the supply and demand of energy. This important characteristic requires a clear capacity to utilize both carbohydrates and lipid fuels and transition between them. This adaptability, especially seen in a healthy metabolic state, is called ‘metabolic flexibility’.[25, 29] Metabolism is largely regulated by nuclear hormone receptors which function as hormone regulated transcription factors that bind DNA and mediate the physiological regulation of gene expression.[16]

1.1.2 Nuclear Receptors (NRs)

As their names imply, the nuclear receptor family are generally found in the nucleus, located mainly at their promoter site (control point for regulating gene transcription) on DNA. NRs

form a superfamily of 48 identified and genetically related proteins which is further divided into the steroid receptor family and the non-steroid receptor family (includes vitamin D receptor (VDR), thyroid hormone receptor (TR) and retinoic receptor (RAR)).[30]

Over the years, it has been established evolutionary relatedness between all the NRs,[31] giving them common structural features such as; (i) A central DNA binding domain (DBD) responsible for targeting the receptor to specific DNA sequences. (ii) A ligand binding domain (LBD) in charge of recognizing specific hormonal and non-hormonal ligands for the biologic response. (iii) A variable length center region between the DBD and LBD.[32] Overall, these structural features are often referred as DNA *cis* elements, also known as hormone response elements (HREs) and activate transcription of target genes.[33] Based on the tendency of function as hetero- or homodimers, Manglesdorf *et al.* proposed four categories of nuclear receptors in which Class 1 include the steroid receptors that function as homodimers, Class 2 involves heterodimerization of NR with retinoic acid receptor (RXR), whereas Class 3 and Class 4 include dimeric or monomeric orphan receptors (Figure 2).[30]

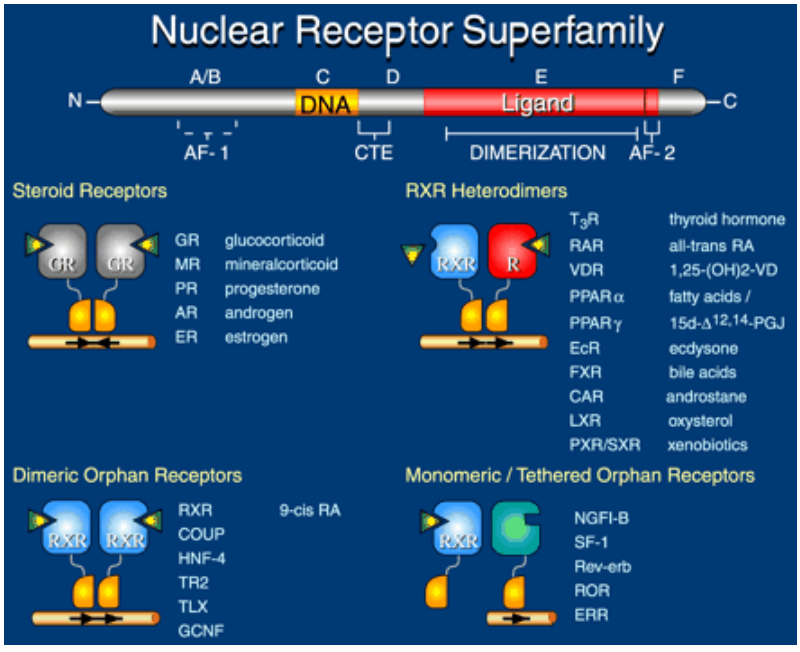

Figure 2. Structure organizations of nuclear receptors. The nuclear receptor superfamily can be broadly divided into four classes based on their dimerization and DNA-binding properties; class 1 receptors include the known steroid hormone receptors classified as homodimers, class 2 receptors heterodimerize with RXR and includes all other known ligand-dependent receptors (excluding steroid hormones as ligand), class 3 and class 4 are classified as homodimers and monomer orphan receptors (there are no obvious ligands), respectively. Receptors with belonging ligands are listed together.[30, 32]

1.1.3 Liver X Receptors (LXRs) and Their Physiological Role

Cholesterol is present in membranes of all animal cells where its function is to build and

maintain characteristics of membranes. Cholesterol is further metabolized to bile acids, steroid hormones and oxysterols, where they have several physiological functions in animals. Steroid hormones have important roles in development, growth and maintenance of homeostasis in animals. Bile acids function as biological cleansing agents in bile and intestine where they increase solubilization of hydrophobic molecules such as lipophilic vitamins and lipids. Oxysterols are oxygenated metabolites of cholesterol and physiological ligands of liver X receptor (LXR).[34-35] In general, oxysterols produced in enzymatic reactions from cholesterol are potent LXR agonists and can be divided into three groups; intermediates of the cholesterol biosynthetic pathway (provisional, 24(S),25-epoxycholesterol (24(S),25-EC) is the only representative of this group), transitional compounds in the synthesis of steroid hormones from cholesterol (e.g. 22(R)-hydroxycholesterol (22(R)-HC)) and other oxygenated metabolites of cholesterol formed by different isoforms of cytochrome P450 (Figure 5a) (CYP450).[36]

Cholesterol and fat hemostasis is an important regulatory system controlled by the nuclear receptor (NR) function, and the two main NRs especially involved in regulation of cholesterol and lipid metabolism are the peroxisome proliferators activated receptors (PPAR) and the liver X receptor (LXR).[32] LXRs belongs to non-steroidal receptor family and was first discovered in 1995 in the human liver (hence the name liver X receptor), as a new member of the nuclear receptor superfamily 'orphan receptors'.[37-38] Subsequently, there has been identified two isoforms of LXRs encoded by separate genes; namely, LXRα and LXRβ (NR1H3 and NR1H2 is the standard nomenclature, respectively). Whereas LXRβ is ubiquitously expressed at low levels in all tissues, LXRα predominates in tissues known to play an important role in lipid metabolism such as the liver, adipose tissue, macrophages, kidney, skeletal muscle and intestine.[38-42] Both LXRα and LXRβ bind to DNA's LXR response elements (LXREs) as heterodimers with the obligate partner 9-*cis* retinoic acid receptor α (RXRα). LXR/RXR heterodimers function as sensors to cellular levels of oxysterols and, when activated by these agonists, mediates responses through a process that is defined by LXREs.[37-38] The crystal structures of the two LXR subtypes have revealed that all the key residues in the ligand binding pocket (LBP) are preserved between the two subtypes (Figure 3).[43]

Exploration in the last decade has shown that the LXR pathway involves induction of target genes (some are shown in Table 1) associated with control of cholesterol, bile acid and

lipoprotein and glucose metabolism either directly through an LXRE or indirectly through interactions with other transcription factors. In addition, LXRs play an important role in regulation of inflammation and intestinal lipid transport through up-regulation of several target genes.[35, 40, 44-45]

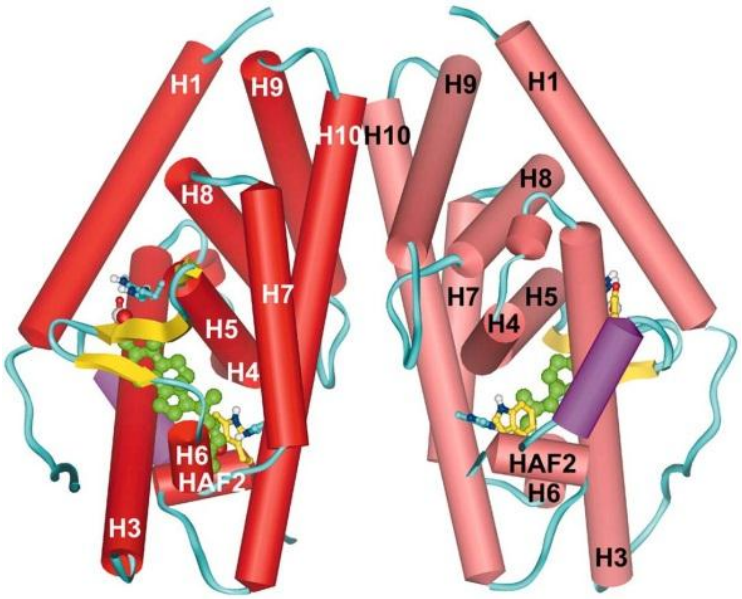

Figure 3. Structure of the LXRβ LBD.
LXRβ/24(S),25-epoxycholesterol/steroid receptor coactivator-1 crystallized as a dimer with an orientation and dimer interface similar to that seen with other nuclear receptors. Helices in the two LXR monomers are shown in red and pink, whereas β-strands are yellow, loops are cyan, and the steroid receptor coactivator-1 helix is magenta. LXR helices 1-10 are labeled H1–H10 and HAF2. Nitrogen, oxygen, and hydrogen atoms are colored blue, red, and white, respectively, whereas carbon atoms are colored green, yellow, cyan, cyan, and yellow in 24(S),25-epoxycholesterol, Glu-281, Arg-319, His-435, and Trp-457, respectively. The same dimer orientation is obtained in LXRα LBD (not shown).[43]

LXR and Cholesterol Homeostasis

As lined out in the foregoing, LXRs function as sensors of oxysterols and thereby having major role in controlling whole-body cholesterol homeostasis in numerous tissues such as liver, intestine, macrophages, adipose tissue and possible muscle tissue. Oxygenated metabolites of cholesterol, that is to say oxysterols, as physiological ligands of LXR were mentioned for the first time by B.A. Janowski *et.al.*[46] Since then, LXR research has been prosperous. Generation and availability of the phenotypes of LXR knock-out mice has been useful tools to uncover conclusive evidence for the role of LXR in cholesterol metabolism. These mice exhibited an increased accumulation of cholesteryl esters in their livers when challenged with a high-fat, high-cholesterol diet.[47-48] Studies over the past 5-10 years,[49-50] also discussed in the work done by Steffenson and Gustavsson,[48] have described impaired expression of hepatic genes involved in cholesterol homeostasis such as cholesterol 7α-hydroxylase, 3-hydroxy-3-methyl-glutaryl-CoA (HMGC) synthase/reductase,

farnesyldiphosphate synthase and squalene synthase in LXRα-deficient mice. On the contrary, LXRβ-deficient mice failed to show these modulations suggesting a more prominent role of LXRα than LXRβ as a regulator of cholesterol metabolism, and that LXRα and LXRβ have at least some distinct target genes.

Recent publications have conclusively reported that LXRs are the primary transcriptional regulators in the process of removing excess cholesterol from peripheral tissues and the body through the pathway known as 'reverse cholesterol transport' (RCT).[35, 51-52] LXRs control this pathway by directly inducing the expression of ATP-binding cassette transporters (ABC) A1, G1, G5 and G8. Thereby promoting efflux of phospholipids and cholesterol from several cells (among others, lipid-laden macrophages) to apolipoprotein A-I (APOA-I) and high density lipoprotein (HDL), and by limiting cholesterol absorption in the intestine (Figure 4). In LXR-deleted mice a significant reduction of HDL has been found,[48] a similar symptom are likewise seen in patients with Tangiers diseases. Tangier disease, a condition characterized by low levels of HDL and cholesterol accumulation in macrophages, is caused by mutations in the ABCA1.[52]

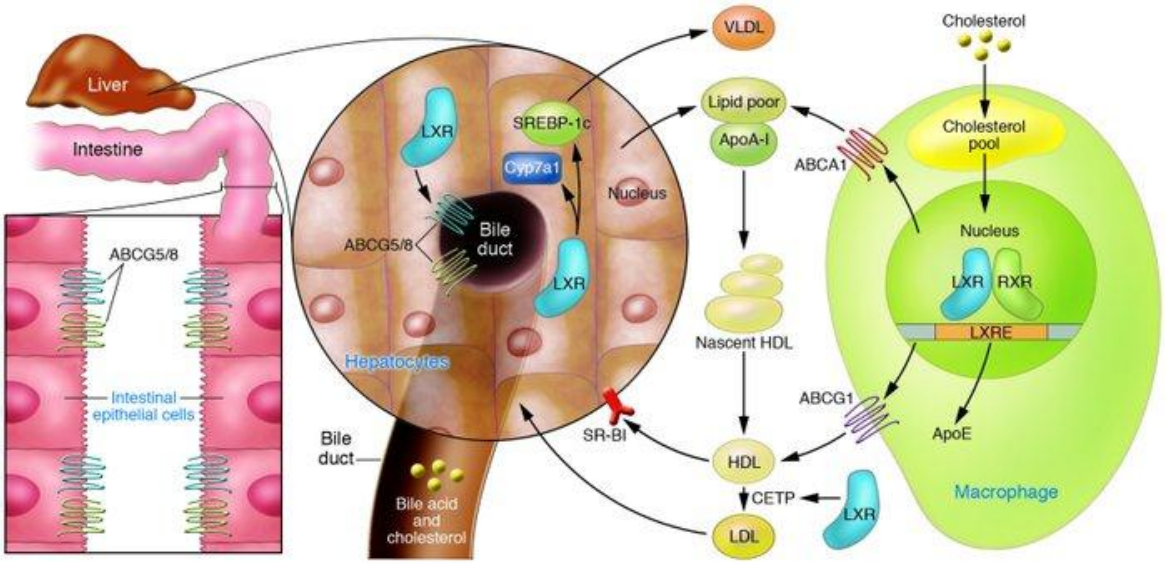

Figure 4. Regulation of reverse cholesterol transport by LXRs from macrophages. The uptake of modified lipoproteins by macrophages results in increased LXR transcriptional activity and efflux of cholesterol to lipid-poor apoA-I by ABCA1 and to HDL by ABCG1.Induction of hCETP expression transfers lipid from HDL to LDL. Once HDL/LDL is taken up by the liver, LXR promotes net cholesterol excretion.[52]

Other essential genes for cholesterol homeostasis regulated by the LXRs transcribe enzymes lipoprotein lipase (LPL), human cholesteryl ester transport protein (hCETP) and phospholipid transfer protein (PLTP).[52] The activity of hCETP involves exchanging

cholesteryl esters out of HDL for triglycerids (TG) having the net effect of reducing HDL levels, while PLTP transfers surface phospholipids from TG-rich lipoproteins (VLDL) to HDL during TG-lipolysis. LPL is secreted by many tissues (manly in in heart, adipose tissue, skeletal muscle, kidney, and mammary gland) of the body and is the principal enzyme responsible for lipoprotein metabolism, it hydrolysis TGs in VLDL releasing FFA to the peripheral tissue.[52]

LXR and Regulation of Fatty Acid Metabolism

The key role of LXR in fatty acid metabolism was established when Repa *et al.* and others found that LXR induces sterol regulatory element binding proteins (SREBPs) expression, and the expression of carbohydrate responsive element-binding protein (ChREBP) by directly binding to LXREs.[45, 53-54] SREBPs are membrane-bound transcription factors significant to the regulation of lipid homeostasis and exist in three isoforms; SREBP-1a, SREBP-1c and SREBP-2. Most organs, including the liver and adipose tissue, express largely isoforms SREBP-1c and SREBP-2. In vivo studies with transgenic and knockout mice suggest that SREBP-1c have a main role in fatty acid and glucose/insulin metabolism, whereas SREBP-2 is specific for cholesterol synthesis.[55-56] Mediating insulin signaling, SREBP-1c stimulates expression of several enzymes involved in lipogenesis, such as fatty acid synthase (FAS) and acetyl CoA carboxylase (ACC). Both FSA and ACC carboxylase are direct as well as indirect targets of LXR.[48] Furthermore, it has been demonstrated that overexpression of SREBP-1c in β-cells of the islets of the pancreas leads to lipid accumulation and finally apoptosis of these cells, a salient feature of diabetes.[57]

ChREBP is a glucose sensitive transcription factor that promotes hepatic conversion of excess carbohydrate to lipids.[45] Under basal conditions inactive ChREBP is located in the cytosol, but it is rapidly translocated to the nucleus at high glucose concentrations.[58] A study published in 2006 demonstrated in leptin-deficient (*ob/ob*) ChREBP knock-out or suppressed mice (well-characterized mouse model of obesity) that these animals had markedly reduced lipogenesis and glucose plasma levels.[59] That the activation of LXR not only increases expression of ChREBP, but also modulates ChREBP activity, was again augmented for in the work by Chang and colleges,[60] where they have revealed that LXR agonist treatment of mice is associated with up-regulation of ChREBP and thereby enhancing expression of many lipogenic genes such as FAS, ACC, and stearoyl CoA desaturase (SCD)-1.

ACCs play a rate-limiting role in fatty acid biosynthesis in plants, microbes, mammals and humans; it catalyzes the synthesis/carboxylation of acetyl-CoA to malonyl-CoA. Malonyl-CoA is a critical bi-functional molecule, i.e., a substrate of FAS for acyl chain elongation in the fatty acid synthesis and an inhibitor of transporting long-chain fatty acids across the membrane for fatty acid beta-oxidation.[61] A supposed LXRE identified in the ACC has displayed to bind both thyroid receptors, LXRα and LXRβ, which suggests that ACC gene expression theoretically can be regulated by these nuclear receptors.[62]

In positive balance, lipids stored in adipose tissue can originate from dietary lipids or from non-lipid precursors such as carbohydrates, and are therefore susceptible to be converted to fatty acids in the intermediary metabolism. This process is known as *de novo* lipogenesis (DNL).[63] FAS is a multifunctional enzyme, vital in the pathway of the DNL catalyzing all the steps in conversion of malonyl-CoA. Previous work has presumed that the effects of LXRs on FAS expression have been secondary to the induction of SREBP-1c.[64] However, demonstrated in macrophage- and liver cell lines, as well as *in vivo* in livers of mice, FAS promoter contains a conserved high-affinity binding site for LXR suggesting FAS as a direct and indirect LXR target gene which requires interaction with both transcription factors for maximal induction.[64]

SCD is the rate-limiting enzyme in the cellular synthesis of monounsaturated fatty acids from saturated fatty acids; an important step in the generation of triglycerides for transport and storage as well as preserving cellular membrane flexibility.[48] Studies executed in the last century have publicized that SCD activity is decreased in rat liver during starvation and diabetes and is rapidly induced to high levels upon re-feeding high carbohydrate diets or upon insulin administration. Moreover, obese hyperglycemic mice are shown to have an elevated activity of SCD and higher depositions of body fat than their lean counterparts.[65-66] A positive correlation between SCD-1 activity in skeletal muscle (up-regulated) and the percentage of body weight has also been reported in extremely obese humans.[66] In T2MD, SCD activity is increased, apparently in response to increased levels of plasma insulin.[66] Despite the fact that there is not yet been detected a LXRE in SCD-1 gene, it has been reported a putative LXRE in the promoter region of SCD-1 gene signifying that LXRs either directly or secondary are involved in diseases caused by altered SCD activity.[67]

Table 1. LXR Target Genes

	Function of Protein	Regulation	References
Cholesterol metabolism			
ABCA1	Mediates the active efflux of cholesterol from cells to apolipoproteins	↑ LXRE	68
ABCG1	Mediates the active efflux of cholesterol and phospholipids from cells to apolipoproteins	↑	69
ABCG5/8	Important role in enterohepatic sterol transport	↑	70
ApoCI/IV/II	Cofactor for LPL in hydrolysis of triglyceride	↑ LXRE	71
Apo E	Facilitates cholesterol efflux outside the enterohepatic axis	↑ LXRE	71
hCETP	Mediates transfer of cholesterol esters from HDL to triglyceride-rich lipoproteins	↑ LXRE	72
LPL	Hydrolyzes triglycerides in circulating large lipoproteins	↑ LXRE	73
PLTP	Transfer phospholipids from triglyceride-rich lipoproteins to HDL	↑	74
SR-B1	HDL receptor involved in reverse cholesterol transport	↑ LXRE	75
Lipid metabolism			
ACC	Carboxylate acetyl-CoA to malonyl-CoA for synthesis off fatty acids	↑(LXR is involved in a complex that binds a thyroid hormone response element)	62
FAS	Catalyzes the formation of long-chain fatty acids from acetyl-CoA	↑ LXRE	62
SCD-1/2	Rate-limiting enzyme in transformation of monounsaturated fatty acids from saturated fatty acids	↑	64
SREBP1c	Transcription factor that controls expression of several genes involved in lipogenesis	↑ LXRE	53-54
ChREBP	Transcription factor that controls genes involved in hepatic conversion of excess carbohydrate to lipids	↑ LXRE	45
PPARγ	Transcription factor that controls genes involved in lipid metabolism and transport of free fatty acids across cell membranes	↑	76
Carbohydrate metabolism			
G6-Pase	Enzyme which convert glucose-1-phosphate to glucose-6-phosphate	↓	74
GLUT-4	Glucose transporter	↑ LXRE	77
GK	Glucokinase	↓	74
PEPCK	Rate-limiting enzyme in gluconeogenesis	↓	74, 78
PDK4	An inhibitor of glycolysis	↑	79
Energy homeostasis			
UCP1	Proton carrier in the mitochondrial membrane	↑↓	80
UCP2	Proton carrier in the mitochondrial membrane	↑	80

A minor overview of some of the genes directly regulated by LXR or by LXR modulators. ↑, up-regulated; ↓ down-regulated. Modified from Steffensen *et al.* and Kalaany *et al.*.[48, 81]

LXR and Regulation of Glucose Metabolism

The first reports about LXR placed the nuclear receptor as a sensor of cholesterol and lipid metabolism,[48] new data indicate improve glycemic control in diabetic rodent models. Administration of the non-steroidal LXR agonist T0901317 (Figure 5b) significantly reduced plasma glucose concentration in *ob/ob* mice and Zucker diabetic fatty rats by suppressing gluconeogenic genes such as pyruvate carboxylase, phosphoenolpyruvate carboxykinase (PEPCK), fructose 1,6-bisphosphatase, and glucose 6-phosphatase (G6-Pase) (Table 1) leading to decreased hepatic glucose output.[78, 82]

Even though the mechanism through which LXR agonists improve carbohydrate metabolism is probably complex, several groups have shown a link between LXR and improved insulin sensitivity in different mice models. Ross and colleagues showed that T0901317 increased basal (GLUT-1 dependent), but not insulin-stimulated (GLUT-4 dependent) glucose uptake in LXRα-expressing adipocytes.[84] In contrast, Dalen *et al.* detected excitation of GLUT-4 expression and insulin-induced glucose uptake by T0901317 in both mouse and human adipocytes.[77] A slight but noteworthy increase in mRNA levels for GLUT-4 in mouse skeletal muscle was also detected. LXRE was identified within the promoter regions of mice and human GLUT-4 genes, and it was exhibited that the LXR/RXR heterodimer binds to this LXRE and stimulates transcription.[77] It has been postulated that activation of LXRs in β-cells through T0901317 further leads to glucose-induced insulin secretion and insulin biosynthesis and has been linked to induce expression of GLUT-2 as well as of glucokinase (the first and rate-limiting enzyme of glycolytic pathway).[85-86]

On the other hand, LXR agonists did not affect blood glucose concentrations in normoglycemic animals, similarly insulin sensitivity was not affected in LXRα- and LXRβ-deficient mice or when lean, normoglycemic mice were treated with an LXR agonist. Moreover, these changes did not upset the gluconeogenic fluidity *in vivo*, since neither pharmacological LXR activation nor LXR absence influence endogenous glucose generation.[78, 87-88]

1.1.4 Effect of 22(S)-Hydroxycholesterol (22(S)-HC) on Glucose- and Lipid Metabolism trough LXRs

The imperative role of LXR as a transcription factor important for the turnover of fat and cholesterol in the body along with glucose metabolism is well recognized. The receptors ties-up and are activated by synthetic non-steroidal LXR ligands (e.g. T0901317) or specific cholesterol metabolites like oxysterols (Figure 5a and b).[89] Naturally appearing agonists for LXRs include 24(S),25-EC (liver), 25-hydroxycholesterol, 24(S)-hydroxycholesterol (24(S)-HC; brain) and 22(R)-HC (adrenal gland). To activate LXR, these molecules require a stereogenic oxygen (a strong hydrogen acceptor) at either carbon 22, 24 or 27 (Figure 5a); illustrated by 24(S),25-EC being a potent LXR activator while cholesterol does not affect the LXRs at all.[43, 46, 90]

The synthetic 22(S)-hydroxycholesterol (22(S)-HC) isomer of the naturally occurring 22(R)-HC behaves more like an antagonist; repressing certain genes involved in lipogenesis and lipid handling that result in reduced synthesis of complex lipids.[89] Thus, 22(S)-HC fit the LXRα- and LXRβ ligand binding pocket (competitively and with high affinity) as well as 22(R)-HC, due to stearic/stereoselective hindrance it does not complete the same critical interactions to form transcriptionally active complexes as its natural enantiomer.[90-91]

Docking study of T0901317 and 22(S)-HC have shown that both substances incorporate into the LBD of LXRs. Hessvik and her colleagues have in their work concluded that while several lipogenic genes are induced by T0901317 in myotubes, HepG2 (human liver carcinoma) cells and the human Simpson-Golabi-Behmel syndrome (SGBS) preadipocyte cell strain, representing human skeletal muscle, liver and white adipose tissue, respectively, effect of 22(S)-HC differs between the cell types.[92] In myotubes, most lipogenic genes were down-regulated or unchanged by 22(S)-HC, whereas a more diverse pattern was found in HepG2 and SGBS cells. Treatment with 22(S)-HC induced SREBP-1 in SGBS and HepG2 cells, but not in myotubes. FAS were down-regulated by 22(S)-HC in myotubes, up-regulated in SGBS and unchanged in HepG2 cells. DNL were increased by T0901317 in all cell models, but decreased in myotubes and HepG2 cells and increased in SGBS cells when affected by 22(S)-HC. Moreover, basal glucose uptake increased in myotubes and tended to increase in SGBS cells when treated with 22(S)-HC. T0901317 did not counteract the effects of 22(S)-HC on glucose utilization, but 22(S)-HC counteracted the effects of T0901317 on lipid metabolism.[92]

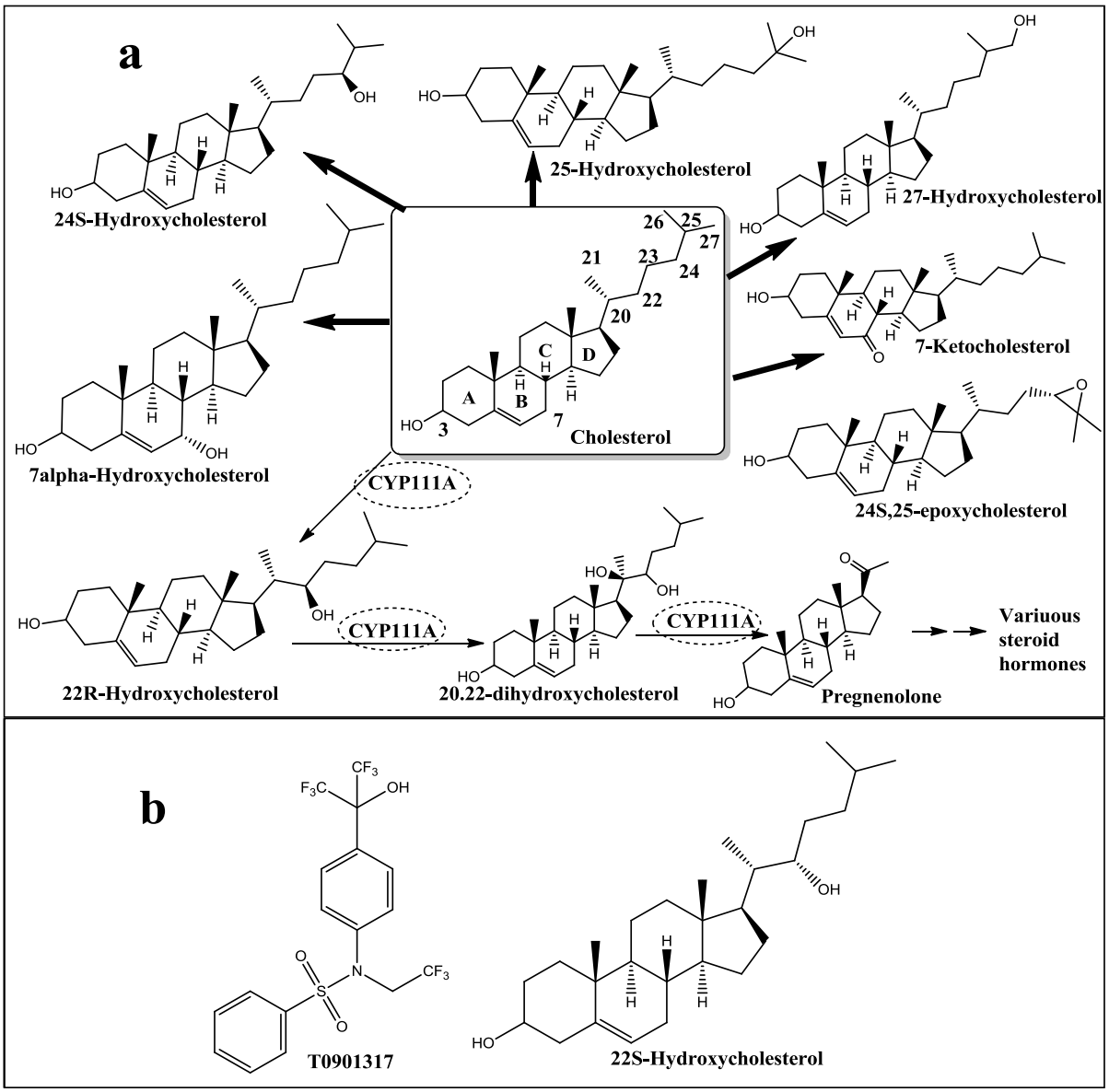

Figure 5. a) Hydroxycholesterol are oxygenated cholesterol metabolites generated through enzymatic reactions, 'reactive oxygen species' (ROS)-dependent oxidations or derived from alimentary sources, e.g. 24S,25-epoxycholesterol is one of the oxysterols not directly derived from cholesterol,[60] **b)** Synthetic LXR ligands, where the non-steroidal T0901317 is an agonist while 22S-Hydroxycholesterol works as an antagonist.[93]

An LXR modulator, with properties like 22(S)-HC might therefore be a potential model-substance for affecting LXR-regulated processes differently in various cell-types. Ability of 22(S)-HC to modify skeletal muscle lipid accumulation and reduce lipogenesis indicate a potential role for 22(S)-HC or a similar 22(S)-HC analogue in the treatment of obesity and type 2 diabetes/insulin resistance.

Synthetic Strategy behind Formation of 22(S)-HC Pharmacophore

As lined out in the previous section the anticipated pharmacophore is the upper right scaffold of the molecule. This is illustrated by the structure's -mimicking features. The strategy aims at new compounds mimicking the antagonistic properties of, as opposed to synthetic agonists of LXRs demonstrating side effects such as fatty liver, 22(S)-HC behaves differently. The aims for the new compounds are (1) they down-regulates genes involved in lipid formation and (2) increases glucose uptake. Furthermore, there has been reported a clear correlation between *in vitro* and *in vivo* biology for 22(S)-HC.[92] Even though 22(S)-HC is generic and therefore a substance patent is not possible, the molecule may be used as a lead candidate in the search drugs against T2DM and obesity.

As shown in figure 6 and scheme 6, the chemistry suggested by my supervisor Pål Rongved identifies two routes to the pharmacophore moiety. The first method is the reaction involving allyl boranes. The reaction may accomplish the right stereochemistry in high yield (98.5% reported). [94] However, it involves many steps, and the product generated is an olefinic group having little flexibility in further functionalization. On the contrary, the second method is based on oxazolidinone chemistry (Evans) yielding the right stereochemistry from commercially available starting materials with few steps involved than the Hoffman/Yamamoto chemistry.[95]

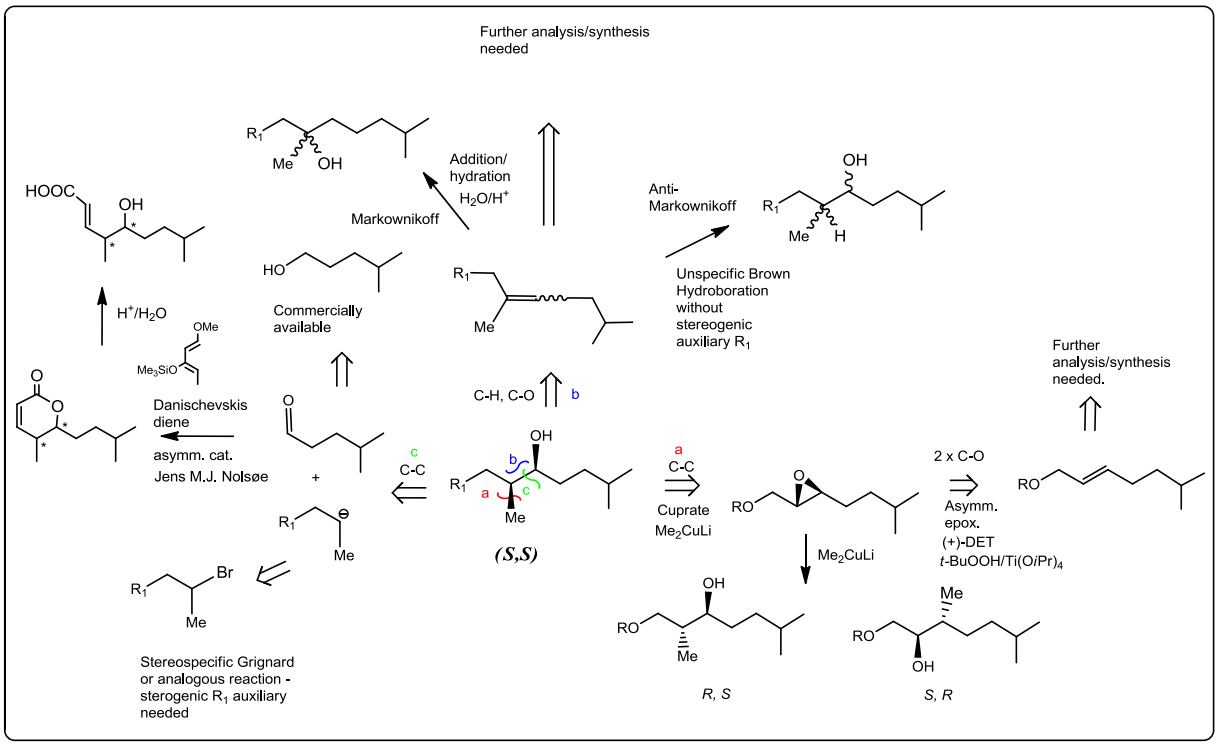

Figure 6. Retrosynthetic analysis of 22(S)-HC pharmacophore.

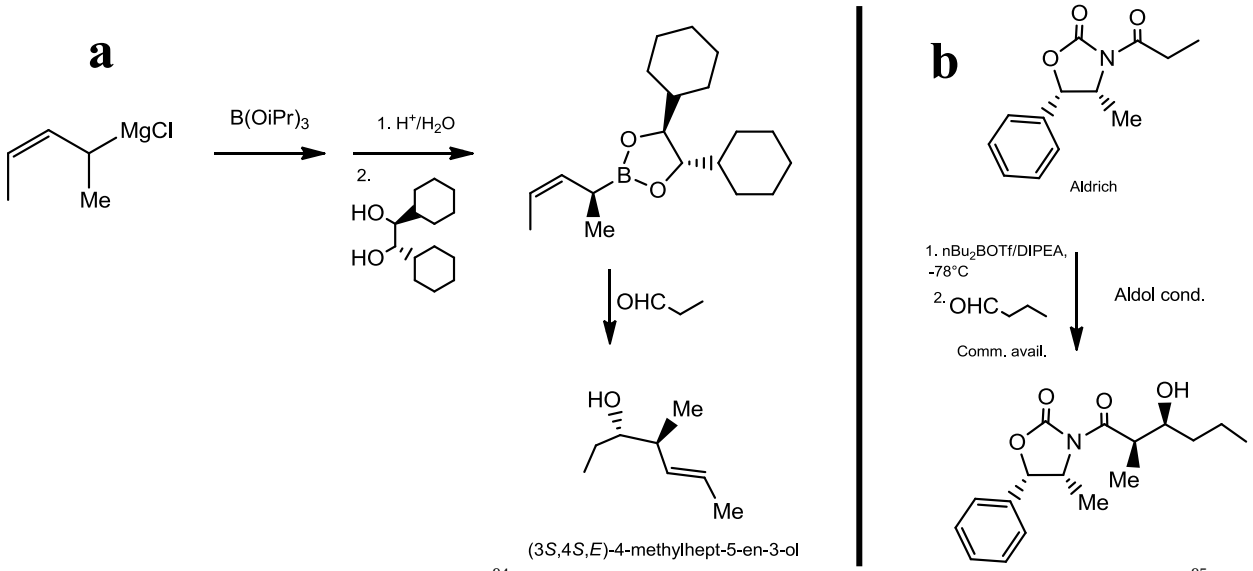

Scheme 6. a) The Hoffmann/Yamamoto reaction. [94] b) Evans oxazolidinone chemistry.[95]

1.2 Aim of Thesis

The aim of this thesis is to:

1. Develop high yielding synthetic methods of the pharmacophore of 22(S)-hydroxycholesterol based on classical stereoselective synthetic methods to be used further in the synthesis of new class of low-molecular regulators of liver X receptor.

2. Determine the stereochemistry of the pharmacophore-comprising molecule.

3. To synthesize new 22(S)-hydroxycholesterol analogues, which can subsequently be tested biologically to identify, if possible, new lipid-lowering and anti-diabetic drug candidates.

2 Results and Discussion

2.1 Synthesis of Compounds I-IVb

Five compounds, see figure 7, were synthesized to generate new analogues of 22S-HC to be tested biologically to identify, if possible, new lipid-lowering and anti-diabetic drug candidates (not shown). Compounds **II** and **III** have to our knowledge heretofore not been described in the literature.

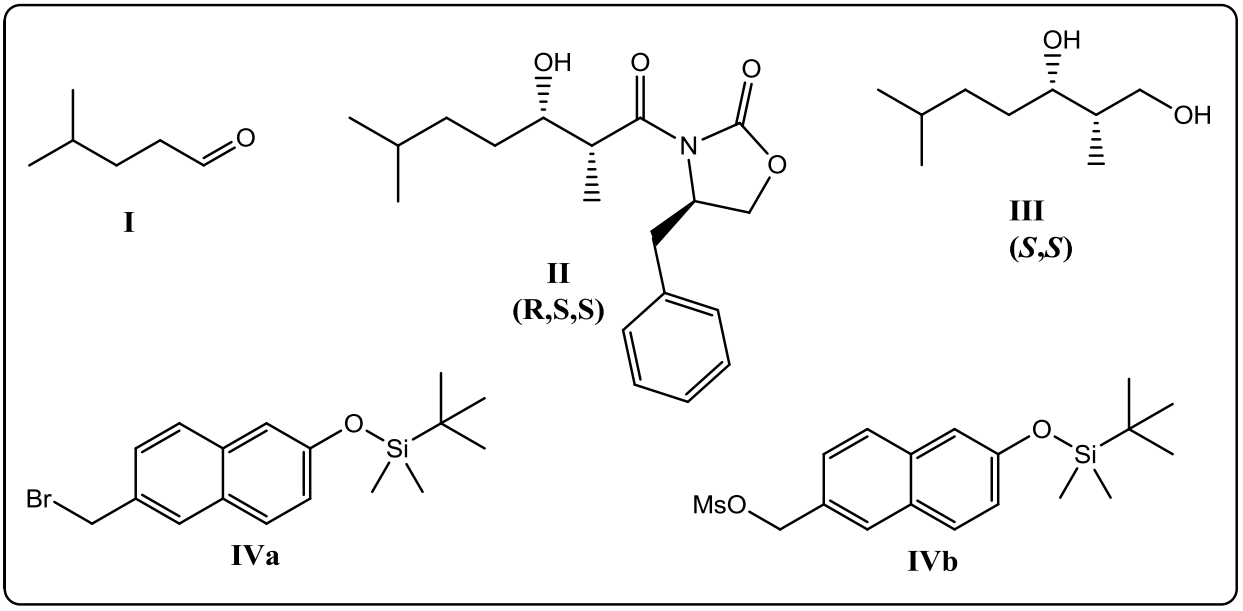

Figure 7. Aldehyde (1), optically pure ligands (II and III) and naphatyl derivatives (IVa and IVb) to be utilized in synthesis of new 22S-HC analogues.

2.1.1 Synthesis of 4-Methylpentanal (I)

Strategy 1

4-methylpentanal (**I**) was synthesized from 4-methylpentanol according to John Xiaoqinag He *et al.*,[96] see scheme 7. The procedure for the synthesis of **I** is shown in section 5.2.1 and the yields and reaction conditions are listed in table 2.

John Xiaoqinag He *et al.* reported the synthesis of 4-methylpentanal, **I**, in 63% yield from 4-methylpentanol and Pyridinium chlorochromat (PCC) in methylene chloride (DCM) for 2 hours under nitrogen atmosphere.[96] Another procedure using Swern conditions was available,[97] and is discussed in **Strategy 2**. The purification procedure used by John

Xiaoqinag He and coworkers was not available to us. Instead of Florisil®, SiO_2 was used for filtration followed by distillation with good success. Starting material was only observed in the crude product, so distillation and the washing procedure involving simple filtration and washing with DCM worked rather well.

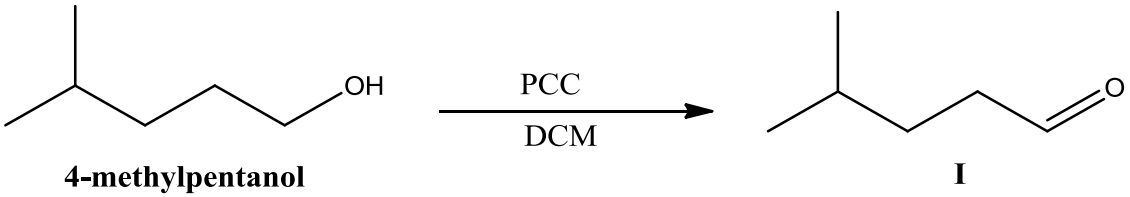

4-methylpentanol **I**

Scheme 7. Preparation of 4-methylpentanal (**I**)

Table 2. Reaction conditions and yields in synthesis of aldehyde (I)

Experiment	*Temperature*	*Elapsed hours**	*Yields % (Product)*
1	Room temperature	2	26
2	Room temperature	24 h	11
3	30ºC**	24 h	9

*How long the reaction was left to stir before work-up
**Liebig's cooler was attached so the solvent would not vaporize into the air

A search of the literature revealed several publications addressing oxidation of 4-methylalcohol to **I** using PCC,[96, 98-101] where one of the studies in addition have reported a yield of 40%. [99] However, in the published work either the aldehyde was used further without being purified, or the reaction was stopped after filtration and washing. An important part of our procedure is to obtain a purified product; therefore, distillation subsequent to filtration played a vital role to get rid of the starting material and any waste products.

When stored at room temperature, the aldehyde is highly unstable; the compound is rapidly oxidized when unprotected from air. Therefore, the best storage condition was found to be under nitrogen at -15ºC to -12ºC. With these necessary precautions, storing the aldehyde in freezer was sufficient; no change in composition was observed when the samples were tested after two weeks. A slight decomposition was however detected after 6 weeks of storage. As listed in section 4.2.1, the ^{1}H NMR spectrum looks just like the expected.

As seen in table 2, the critical factor for achieving high yields in these reactions is neither a long elapsed time nor heat to overcome the energy barrier under distillation; therefore it was considered whether it might have been the solvent that was the problem. Thin layer chromatography (TLC) analyses of DCM after evaporation (rotary evaporator) and

distillation confirmed presence of a compound in the DCM. It is likely but not conclusive that an amount of compound **I** have been collected with the DCM. It could have been a good idea to try a different solvent, but then one have to consider the important role of boiling point and polarity. The aldehyde is a quite polar molecule with a boiling point of ~120ºC. Since DCM had a sufficient boiling point (39.8ºC) and a polar aprotic character, it was an ideal solvent for the reaction. Tetrahydrofuran (THF) and Methyl-t-Butyl Ether (MTBE) could have been good candidates as they have similar, though a little higher, boiling point (66ºC and 55.2 ºC, respectively) and at the same time are polar and aprotic.[102]

Another problem that is of relevance is the semiliquid form of the aldehyde getting stuck on different equipment, i.e. under distillation, which can also be the reason for the low yield. The low yields in experiment 2 and 3 could in fact also be attributed to a relative large mechanical loss as it was only run on small scale.

All in all, oxidation using PCC proved successful, but the yields and the reproducibility were only decent. This can in part be attributed to the low stability of the compound and the purification procedures that need to be undertaken to produce pure product.

Strategy 2

PCC is not particularly hygroscopic, is stable and very convenient to store. In addition, it is commercially available. PCC is soluble in many organic solvents, and especially DCM at room temperature, and has been used to transform alcohols to aldehydes and ketones in high yield. However, Chromium (VI) compounds are toxic and must be handled with care. Another disadvantage is the formation of gelatinous materials that complicate product separation. Addition of Celite, powdered molecular sieves or magnesium sulfate to PCC oxidation reaction mixtures can make the work-up easier, because the reduced chromium salts are withdrawn to these solids, which can then be freely removed by filtration.[103] These drawbacks do not occur when dealing with Swern oxidation.

The Swern Oxidation of alcohols eludes the use of toxic metals such as chromium, and can be carried out under very mild conditions. Reaction allows generation of aldehydes and ketones from primary and secondary alcohols, respectively. Furthermore, aldehydes do not

react further to give carboxylic acids. A drawback is the production of the stinking side product dimethyl sulphide.[103]

4-methylpentanal (**I**) was synthesized from 4-methylpentanol according to Sepe *et al*.[97] The primary alcohol was submitted to oxidation under Swern conditions, se scheme 8; the procedure is shown in section 6.2.1 and the yield and reaction conditions are listed in table 3.

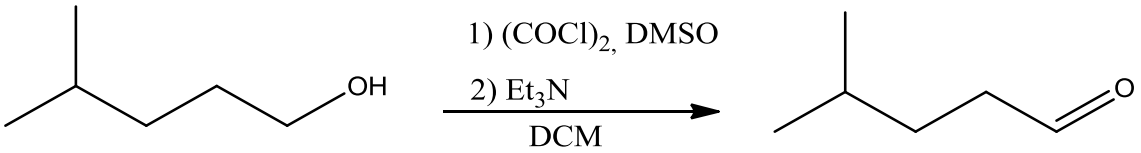

4-methylpentanol **I**

Scheme 8. Primary alcohol submitted to oxidation under Swern conditions

Table 3. Yield obtained in the synthesis of the aldehyde (I) under Swern condition

Experiment	*Temperature*	*Reaction time*	*Yields % (Product)*
1	-78ºC → room temperature	1.5 h	32

Sepe and coworkers reported the synthesis of 4-methylpentanal, **I**, in 97 % yield (unpurified) from 4-methylpentanol under Swern condition. The procedure was used without changing of parameters assuming that the yield would be improved compared to the PCC procedure. Nonetheless, when the refinement procedure was included the yield dropped, representing almost the same yield as gained with the use of PCC. This again amplifies the fact that the low stability of the compound and the purification method involving distillation affects the yield and reproducibility in synthesis of compound **I**.

2.1.2 Synthesis of 4-(R)-Benzyl-3-(3-(S)-hydroxy-2(S),6-dimethyl-heptanoyl)-oxazolidin-2-one (II)

As lined out in the theory section, naturally appearing agonists require a stereogenic carbon at either carbon 22, 24or 27 (Figure 5a). 22(S)-HC fit the LXRα- and LXRβ-LBD with high affinity. Nevertheless, it behaves more like an antagonist compared to its natural enantiomer 22(R)-HC operating more as an antagonist. In order to utilize **I** in the synthesis of new 22S-HC analogues, the next reaction step must be stereoselective.

A *syn* aldol adduct 4-(R)-Benzyl-3-(3-(S)-hydroxy-2(S),6-dimethyl-heptanoyl)-oxazolidin-2-one (**II**), with the same configuration as 22(S)-HC, was synthesized from an aldol condensation of the enolborate derived from (R)-4-benzyl-3-propionyloxazolidin-2-one to the aldehyde(**I**), see scheme 9; the procedure for the synthesis of **II** is shown in section 5.2.2 and the yield and reaction conditions are listed in table 4.

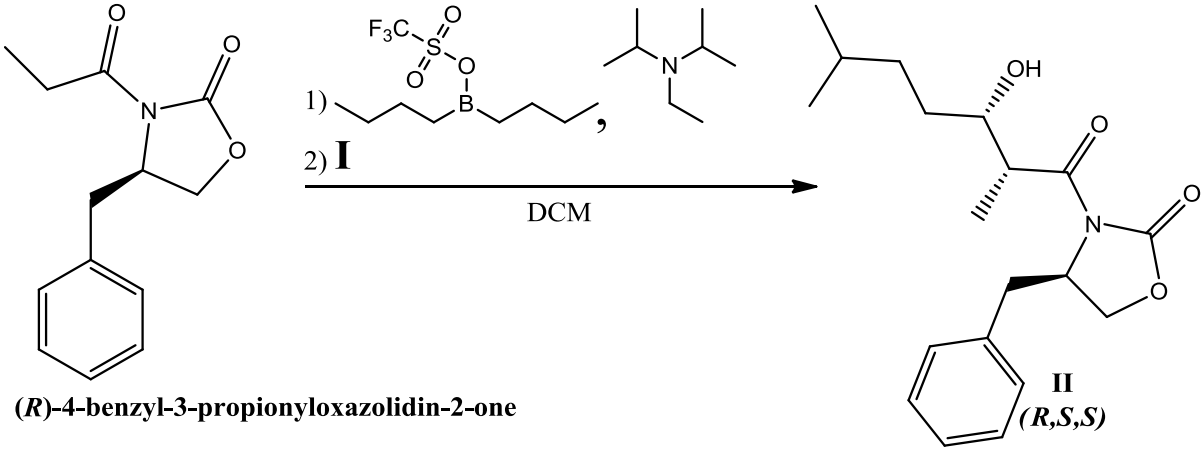

Scheme 9. Preparation of *syn* aldol adduct (**II**)

Table 4. Reaction conditions and yield obtained in the synthesis of the compound II

Experiment	*Temperature*	*Reaction time*	*Yields % (Product)*
1	0ºC →(-78)ºC→ room temperature	3 h	83

Tsutsumi *et al.* and others have reported good yields and excellent diastereoselectivity with (R)-4-benzyl-3-propionyloxazolidin-2-one in nucleophilic additions based on Evans aldol reaction resulting in *syn* aldol product.[104-105] Evan's chiral oxazolidinones have been extensively engaged in asymmetric synthesis, in particular, the aldol reactions of aldehydes with lithium or boron enolates have been found to give high diastereoselectivities in the presence of oxazolidinone as the chiral support.[106]

Tsutsumi and colleagues have in their work stated 92% yield of the *syn* aldol product under argon atmosphere.[104] It was suggested/assumed that our aldehyde (**I**) would react in similar manner, so the procedure was used without changing conditions. TLC analysis of the reaction mixture after termination of the reaction displayed that not all of the starting material had reacted; this is probably the reason for a lower yield than reported, alternatively, it could be due to mechanical loss during work-up.

Thus, Evans asymmetric aldol reaction using the boron enol ether afforded the product **II** in good yield (the difference in yield is believed to be neglectible).[1]H NMR analysis (300 MHz) of the reaction mixture indicated a 95:5 mixture of two diastereomeres, however, the stereochemistry of the newly generated chiral centers was confirmed as *S,S* by X-ray crystallography done by chemistry professor Carl Henrik Gørbitz at University of Oslo, se section 5.2.3 for recrystallization procedure.

2.1.3 Synthesis of (2S,3S)-2,6-dimethylheptane-1,3-diol (III)

(2S,3S)-2,6-dimethylheptane-1,3-diol (**III**) was obtained from compound **II** by reductively removing the auxiliary (R)-4-benzyloxazolidin-2-one, se scheme 10. The procedure for the synthesis of **II** is shown in chapter 5.2.4 and the yields and reaction conditions are listed in table 5.

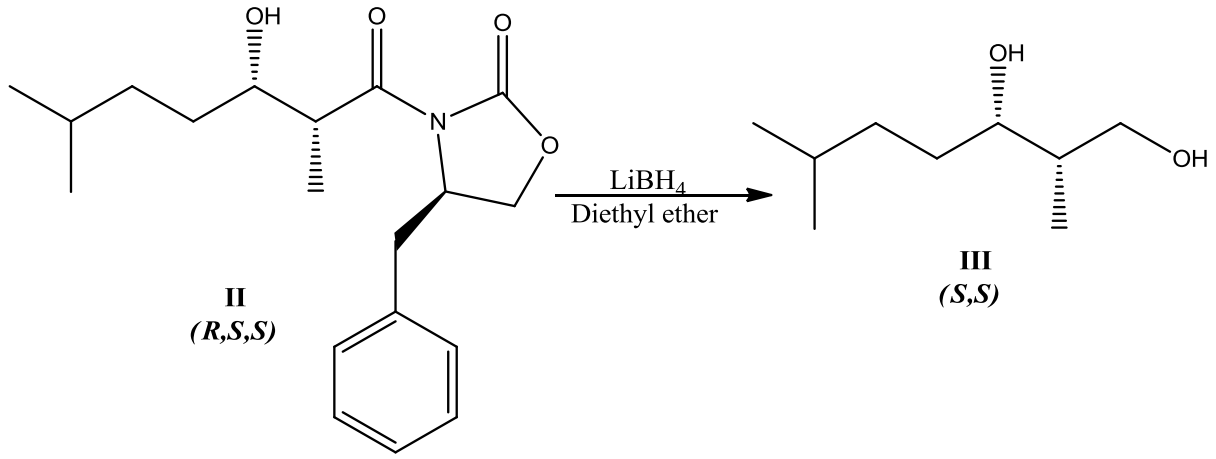

Scheme 10. The auxiliary can be reductively removed by simple exposure to lithium borohydride ($LiBH_4$) in diethyl ether to provide primary alcohol **III** in high yield.

Table 5. Reaction conditions and yields obtained in the synthesis of compound III

Experiment	*Temperature*	*Elapsed hours**	*Yields % (Product)*
1	Room temperature	1	0
2	Room temperature	1	66 %
3	Room temperature	2	82 %
4	Room temperature	3	91 %

*How long the reaction was left to stir before work-up

Burges *et al.*[107] have in their work reported a method which could have been used to synthesize the title compound. The literature describes the synthesis of (2R,3R)-2,6-dimethylheptane-1,3-diol (enantiomer of complex **III**) with high diastero-control to the *syn* adduct by using catecholborane rhodium catalyst. The starting material is optically pure and

the reaction conditions do not lead to racemization. Other reaction conditions with spectroscopic data were not specified. However, the method was not tried; instead Evan's chiral oxazolidinones was used to obtain the right stereochemistry thereby chemoselectively removing the auxiliary to achieve the desired compound.

Sodium borohydride ($NaBH_4$) is the favored reducing agent for chemoselective reductions of aldehydes and ketones. However, it is sometimes forgotten that $NaBH_4$ can simply be customized to form either a stronger or more selective reducing agent.[108] Lithium borohydride ($LiBH_4$), easily prepared from $NaBH_4$, but also commercially available[1] is reported to be a selective reducing agent. The advantage of using $LiBH_4$ in chemoselective, diastereoselective and enantioselective reactions is possibility to use ether-type solvents.[109] Several publications have demonstrated the use of $LiBH_4$ reductively removing the supporting moiety(R)-4-benzyloxazolidin-2-one to obtain an alcohol in high yield along with the intact oxazolidinone chiral auxiliary.[110-111]

As seen in table 5, the decisive factor for achieving high yields in these reactions is the long elapsed time before work-up. A long time (3 hours or more at room temperature) allows the starting material to fully reduce the starting material that can be isolated through flash chromatography. Moreover, it is essential to take into account the quality of the reductive agent. The first experiment ended in 0% yield; a new batch of $LiBH_4$ dramatically affected the yield raising it to more than 60% between entry 1 and 2 in table 5. When all the above mentioned precautions are made, the yields are usually good to excellent.

Entry 2 and 3 (table 5) ended up giving the title compound as a colorless oil. Despite the fact that ^1H NMR did show a pure compound **III**, it is conceivable, but not decisively, that the experiments have given a contaminated diol. In contrast, the last experiment generated **III** as a colorless solid. A crystallization procedure was performed to determine the stereochemistry of the newly generated chiral centers, see section 5.2.5, but was not able to produce high-quality crystals for X-ray crystallography.

[1] 5 grams costs 570.35 euros as of 01.mai.2012 from Sigma-Aldrich

2.1.4 Synthesis of ((6-(bromomethyl)naphthalen-2-yl)oxy)(tert-butyl)dimethylsilane(IVa)

((6-(bromomethyl)naphthalen-2-yl)oxy)(tert-butyl)dimethylsilane (**IVa**) was synthesized from (6-((tert-butyldimethylsilyl)oxy)naphthalen-2-yl)methanol. The benzyl alcohol was submitted to a simple bromination under Appel condition, se scheme 11; the procedure for the synthesis of **IVa** is shown in section 5.2.6 and the yields and reaction conditions are listed in table 6.

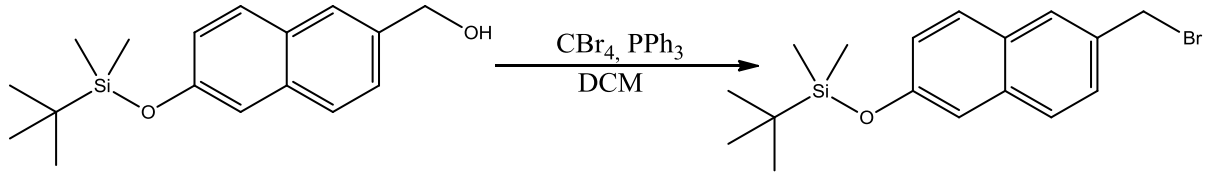

(6-((tert-butyldimethylsilyl)oxy)naphthalen-2-yl)methanol **IVa**

Scheme 11. Benzyl alcohol submitted to bromination under Appel conditions.

Table 6. Yield obtained in the synthesis of the naphatyl-analogue IVa under Appel condition

Experiment	*Temperature*	*Reaction time*	*Yields % (Product)*
1	0ºC	3 h	89

Appel's reaction was originally described in 1971 by Professor Rolf Appel at the University of Bonn in Germany. The reaction between triphenylphospine and tetrahalometane (CCl_4, CBR_4) forms a salt known as Appel's salt. The transformation of alcohols into the corresponding halides is easily done by treating the alcohol with Appel's salts (Figure 8). It is a convenient method conducted under mild conditions, the yields are normally high.[112]

As with the synthesis of compound **II-III**, it was anticipated that the yield would be deeply affected by how long the reaction was left to stand and stir before filtration and further work-up. Because of this, the reaction was left for 3 hours and not tested in advance. The reaction was carried out under nitrogen atmosphere and the TLC analysis of the reaction mixture after 3 hours did not show any other byproducts. Therefore, instead of flash chromatography, filtration through a silica plug was used (a necessary step) to get rid of Ph_3P/Ph_3=O. The yield was good and there is no trace of starting material in the NMR spectra, see appendix **B.9** and **B.10**.

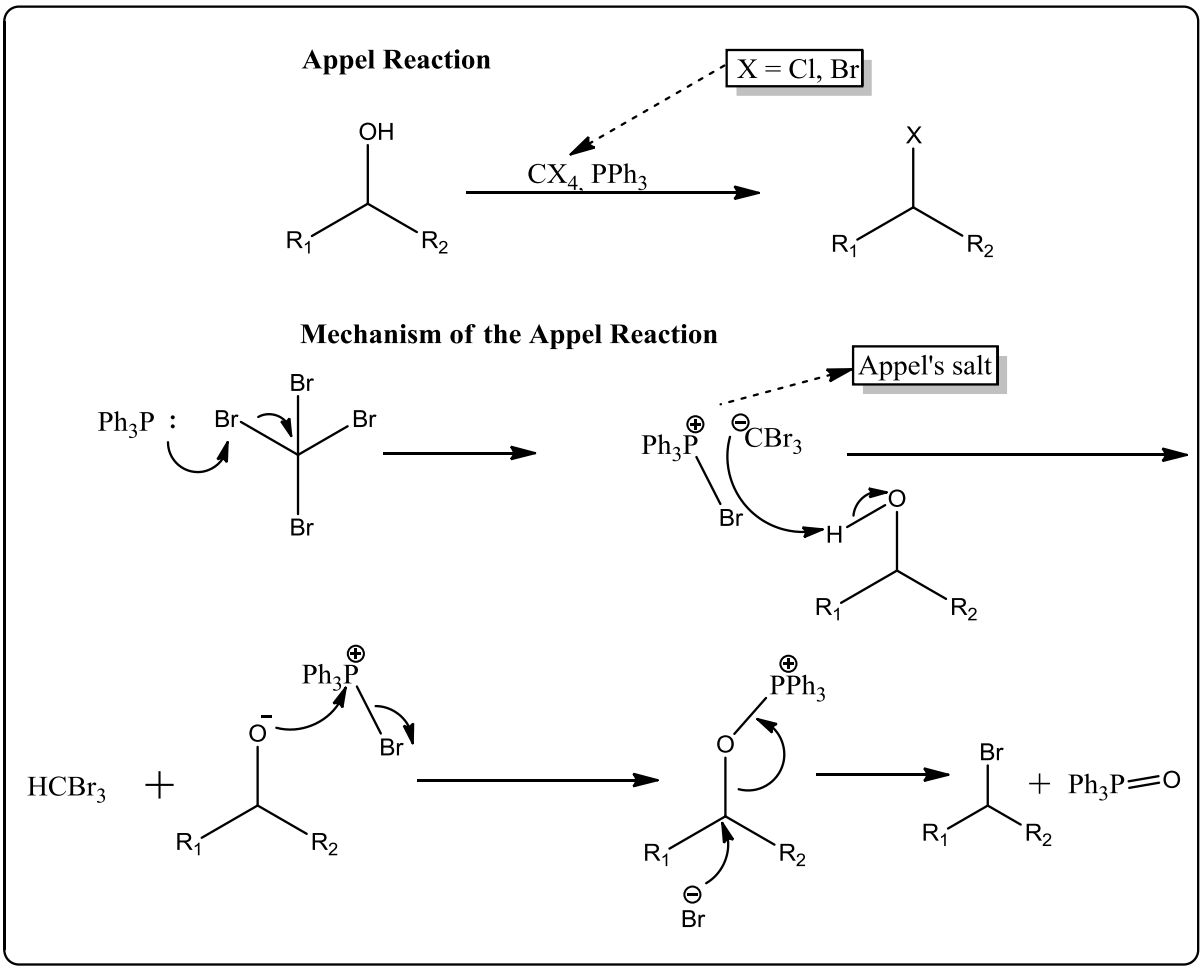

Figure 8. Mechanism of the Appel reaction.[112]

2.1.5 Synthesis of (6-((tert-butyldimethylsilyl)oxy)naphthalen-2-yl)methyl methanesulfonate (IVb)

A publication by Marcotullio and coworkers from 2006,[113] described a simple method for the conversion of alcohols to tosylates and mesylates. The transformation of aromatic alcohols to the corresponding mesylate form is not described in Marcotullio's work, but it was anticipated that (6-((tert-butyldimethylsilyl)oxy)naphthalen-2-yl)methanol would react in a parallel manner, so the technique was used without changing the reaction conditions (scheme 12 and table 7). The reaction procedure is outlined in section 5.2.7.

Marcotullio *et al.* stated the preparation of two secondary mesylates in 85% and 86% yield from different alcohols for 2 hours in room temperature where the mesyl chloride was added drop-wise. Under these conditions, it was reasonable to reduce the rate of reaction by cooling it to 0ºC at the beginning instead of adding mesyl chloride drop-wise to better control the response rate. TLC analyses of the reaction mixture after half an hour and after 1, 3 and 4

hours for entry 1, 2 and 3, respectively, did not show any byproducts. TLC analyses of entry 1 after 2 hours showed two distinct spots indicating that not all the starting material had reacted. The reaction was however stopped prematurely, in order to see if the anticipated product had formed at all. Purification of the reactions was obtained by filtration trough a SiO_2 plug as a substitute of flash chromatography to get rid of the starting material giving overall fine yields.

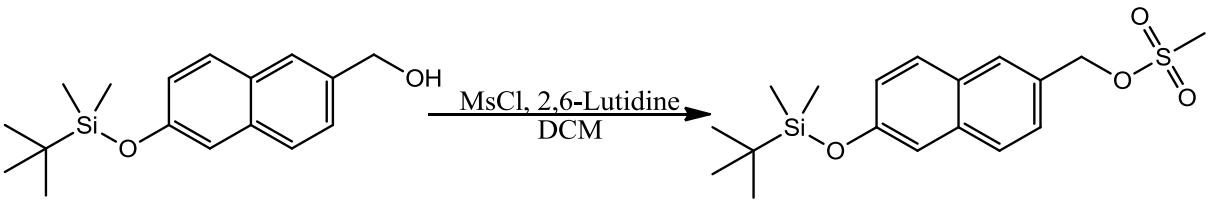

(6-((*tert*-butyldimethylsilyl)oxy)naphthalen-2-yl)methanol **IVb**

Scheme 12. A simple method for the conversion of the aromatic alcohol to corresponding mesylate structure.

Table 7. Yield obtained in the synthesis of the naphatyl-analogue IVb

Experiment	*Temperature*	*Reaction time*	*Yields % (Product)*
1	Room temperature	2 h	49
2	Room temperature	6 h	67
3	Room temperature	24 h	70

While efforts with the compound **IVb** progressed, it was shown that in solution the product was quite unstable, likely because it is a highly reactive compound. When exposed to even minute amounts of water and/or acidic solvents such as deuterated chloroform ($CDCL_3$-d), it seemed like mesylate moiety was furnished returning a NMR spectrum and TLC analysis similar to the starting material. This was first detected by ^1H NMR, where the solvent used was $CDCL_3$-d which subsequently was found to be contaminated with a small quantity of water. For assurance, ^1H NMR of the end product was taken with another batch of $CDCl_3$-d in addition to deuterated dimethyl sulfoxide (DMSO- d_6). NMR spectra of $CDCl_3$-d demonstrated the same signals as before, whereas DMSO- d_6 gave an additional signal for one proton. It is possible, but not definite, that the additional signal is from one of the protons on methylene located on the mesylate group. However, as listed in section 4.2.5, the ^{13}C NMR spectrum obtained from DMSO-solution looks just like expected (appendix **B.13**). All in all, it is quite likely that the product formed is **IVb** and that the compound is probably quite unstable in solution when exposed to water or acidic solvents.

2.1.6 Attempted Synthesis of (2S,3S)-1-((6-((tert-butyldimethylsilyl)oxy)naphthalen-2-yl)methoxy)-2,6-dimethylheptan-3-ol (V)

Synthesis of the title compound, considered to provide similar response as 22S-HC, has to our knowledge heretofore not been described in the literature. The synthesis was carried out based on reaction conditions suggested by senior research scientist Marcel Sandberg from the external synthesis laboratory Synthetica AS. However, the desired product was not achieved. The general reaction is outlined in scheme 13. The results of the reactions are shown in table 8 and the experimental details can be found in chapter 5.2.8.

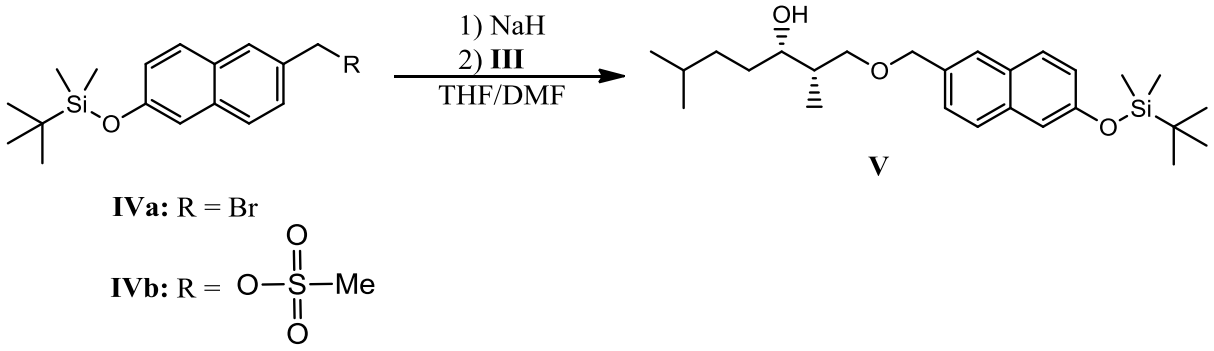

Scheme 13. General procedure for the synthesis of composite **V** using reaction conditions proposed by Marcel Sandberg.

Table 8. Attempted synthesis of molecule V from III, IVa, and IVb

Experiment	*Compound*	*mmol compound*	*mmol **III***	*Reaction condition*
1	**IVa**	0.280	0.312	Room temperature for 24 h
2	**IVa**	0.280	0.312	Room temperature for 2 h with addition of potassium iodide*
3	**IVa**	0.280	0.312	At 50 ºC for 3 h
4	**IVb**	0.240	0.267	Room temperature for 24 h
5	**IVb**	0.546	0.606	0ºC for 5 h

*10% mmol of the material quantity of **III**

The reactions were performed under nitrogen atmosphere and followed on TLC to see if the starting material were consumed and the product achieved. The problem seemed to be reactivity of the compounds combined shortcomings of the purification step. Overlying bands in TLC and complex mixtures proved hard to separate, but given more time to optimize the solvent systems used this could have been manageable. In contrast, entry 5 gave a discrete spot on TLC. It was more non-polar matched to the starting material in addition not having the same color similarity when treated with *p*-anisaldehyde. Because of its hydrophobic

character, purification by filtration trough a pad of silica was executed to get rid of the starting material and any other products. Still the desired product was not achieved. ^{1}H NMR spectrum, see appendix **B.15**, did not reveal any protons of the naphatyl constituent, likewise ^{13}C NMR did not show any expected signals for the same part of the molecule . At this point it was concluded that the procedure using **IVa** and **IVb** in the presence of compound **III** and sodium hydride (NaH) to make the title composite is not working.

2.1.7 Attempted Synthesis of 4-((((2S,3S)-3-hydroxy-2,6-dimethylheptyl)oxy)methyl)-N,N-bis((2-(trimethylsilyl)ethoxy)methyl)benzenesulfonamide (VI)

Attempt to synthesize another 22S-HC analogue (**VI**) from **III** failed to give significant and usable results. Synthesis of **VI** is to our knowledge not yet been described in the literature. The approach (scheme 14), based on the work done by my supervisor associate professor Pål Rongved and senior research scientist Marcel Sandberg from Synthetica AS, was not successful; the synthesis did not end in the isolation of the intermediate-2 (**I-2**). The experimental details for the synthesis of intermediate-1(**I-1)** and **I-2** can be found in chapters 5.2.9 and 5.2.10, respectively whereas the reaction conditions are listed in table 9.

The preparation of the title compound takes place over three steps. The first step deals with a conventional amine sulfonation, while the second step involves linkage of the newly formed sulfonamide, **I-1**, with the stereogenic diol **III**. The generation of sulfonamides has up to date practically relied on the treatment of sulfonyl chlorides with different nucleophiles such as ammonia or amines.[114-115] Handling with ammonia gives primary sulfonamides, whereas primary and secondary amines gives *N*-alkyl and *N*,*N*-dialkyl sulfonamides, respectively.[115] The last operation of the synthesis is a simple alkylation with 2-(Trimethylsilyl)ethoxymethyl (SEM) chloride protecting the nitrogen moiety as a tertiary sulfonamide.

Both step 1 and step 2 was done under nitrogen atmosphere and was closely monitored by TLC. Sadly, as with the synthesis of **V**, the problem in both steps seemed to be reactivity and purification. It was not practicable to purify the cruide residue in step 1 due to the high amount of impurities, but given more time to optimize the solvent systems used this might have been amendable. The cruide was used without further purification. Though overlapping spots were demonstrated by TLC analyses after step 2, column chromatography was

performed returning a quite polar product assumed to be compound **I-2**. However, what anticipated being pure fractions from chromatography indeed gave very complex mixture when analyzed by ^{1}H NMR. ^{13}C NMR demonstrated nevertheless some traces of the desired molecule.

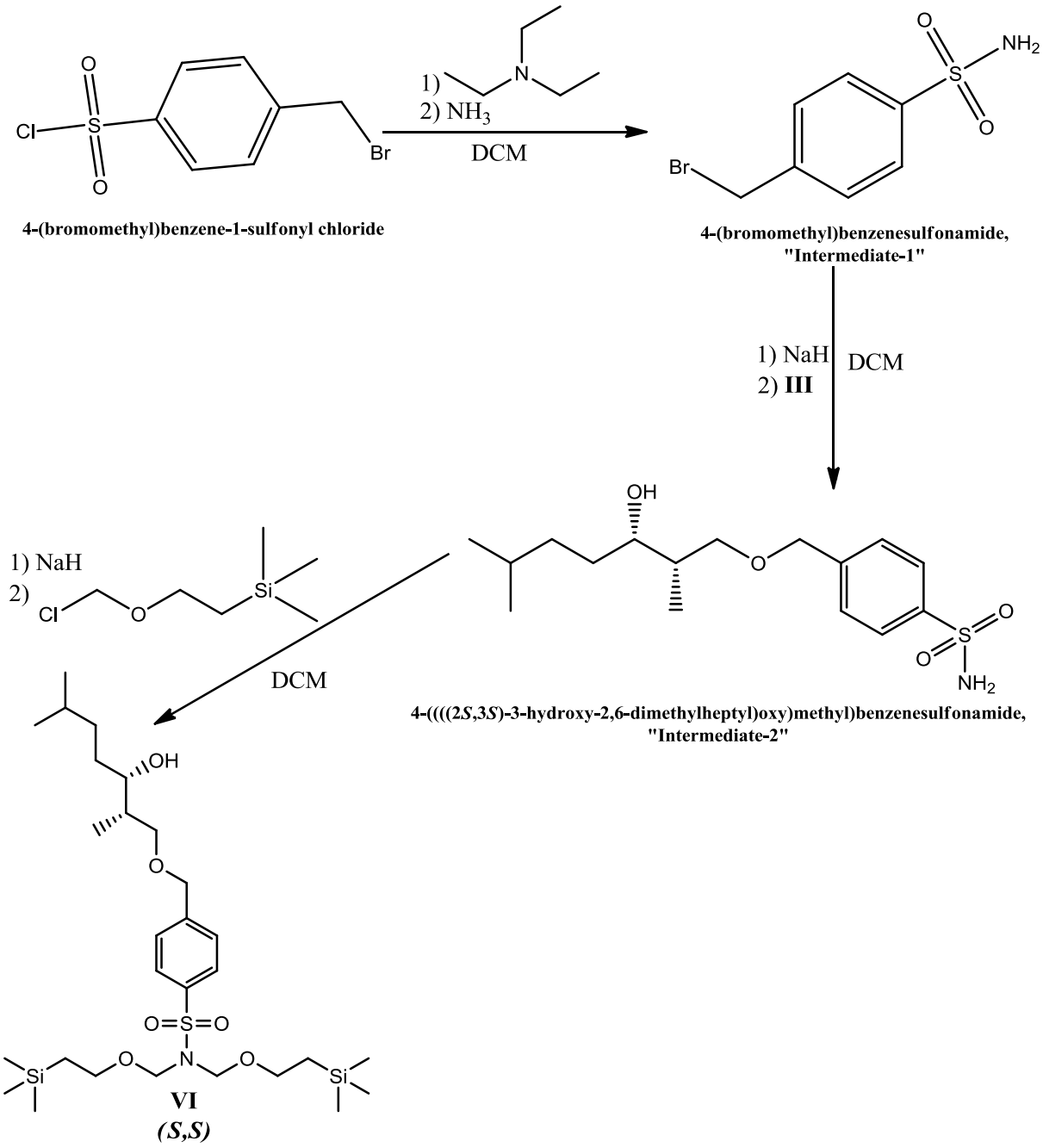

4-(bromomethyl)benzene-1-sulfonyl chloride

4-(bromomethyl)benzenesulfonamide, "Intermediate-1"

4-((((2*S*,3*S*)-3-hydroxy-2,6-dimethylheptyl)oxy)methyl)benzenesulfonamide, "Intermediate-2"

Scheme 14. General procedure for the synthesis of molecule **VI** based on the work by Pål Rongved and Marcel Sandberg

Table 9. Yield obtained in the synthesis intermediate-1 and -2 in attempted synthesis of

Experiment	*Temperature*	*Reaction time*	*Yields g (Product)*
1	0ºC	1.5 h	0.501 (intermediate-1)*
2	0ºC → Room temperature	4 h	n/a (intermediate-2)

*Product used in the next reaction without isolation, achieved yield implicate cruide residue

It was suggested that the sulfonamide **I-1** could have first been protected with SEM before reacting it with the diol to achieve **VI.** The problem with the described scheme could have been treatment with NaH. Even though the base also could remove acidic protons at the sulfonamide group at 0 ºC first, it could as well deprotonate the secondary alcohol at room temperature. Currently, the procedure involving linkage of **I-1** with **III**, and using the protection with SEM as the last step, is not effective and due to limited time altering the procedure, it was not attempted.

3 Concluding remarks

A process for developing new 22(S)-hydroxycholesterol analogues have been studied with emphasis on obtaining high yields and pure end products comprising the anticipated pharmacophore of 22(S)-hydroxycholesterol, antagonizing the liver X receptor. The synthesis and purification of compounds has been the vulnerable factor of this project; therefore, it has been invested more time to understand the reactions and especially the work-up and purification steps. Longer reaction time did have a dramatic effect on the yields obtained in some systems.

Five chiral and achiral compounds, **I-IVb**, were synthesized with yields ranging from 9-91 %, respectively, to be utilized in the synthesis of new modulators of the liver X receptor. The synthesis of aldehyde **I** using either PCC or Swern oxidation gave the poorest yields (9-32%), whereas the synthesis of pharmacophore-comprising molecule **III** by reduction gave well to excellent yields (66-91%).

Both compound **II** and compound **III** are new and not hitherto described in the literature. The developed process described in this master thesis has given the desired stereochemistry, which has been confirmed by X-ray crystallography. In this context, it has been established method of providing high-quality crystals of the composite **II**.

The syntheses of two different 22(S)-hydroxycholesterol analogues were attempted through various synthetic routes to be tested biologically to identify new lipid-lowering and anti-diabetic drug candidates. First, the attempted ether formation of **III** with **IVa** and **IVb** failed under various conditions. Second, the synthesis of the analogue **VI** via the attempted alkylation of **III** with the intermediate **I-2** produced multiple products indicating a higher reactivity of compound **III** when treated with sodium hydride, however, complex **I-2** could not be isolated.

4 Spectroscopic Interpretation and Characterization of Compounds

4.1 General Information About Spectrometric and Physical Identification

Compounds that already were described in the literature are here only documented with ^{1}H NMR. New compounds are characterized by using ^{1}H NMR and ^{13}C NMR. In addition, the intention was to document the different compounds using liquid chromatography-mass spectrometry, but due to running problems with the mass spectrometry system it was not manageable.

The ^{1}H NMR and ^{13}C NMR shift values are attributed to each atom with the help of 2D NMR technique COSY and similar data obtained from the starting material or published work. NMR elucidation book by Silverstein, Webster and Kiemble was also made use of during characterization.[116] The industry standard software ChemBioDraw Ultra 12.0.2 and ChemBio3DUltra 12.0.2, used to require electronic description of molecules and reactions, have been utilized to predict NMR shifts.

A widespread set of ^{1}H NMR signal appear in some spectrums that cannot be allocated to specific products. $CDCl_3$-d will contain a small amount of $CHCl_3$ which will give a peak at 7.26 ppm. DMSO-d_6 will give a peak at 2.05 ppm as its residual peak. A singlet at 2.10 ppm in $CDCl_3$-d is due to acetone contamination. Ethyl acetate will give a singlet at 2.05 ppm, a quartet at 4.12 ppm and a triplet at 1.26 ppm in $CDCl_3$-d. Hexane will give a triplet at 0.88 ppm and a multiplet at 1.26 ppm in $CDCl_3$-d. If $CDCl_3$-d and DMSO- d_6 contain a small amount of water, a peak will show up at 1.56 ppm and 2.84 ppm, respectively.

4.2 Spectroscopic Characterization of the Compounds

4.2.1 Characterization of Compound I

This aldehyde (**I)** has already been characterized in the literature by John Xiaoqinag He and colleagues, and the acquired NMR spectrum are in conformity with the published data.[96] The ^{1}H NMR shifts are assigned to each proton, as outlined in figure 9, and are listed in table 10. The spectrum is shown in appendix **B.1**.

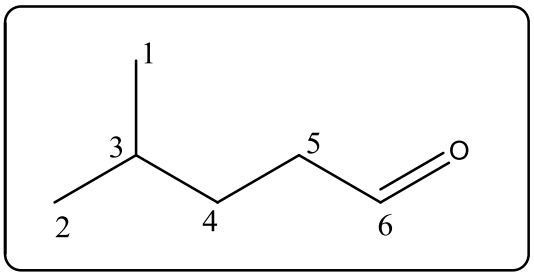

Figure 9. Atom numbering of compound I

Table 10. Assignment of ^{1}H NMR shifts values to compound I

Position	$^{\delta}$ H	*Multiplicity*	*Coupling constant (J Hz)*
1, 2	0.89	d	6.2
3, 4	1.48-1.6	m	-
5	2.41	t, d	8.0, 1.9
6	9.75	t	1.9

To see if the aldehyde decomposes over time at -15ºC to -12ºC a new ^{1}H NMR spectrum was obtained after 6 weeks of storage that show comparable shift values. However, a new peak has emerged more downfield versus CHO-group which could be due to aldehyde oxidation to the corresponding carboxylic acid. The change however is small but noteworthy.

4.2.2 Characterization of Compound II

Syn aldol adduct **II** is a new compound and thus no spectrometric data for this have been published. However, the spectra obtained from the starting material (R)-4-benzyl-3-propionyloxazolidin-2-one (appendix **A.1** and **A.2**) and the aldehyde **I** were used to determine whether the different coupling reactions had occurred or not. A COSY spectrum was also taken to correlate the different protons to their specific positions. This made the elucidation

possible. The structure was also confirmed by crystallography done by Professor Carl Henrik Gørbitz at Department of Chemistry, University of Oslo. The different shift values are assigned to each position, as shown in figure 10, in table 11. The ^{1}H NMR spectrum is shown in appendix **B.3** and ^{13}C NMR spectrum in appendix **B.4**.

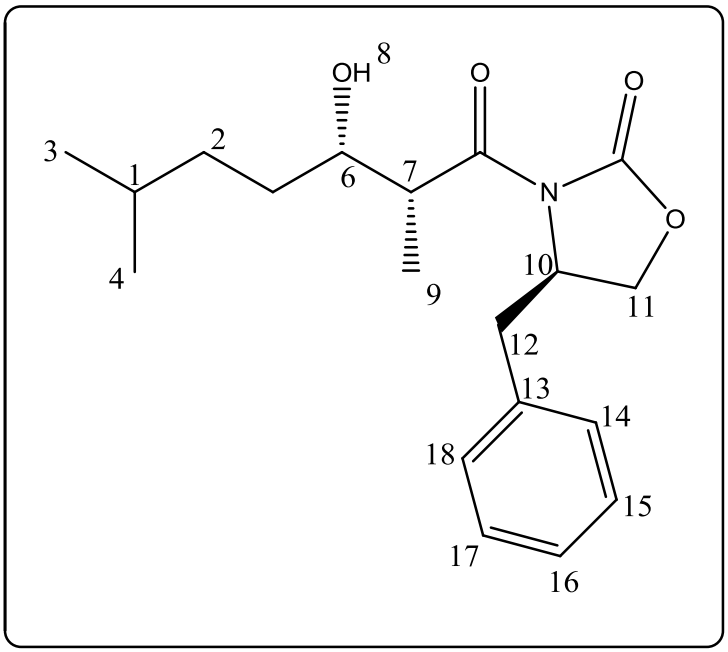

Figure 10. Atom numbering of compound II

Table 11. Assignment of ^{1}H NMR shifts values to compound II

Position	$^{\delta}$ H	*Multiplicity*	*Coupling constant (J Hz)*
1, 2, 5	1.05-1.16, 1.22-1.56	m, m	-
3, 4	0.82	d	6.6
6	3.79-3.89	m	-
7	3.69	qd	7.0, 2.6
8, 11	2.72	dd	13.4, 9.4
9	1.18	d	7.1
10	4.63	ddt	10.6, 6.9, 3.3
11	3.17	dd	13.4, 3.1
12	4.06-4.20	m	-
13-18	7.09-7.30	m	-

In the spectrum, one can see that the protons located at position 11 have different chemical shift value compared to each other. The difference in shift values is likely because of different stereochemistry at the adjacent carbon. It is believed that the proton in position 11 pointing back is shielded by the proton in position 10, which means that backward-looking hydrogen in 11th position would have a higher shift value than the proton pointing forward. The same augment too stand for the two protons in position 5, but as a result of non-sufficient

separation these peaks come as multiplets in the ppm area 1.05-1.16, 1.22-1.56. Furthermore, the ^{13}C NMR spectrum of **II** shows 17 distinct peaks, a total count of 19 carbons, whereas ^{13}C NMR spectrum of the oxazolidinone starting material count for 13 peaks (13 carbons).

4.2.3 Characterization of Compound III

Pharmacophore-comprising molecule **III** is a new compound and thus no spectroscopic data for this have been published. It will nevertheless have similar characteristics as molecule **II** so the elucidation would be quite alike without the oxazolidinone auxiliary. Each ^{1}H NMR signal are assigned to a proton in position as show in figure 11 and are listed in table 12. The ^{1}H NMR spectrum is shown in appendix **B.6**.

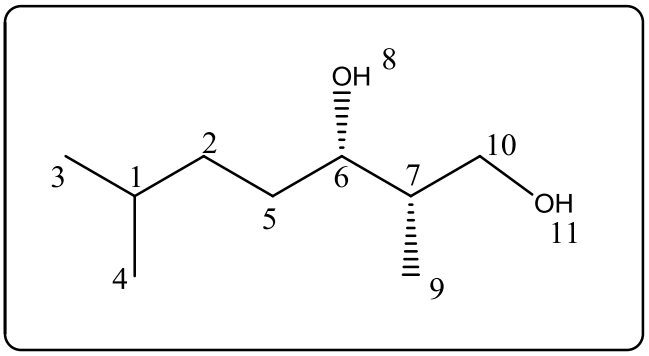

Figure 11. Atom numbering of the diol III

Table 12. Assignment of ^{1}H NMR shifts values to compound III

Position	$^{\delta}$ H	*Multiplicity*	*Coupling constant (J Hz)*
1, 2, 5	1.04-1.20, 1.25-1.60	m, m	-
3, 4, 9	0,87	d	6.6
6	3.76	s	-
7	1.75	d	6.2
8	3.64	d	4.8
10,11	3.32	d	6.5

The characteristic peaks for **III** is a doublet at 3.64 ppm. The carbonyl group is no longer there revealing a new coupling pattern for two hydrogen atoms. The absence of several peaks in the aromatic area both in ^{1}H NMR and ^{13}C NMR proves that there is no unreacted **II** in the sample. Another evidence for effective cleavage is the presence of two protons which according to COSY does not connect with any other protons; these signals can be assigned to hydrogen from the hydroxyl-groups. In addition, the hydrogen from the stereogenic center connected to the methylene group has moved further upfield to 1.75 ppm. This is consistent

with the CH-group is now positioned next to a less strongly electron-withdrawing group, CH_2 versus a carbonyl group.

4.2.4 Characterization of Compound IVa

Both ^{1}H NMR- and ^{13}C NMR spectrum of **IVa** showed similar pattern and expected number of peaks compared to the starting material (6-((tert-butyldimethylsilyl)oxy)naphthalen-2-yl)methanol. The only difference is the signal from the CH_2-group linked to bromine in the product and to hydroxyl in the starting material. Signal/peak from the fraction has moved upfield, in both ^{1}H NMR and ^{13}C NMR in harmony with the CH_2-group vicinal to the more electron-withdrawing bromine compared to the hydroxyl group. The different shift values are assigned to each position, as shown in figure 12, in table 13. The ^{1}H NMR spectrum is shown in appendix **B.9**.

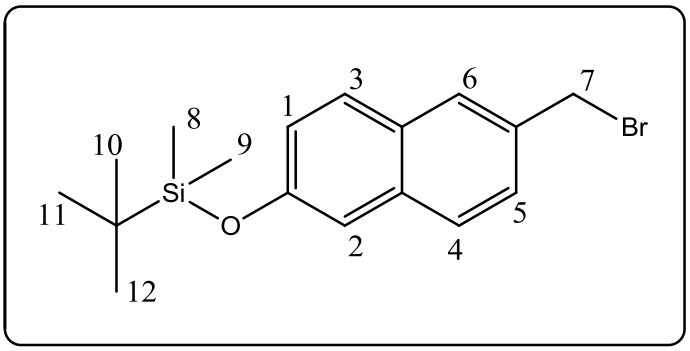

Figure 12. Atom numbering of compound IVa

Table 13. Assignment of ^{1}H NMR shifts values to compound Iva

Position	$^{\delta}$ H	*Multiplicity*	*Coupling constant (J Hz)*
1	7.09	dd	8.8, 2.4
2, 3, 6	7.68-7.76	m	-
4	7.18	d	2.3
5	7.45	dd	8.5, 1.8
7	4.66	s	-
8, 9	0.25	s	-
10-12	1.02	s	-

4.2.5 Characterization of Compound IVb

Complex **IVb** is a quite reactive and unstable when exposed to water and acidic solvents, therefore characterization have been challenging. However, similar splitting patterns have been observed in the starting material and complex **IVa**, which makes the elucidation

possible. The different shift values are assigned to each position, as shown in figure 13, in table 14. The ^{1}H NMR spectrum is shown in appendix **B.11**, and ^{13}C NMR spectrum in appendix **B.13**.

First detected by ^{1}H NMR, where the solvent used was $CDCL_3$-d (later found to be contaminated with water), demonstrated no signals of the mesylate moiety returning a NMR spectrum similar to the starting material. For securing a good result, ^{1}H NMR of the complex was taken with another batch of $CDCl_3$-d, however the result as same as before; nor did ^{13}C NMR spectrum show any additional peaks. Subsequently, DMSO- d_6 was used. ^{1}H NMR obtained through DMSO- d_6 resulted in an additional signal for one proton. It is possible that the additional peak is from one of the protons on methylene located on the mesylate group. Furthermore, the same spectrum reported as well a signal consistent with the CH_2-groupe being positioned adjacent to a stronger electron-withdrawing group, i.e. mesylate, in contrasted with hydroxyl group. On top, ^{13}C NMR spectrum obtained from DMSO-solution, see appendix **B.13**, do show the anticipated number of signals.

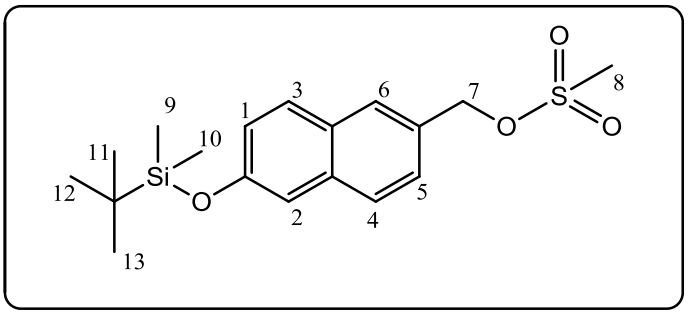

Figure 13. Atom numbering of compound IVb

Table 14. Assignment of ^{1}H NMR chemical shifts values to compound IVb

Position	$^{\delta}$ H	*Multiplicity*	*Coupling constant (J Hz)*
1	7.13	d	8.8
2, 3, 6	7.79-7.91	m	-
4	7.30	s	-
5	7.49	d	8.6
7	4.89	s	-
8	3.32	s	-
9, 10	0.24	s	-
11, 12, 13	0.98	s	-

5 Experimentally

5.1 General Experimental Procedures

All reagents were bought from Sigma-Aldrich and used without further purification unless otherwise noted. Merck 250 µm silica gel 60 F_{254}-plates were used for thin layer chromatography testing (TLC) unless otherwise specified. The TLC analyses were visualized using UV-light (254nm) or developed with potassium permanganate or *p*-anisaldehyde. For column chromatography and filtration trough a pad of silica Merck silica 60 mesh (35-70 µm) is used unless noted otherwise.

^{1}H and ^{13}C NMR were recorded on Bruker DPX 300 and Bruker AVII 400 instrument equipped with a BACS-60 and a BACS-120 automatic sample changer, respectively. All experiments were performed at 25°C.DMSO-d_6 and $CDCl_3$-d were used as NMR solvents and as reference when tetramethylsilane (TMS) standard was unavailable. Proton shifts ($^{\delta}H$) are measured in parts per million (ppm) relative to an internal standard. In $CDCl_3$-d the peaks are given in ppm relative to the TMS calibrated to 0.00 ppm and the $CHCl_3$ residual peak at 7.26 ppm. In DMSO-d_6 the peaks are given relative to the solvent signal at 2.50 ppm.^{1}H NMR signals are reported with number of protons integrated for each peak, peak splitting pattern: s (singlet), d (doublet), t (triplet), m (multiplet) and any potential coupling constants (J), which are given in Hz.

5.2 Methods

5.2.1 Synthesis of 4-methylpentanal (I)

The compound was synthesized according to the procedure by John Xiaoqinag He and coworkers[96], and by the use of Swern conditions described the work by Sepe *et al.*[97]

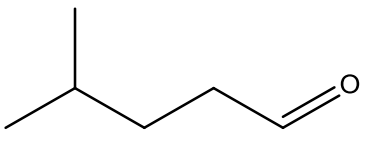

4-methylpentanal
Molecular Weight: 100,16

Synthesis of Compound I via PCC

Procedure 1: A solution of 4-methylpentanal (15.0 g, 147 mmol) in DCM (0.5 L) under nitrogen atmosphere was added PCC (47.50 g, 220 mmol) in portions and the mixture was stirred for 2 hours at room temperature. By addition of PCC, the reaction mixture changed color into black. After 2 hours, the reaction mixture was added Celite, filtered through a pad of silica and concentrated *in vacuo* (mild vacuum and temperature ~30ºC in water bath). Distillation yielded the title compound as colorless oil.

Yield: 3.9 g, 39.05 mmol, 26%

Procedure 2: A solution of 4-methylpentanal (4.0 g, 39.15 mmol) in DCM (133 mL) under nitrogen atmosphere was added PCC (12.67 g, 58.78 mmol) in portions and the mixture was stirred for 24 hours at room temperature. By addition of PCC, the reaction mixture changed color into black. The next day the reaction mixture was added Celite, filtered through a pad of silica and concentrated *in vacuo* (mild vacuum and temperature ~30ºC in water bath). Distillation yielded the title compound as colorless oil.

Yield: 0.415 g, 4.14 mmol, 11%

Procedure 3:: A solution of 4-methylpentanal (4.0 g, 39.15 mmol) in DCM (100 mL) under nitrogen atmosphere was added PCC (12.67 g, 58.78 mmol) in portions and the mixture was stirred for 24 hours at 30ºC with Liebig's cooler attached. By addition of PCC, the reaction mixture changed color into black. The next day the reaction mixture was added Celite, filtered through a pad of silica and concentrated *in vacuo* (mild vacuum and temperature ~30ºC in water bath). Distillation yielded the title compound as colorless oil.

Yield: 0.369 g, 3.68 mmol, 9%

^{1}H NMR (300 MHz, CDCl3): δ 9.75 (t, J = 1.9 Hz, 1H), 2.41 (td, J = 8.0, 1.9 Hz, 2H), 1.60 – 1.48 (m, 3H), 0.89 (d, J = 6.2 Hz, 6H) which are in consensus with published data.[96] The ^{1}H NMR spectrum for this compound is shown in appendix **B.1**.

Synthesis of Compound I trough Swern Oxidation

DMSO (2.22 mL, 31.27 mmol) was added drop wise to a solution of oxalyl chloride (1.47 mL, 17.12 mmol) in DCM (50 mL) at minus 78ºC. After stirring for 5 minutes a solution of 4-methylpentanol (4.0 g, 39.15 mmol) in DCM (10 mL) was added drop wise over 5 minutes. After stirring at minus 78ºC for 40 minutes triethylamine (8.2 mL, 58.79 mmol) was added and the mixture was allowed to reach room temperature over 40 minutes. The mixture was diluted with DCM (50 mL), washed with saturated aqueous NH_4Cl (3x30 mL) and brine (1x20 mL). The organic layer was dried ($MgSO_4$) and distilled. Distillation gave the title compound as colorless oil.

Yield: 1.26 g, 12.58 mmol, 32%

^{1}H NMR (300 MHz, CDCl3): δ 9.77 (t, J = 1.9 Hz, 1H), 2.52 – 2.23 (m, 2H), 1.71 – 1.46 (m, 3H), 0.91 (d, J = 6.2 Hz, 6H) which are in consensus with published data.[96]

5.2.2 Synthesis of 4-(R)-Benzyl-3-(3-(S)-hydroxy-2(S),6-dimethyl-heptanoyl)-oxazolidin-2-one (II)

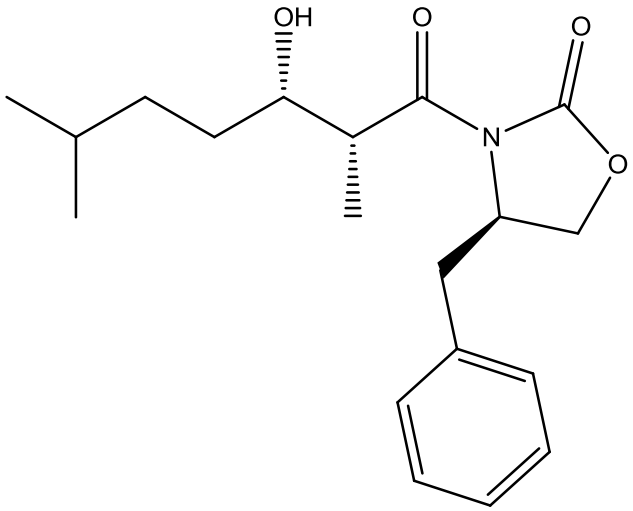

(*R*)-4-benzyl-3-((2*S*,3*S*)-3-hydroxy-2,6-dimethylheptanoyl)oxazolidin-2-one
Molecular Weight: 333,42

To a cooled solution (0ºC) of (R)-4-benzyl-3-propionyloxazolidin-2-one (3.51 g, 16.01 mmol) in dry DCM (30 mL) was added slowly di-n-butylbortriflate (1 M in DCM, 16.5 mL, 16.5 mmol) followed by *N*,*N*-diisopropylethylamine (3.15 mL, 18.08 mmol) (changed color to orange). The reaction mixture was stirred at 0ºC for 30 minutes and cooled to -78ºC. Distilled 4-methylpentanal (1.665 g, 16.62 mmol) was added in portion. The reaction mixture was kept at -78ºC for 30 minutes, allowed to reach room temperature and stirred for 2 hours. A brown

color was observed. The reaction mixture was quenched by addition of 12 mL phosphate buffer (pH ~7.00) and methanol (34 mL). This solution was treated with 32 mL methanol:30 % H_2O_2 (2:1) and stirred for 1 hour at room temperature. Saturated aqueous NH_4Cl was added and the aqueous phase was extracted with DCM (5x10 mL). The organic phase dried ($MgSO_4$), filtered and evaporated under reduced pressure. Flash chromatography on silica gel eluting with hexane:ethyl acetate (80:20) (70:30) (50:50) yielded the title compound as a colorless solid.

Yield: 4.431 g, 13.28 mmol, 83 %

R_f-value: 0.065 in hexane:ethyl acetate (80:20)

Appearance: colorless needle formed crystals

Melting point: 52.1 - 54.6ºC

^{1}H NMR (300 MHz, CDCl3): δ 7.30 – 7.09 (m, 5H), 4.63 (ddt, J = 10.6, 6.9, 3.3 Hz, 1H), 4.20 – 4.06 (m, 2H), 3.89 – 3.79 (m, 1H), 3.69 (qd, J = 7.0, 2.6 Hz, 1H), 3.17 (dd, J = 13.4, 3.1 Hz, 1H), 2.72 (dd, J = 13.4, 9.4 Hz, 2H), 1.56 – 1.22 (m, 4H), 1.18 (d, J = 7.1 Hz, 3H), 1.16 – 1.05 (m, 1H), 0.82 (d, J = 6.6 Hz, 6H). The ^{1}H NMR spectrum of this compound is shown in appendix **B.3**.

^{13}C NMR (75 MHz, CDCl3): δ 177.72 (s), 153.14 (s), 135.15 (s), 129.53 (s), 129.08 (s), 127.54 (s), 71.88 (s), 66.29 (s), 55.21 (s), 42.15 (s), 37.90 (s), 35.20 (s), 31.79 (s), 28.14 (s), 22.70 (s), 22.65 (s), 10.43 (s). The ^{13}C NMR spectrum of this compound is shown in appendix **B.4**.

5.2.3 Recrystallization of 4-(R)-Benzyl-3-(3-(S)-hydroxy-2(S),6-dimethyl-heptanoyl)-oxazolidin-2-one (II)

Charges of 20 mg compound **II** were delivered into eight test tubes. Eight solvents were thereby selected based on their polar properties. Each solvent was dedicated to one test tube and a constant volume of 2 mL of the assigned solvent were added to the each tube. The tubes where the substance did not dissolve were heated and the cylinders where the heat treatment resulted in resolution of compound **II**, were placed at room temperature, refrigerator and freezer (table 15). All the cylinders were monitored daily for 7 days. The most excellent

condition which gave high quality crystals was found to be hexane at room temperature for 24 hours.

Table 15. Conditions for recrystallization of compound II

	Test tube							
	1	2	3	4	5	6	7	8
Solvent	Hexane	Diethyl ether	Dichloromethane	Ethyl acetate	Toluene	Acetone	Methanol	Water
Compound **II**	Insoluble	Soluble	Soluble	Soluble	Soluble	Soluble	Soluble	Insoluble
After heating	Soluble	-	-	-	-	-	-	Soluble
Storage; room temperature	Crystal precipitation (24 hours)*	-	-	-	-	-	-	Soluble
Storage; refrigerator	Crystal precipitation (24 hours)*	-	-	-	-	-	-	Soluble
Storage; freezer	n/a	-	-	-	-	-	-	Crystal precipitation (72 hours)*

In each test tube 20 mg of compound **II** and 2 mL of solvent was added.
* How many hours after heating and storage the crystals were seen

5.2.4 Synthesis of (2S,3S)-2,6-dimethylheptane-1,3-diol (III)

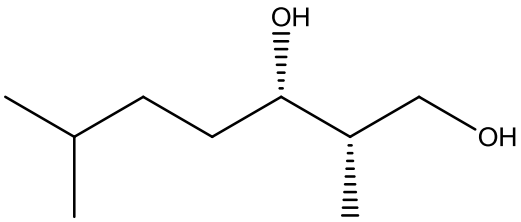

(2*S*,3*S*)-2,6-dimethylheptane-1,3-diol
Molecular Weight: 160,25

Procedure 1: To a cooled (0ºC) solution of 4-(R)-Benzyl-3-(3-(S)-hydroxy-2(S),6-dimethyl-heptanoyl)-oxazolidin-2-one (3.467 g, 10.398 mmol) in diethyl ether (210 mL) water (3.5 mL) followed by $LiBH_4$ (≥ 95%, 0.627 g, 28.79 mmol). The reaction mixture was stirred at 0ºC and then 1 hour at room temperature. Water was added and the water phase was extracted with diethyl ether (3x20 mL) and ethyl acetate (2x10 mL). The organic phase was dried ($MgSO_4$), filtered and evaporated under reduced pressure. Flash chromatography on silica gel

eluting with hexane:ethyl acetate (80:20) (70:30) (50:50) yielded the title compound as a colorless oil.

Yield: 1.093 g, 6.82 mmol, 66%

Procedure 2: To a cooled (0ºC) solution of 4-(R)-Benzyl-3-(3-(S)-hydroxy-2(S),6-dimethyl-heptanoyl)-oxazolidin-2-one (1.87 g, 5.608 mmol) in diethyl ether (113 mL) water (1.89 mL) followed by $LiBH_4$ (≥ 95%, 0.339 g, 14.787 mmol). The reaction mixture was stirred at 0ºC and then 2 hour at room temperature. Water was added and the water phase was extracted with diethyl ether (3x10 mL) and ethyl acetate (2x10 mL). The organic phase was dried ($MgSO_4$), filtered and evaporated under reduced pressure. Flash chromatography on silica gel eluting with hexane:ethyl acetate (80:20) (70:30) (50:50) yielded the title compound as a colorless oil.

Yield: 0.733 g, 4.57 mmol, 82%

Procedure 3: To a cooled (0ºC) solution of 4-(R)-Benzyl-3-(3-(S)-hydroxy-2(S),6-dimethyl-heptanoyl)-oxazolidin-2-one (1.87 g, 5.608 mmol) in diethyl ether (113 mL) water (1.89 mL) followed by $LiBH_4$ (≥ 95%, 0.339 g, 14.787 mmol). The reaction mixture was stirred at 0ºC and then 3 hour at room temperature. Water was added and the water phase was extracted with diethyl ether (3x10 mL) and ethyl acetate (2x10 mL). The organic phase was dried ($MgSO_4$), filtered and evaporated under reduced pressure. Flash chromatography on silica gel eluting with hexane:ethyl acetate (80:20) (70:30) (50:50) yielded the title compound as a colorless solid.

Yield: 0,817 g, 5.098 mmol, 91 %

Appearance: colorless needle formed crystals

Melting point: 47.1- 49.9ºC

R_f-value: 0.21 in hexane:ethyl acetate (50:50)

^{1}H NMR (300 MHz, CDCl3): δ 3.76 (s, 1H), 3.64 (d, J = 4.8 Hz, 2H), 3.32 (d, J = 6.5 Hz, 2H), 1.75 (d, J = 6.2 Hz, 1H), 1.60 – 1.25 (m, 4H), 1.20 – 1.04 (m, 1H), 0.87 (d, J = 6.6 Hz,

9H).The ^{1}H NMR spectrum of this compound is shown in appendix **B.6**.

^{13}C NMR (75 MHz, CDCl3): δ 74.58 (s), 66.94 (s), 39.02 (s), 35.50 (s), 31.87 (s), 28.20 (s), 22.70 (s), 10.09 (s).The ^{13}C NMR spectrum of this compound is shown in appendix **B.7**.

5.2.5 Recrystallization of (2S,3S)-2,6-dimethylheptane-1,3-diol (II)

Charges of 20 mg compound **III** were delivered into eight test tubes. Eight solvents were thereby selected based on their polar properties. Each solvent was dedicated to one test tube and a constant volume of 1.5 mL of the assigned solvent was added to the each tube. The tubes where the substance did not dissolve were heated and the cylinders where the heat treatment resulted in resolution of compound **III**, were placed at room temperature, refrigerator and freezer (table 16). All the cylinders were monitored daily for 7 days. The conditions which achieved crystals were found to be hexane in the refrigerator for 5 days and toluene in the freezer for 3 days. Unfortunately they did not have high enough quality for X-ray crystallography.

Table 16. Conditions for recrystallization of compound III

	Test tube							
	1	2	3	4	5	6	7	8
Solvent	Hexane	Diethyl ether	Dichloromethane	Ethyl acetate	Toluene	Acetone	Methanol	Water
Compound **III**	Insoluble	Well soluble	Well soluble	Soluble	Slightly soluble	Well soluble	Soluble	Insoluble
After heating	Soluble	-	-	-	Soluble	-	-	Soluble
Storage; room temperature	Soluble	-	-	-	Soluble	-	-	Soluble
Storage; refrigerator	Crystal precipitation (5 days)*	-	-	-	Soluble	-	-	Soluble
Storage; freezer	n/a	-	-	-	Crystal precipitation (72 hours)*	-	-	Soluble

In each test tube 20 mg of compound **III** and 1.5 mL of solvent was added.
* How much time after heating and storage the crystals were seen

5.2.6 Synthesis of ((6-(bromomethyl)naphthalen-2-yl)oxy)(tert-butyl)dimethylsilane (IVa)

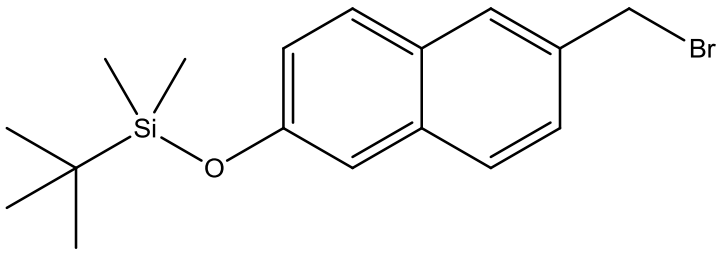

((6-(bromomethyl)naphthalen-2-yl)oxy)(*tert*-butyl)dimethylsilane
Molecular Weight: 351,35

To a cooled solution (0ºC) of (6-((tert-butyldimethylsilyl)oxy)naphthalen-2-yl)methanol (0.525 g, 1.82 mmol) in dry DCM (15 mL) under nitrogen atmosphere was added triphenylphospine (0.715 g, 2.726 mmol). The reaction mixture was stirred at 0ºC for 3 hours before DCM (100 mL) was added. The organic phase was washed with water (25 mL), dried ($MgSO_4$) and concentrated *in vacuo* (mild vacuum and temperature ~30ºC in water bath). Evaporation residue was diluted with hexane (100 mL), filtered through a pad of silica and evaporated under reduced pressure. The title compound appeared as a colorless solid.

Yield: 0.568 g, 1.62 mmol, 89%

R_f-value: 0.86 in hexane:ethyl acetate (70:30)

^{1}H NMR (300 MHz, CDCl3): δ 7.76 – 7.68 (m, 3H), 7.45 (dd, J = 8.5, 1.8 Hz, 1H), 7.18 (d, J = 2.3 Hz, 1H), 7.09 (dd, J = 8.8, 2.4 Hz, 1H), 4.66 (s, 2H), 1.02 (s, 9H), 0.25 (s, 6H).The ^{1}H NMR spectrum of this compound is shown in appendix **B.9**.

^{13}C NMR (75 MHz, CDCl3): δ 154.37 (s), 132.41 (s), 129.56 (s), 128.83 (s), 128.67 (s), 127.86 (s), 127.70 (s), 127.24 (s), 122.83 (s), 115.08 (s), 34.61 (s), 25.86 (s), 18.43 (s), -4.17 (s).The ^{13}C NMR spectrum of this compound is shown in appendix **B.10**.

5.2.7 Synthesis of (6-((tert-butyldimethylsilyl)oxy)naphthalen-2-yl)methyl methanesulfonate (IVb)

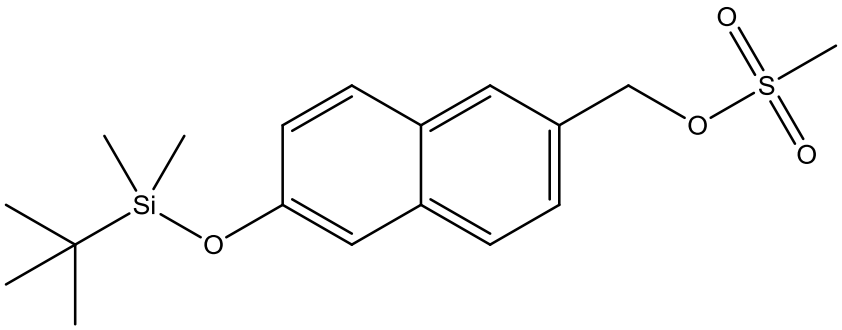

(6-((*tert*-butyldimethylsilyl)oxy)naphthalen-2-yl)methyl methanesulfonate
Molecular Weight: 366,55

Procedure 1: To a cooled solution (0ºC) of (6-((tert-butyldimethylsilyl)oxy)naphthalen-2-yl)methanol (0.100 g, 0,347 mmol) in DCM (3 mL) was added 2,6-Lutidine(0.157 g, 0.17 mL, 1.468 mmol) followed by mesyl chloride (44.4 mg, 0.03 mL, 0.388 mmol). The reaction mixture was stirred at room temperature for 2 hours. The reaction mixture was quenched with water and the aqueous phase was extracted with DCM (2x10 mL). The combined organic phase was washed with 2M HCL and brine, dried ($MgSO_4$) and concentrated *in vacuo* (mild vacuum and temperature ~30ºC in water bath). Evaporation residue was diluted with hexane (10 mL), filtered through a pad of silica and evaporated under reduced pressure. The title compound appeared as a colorless solid.

Yield: 0,062 g, 0.17 mmol, 49%

Procedure 2: To a cooled solution (0ºC) of (6-((tert-butyldimethylsilyl)oxy)naphthalen-2-yl)methanol (0.300 g, 1.041 mmol) in DCM (9 mL) was added 2,6-Lutidine(0.471 g, 0.51 mL, 4.404mmol) followed by mesyl chloride (0,113 g, 0.09 mL, 1.164mmol). The reaction mixture was stirred at room temperature for 6 hours. The reaction mixture was quenched with water and the aqueous phase was extracted with DCM (2x10 mL). The combined organic phase was washed with 2M HCL and brine, dried ($MgSO_4$) and concentrated *in vacuo* (mild vacuum and temperature ~30ºC in water bath). Evaporation residue was diluted with hexane (10 mL), filtered through a pad of silica and evaporated under reduced pressure. The title compound appeared as a colorless solid.

Yield: 0.256 g, 0.69 mmol, 67%

Procedure 3: To a cooled solution (0ºC) of (6-((tert-butyldimethylsilyl)oxy)naphthalen-2-yl)methanol (0.525 g, 1,82 mmol) in DCM (15 mL) was added 2,6-Lutidine(0.838 g, 0.91 mL, 7.82 mmol) followed by mesyl chloride (0,229 g, 0.15 mL, 2.01 mmol). The reaction mixture was stirred at room temperature for 24 hours. The reaction mixture was quenched with water and the aqueous phase was extracted with DCM (2x15 mL). The combined organic phase was washed with 2M HCL and brine, dried ($MgSO_4$) and concentrated *in vacuo* (mild vacuum and temperature ~30ºC in water bath). Evaporation residue was diluted with hexane (20 mL), filtered through a pad of silica and evaporated under reduced pressure. The title compound appeared as a colorless solid.

Yield: 0.467 g, 1.27 mmol, 70%

R_f-value: 0.65 in hexane:ethyl acetate (80:20)

^{1}H NMR (300 MHz, DMSO): δ 7.91 – 7.79 (m, 3H), 7.49 (d, J = 8.6 Hz, 1H), 7.30 (s, 1H), 7.13 (d, J = 8.8 Hz, 1H), 4.89 (s, 2H), 3.32 (s, 1H), 0.98 (s, 6H), 0.24 (s, 3H).The ^{1}H NMR spectrum of this compound is shown in appendix **B.11**.

^{13}C NMR (75 MHz, DMSO): δ 153.45 (s), 133.92 (s), 133.02 (s), 129.58 (s), 128.40 (s), 127.46 (s), 127.25 (s), 127.02 (s), 122.27 (s), 114.49 (s), 46.70 (s), 25.56 (s), 17.98 (s), -4.49 (s).The ^{13}C NMR spectrum of this compound is shown in appendix **B.13**.

5.2.8 Attempted Synthesis of (2S,3S)-1-((6-((tert-butyldimethylsilyl)oxy)naphthalen-2-yl)methoxy)-2,6-dimethylheptan-3-ol (V)

Synthesis of the title compound, considered to provide the same biological response as 22S-HC, has to our knowledge heretofore not been presented in the literature. The synthesis was carried out based on reaction conditions suggested my supervisors Pål Rongved and Marcel Sandberg.

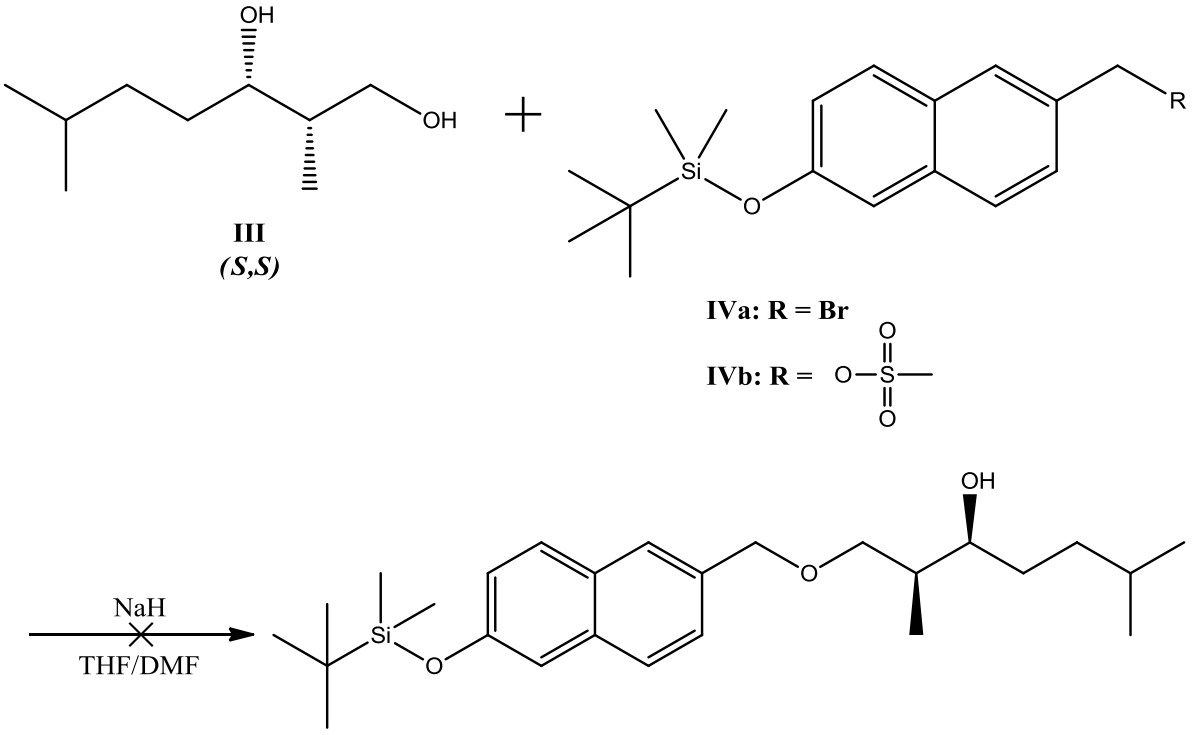

(2*S*,3*S*)-1-((6-((*tert*-butyldimethylsilyl)oxy)naphthalen-2-yl)methoxy)-2,6-dimethylheptan-3-ol
Molecular Weight: 430,70

Attempted synthesis of Compound V Using Compound III and IVa

Procedure 1: A suspension of NaH 60% dispersion in mineral oil (13.3 mg, 0.333mmol) in dry THF (2 mL) and dry DMF (2 mL) was cooled to 0˚C under nitrogen atmosphere before a solution of **III** (50 mg, 0.312 mmol) in dry THF (1 mL) was added drop wise. The reaction mixture was stirred at 0˚C for 30 minutes before a solution of **IVa** (98 mg, 0.280mmol) in dry THF (1 mL) was added. The cooling bath was removed and the reaction mixture was stirred for 24 hours. Saturated NH_4Cl (10 mL) was added, the mixture was extracted with ethyl acetate (5x10 mL), dried ($MgSO_4$), filtered and evaporated under reduced pressure. The product was attempted purified by column chromatography (5% ethyl acetate in hexane), but no product was isolated. Reaction discarded.

Procedure 2: A suspension of NaH 60% dispersion in mineral oil (13.3 mg, 0.333mmol) in dry THF (2 mL) and dry DMF (2 mL) was cooled to 0˚C under nitrogen atmosphere before a solution of **III** (50 mg, 0.312 mmol) in dry THF (1 mL) was added drop wise. The reaction mixture was stirred at 0˚C for 30 minutes before a solution of **IVa** (98 mg, 0.280 mmol) in dry THF (1 mL) was added. The reaction mixture was then again stirred for 30 minutes before potassium iodide (5.1 mg, 0.0312 mmol) was added. The cooling bath was removed and the

reaction mixture was stirred for 2 hours. Saturated NH_4Cl (10 mL) was added, the mixture was extracted with ethyl acetate (5x10 mL), dried ($MgSO_4$), filtered and evaporated under reduced pressure. Liquid chromatography-mass spectrometry (electrospray) (positive) did not show the mass of the molecule ion. Reaction discarded.

Procedure 3: A suspension of NaH 60% dispersion in mineral oil (13.3 mg, 0.333 mmol) in dry THF (2 mL) and dry DMF (2 mL) was cooled to 0˚C under nitrogen atmosphere before a solution of **III** (50 mg, 0.312 mmol) in dry THF (1 mL) was added drop wise. The reaction mixture was stirred at 0˚C for 30 minutes before a solution of **IVa** (98 mg, 0.280 mmol) in dry THF (1 mL) was added. The cooling bath was removed and the reaction mixture was stirred for 2 hours at 50˚C under reflux. Saturated NH_4Cl (10 mL) was added, the mixture was extracted with ethyl acetate (5x10 mL), dried ($MgSO_4$), filtered and evaporated under reduced pressure. Liquid chromatography-mass spectrometry (electrospray) (positive) did not show the mass of the molecule ion. Reaction discarded.

Attempted synthesis of V Using Compound III and IVb

Procedure 1: To a cooled solution of **III** (43 mg, 0.267 mmol) in dry THF (2 mL) and dry DMF (2 mL) was added an suspension of NaH 60% dispersion in mineral oil (10.8 mg, 0.267 mmol) in dry THF (1 mL) drop wise under nitrogen atmosphere. The reaction mixture was stirred at 0˚C for 30 minutes before a solution of **IVa** (88 mg, 0.240 mmol) in dry THF (1 mL) was added. The cooling bath was removed and the reaction mixture was stirred for 24 hours. Saturated NH_4Cl (10 mL) was added, the mixture was extracted with ethyl acetate (5x10 mL), dried ($MgSO_4$), filtered and evaporated under reduced pressure. Liquid chromatography-mass spectrometry (electrospray) (positive) did not show the mass of the molecule ion. Reaction discarded.

Procedure 2: To a cooled solution of **III** (97 mg, 0.606 mmol) in dry THF (4 mL) and dry DMF (4 mL) was added an suspension of NaH 60% dispersion in mineral oil (24.2 mg, 0.606mmol) in dry THF (3 mL) drop wise under nitrogen atmosphere. The reaction mixture was stirred at 0˚C for 30 minutes before a solution of **IVa** (0.2 g, 0.546 mmol) in dry THF (3 mL) was added. The reaction mixture was stirred 0˚C for 5 hours. Saturated NH_4Cl (10 mL) was added, the mixture was extracted with ethyl acetate (5x10 mL), dried ($MgSO_4$), filtered and concentrated under reduced pressure. Evaporation residue was diluted with hexane (20

mL), filtered through a pad of silica and evaporated under reduced pressure. However, the title compound was not achieved. Reaction discarded.

^{1}H NMR and ^{13}C NMR spectrum shows a product which is unlikely to be the title compound; the spectrum of this compound is shown in appendix **B.15** and **B.16**, respectively.

5.2.9 Synthesis of 4-(bromomethyl)benzenesulfonamide (I-1)

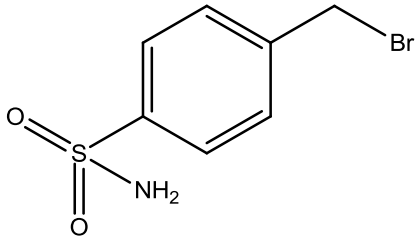

4-(bromomethyl)benzenesulfonamide
Molecular Weight: 250,11

To a solution of 4-(bromomethyl)benzenesulfonyl chloride (1.06 g, 3.93 mmol) in dry DCM (10 mL) under nitrogen atmosphere at 0ºC was added triethylamine (1.10 mL, 7.86 mmol) followed by ammonia (0.5 M in dioxane, 7.86 mL, 3.93 mmol) with stirring. After 1.5 hours at 0ºC 2 M HCL was added to neutralize the reaction mixture, and the agues phase was extracted with DCM (2x15 mL). The combined organic phase was washed with 2 M HCl, brine, dried ($MgSO_4$), filtered and concentrated. The procedure yielded the cruide residue as a pale yellow solid, used without further purification.

Yield: 0.501 g (of the cruide residue)

5.2.10 Attempted synthesis of 4-((((2S,3S)-3-hydroxy-2,6-dimethylheptyl)oxy)methyl)benzensulfonamide (I-2)

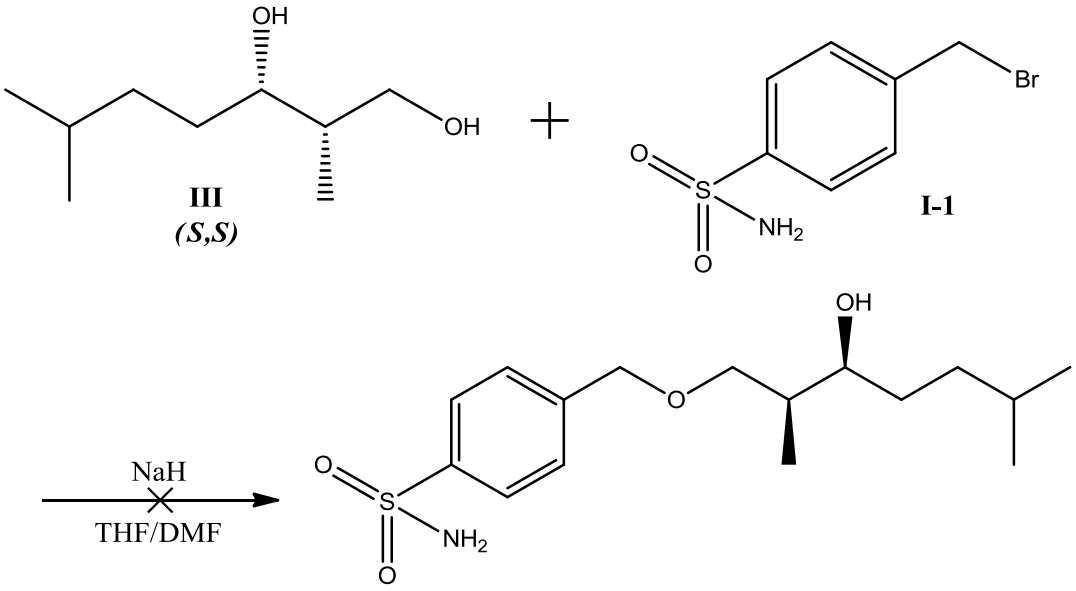

4-((((2*S*,3*S*)-3-hydroxy-2,6-dimethylheptyl)oxy)methyl)benzenesulfonamide
Molecular Weight: 329,45

To a solution of **III** (174 mg, 1.08 mmol) in THF/DMF (2 mL each) under nitrogen atmosphere was added a suspension of NaH 60% dispersion in mineral oil (49.6 mg, 1.24 mmol). After stirring at 0ºC for 20 minutes, composite **I-1** (0.270 g, 1.08 mmol) in THF (2 mL) was added. The reaction mixture was allowed to reach room temperature and stirred for 4 hours. Saturated NH_4Cl was added (15 mL) and the aqueous phase was extracted with diethyl ether (3x10 mL). The combined organic extract was washed with brine, dried ($MgSO_4$), filtered and concentrated. Purification by flash chromatography hexane:ethyl acetate (70:30) a compound as an orange oil which on TLC (30% ethyl acetate in hexane) gave an R_f-value of 0.18. However, ^{1}H NMR shows no single product.

^{1}H NMR and ^{13}C NMR spectrum of the orange compound in $CDCl_3$-d are given in appendix **B.17** and **B.18**, respectively

References

[1]. A. A. Tuah Nik, Cressida Amiel, Samrina Qureshi, Josip Car, Balvinder Kaur and Azeem Majeed: Transtheoretical model for dietary and physical exercise modification in weight loss management for overweight and obese adults. Cochrane Database of Systematic Reviews, (2011).
[2]. WHO: "Obesity and overweight." (2012) <http://www.who.int/mediacentre/factsheets/fs311/en/index.html> [Accessed 1.apr. 2012].
[3]. Bret H. Goodpaster: Measuring body fat distribution and content in humans. Current Opinion in Clinical Nutrition & Metabolic Care **5**,(2002), 481-487.
[4]. S. M. Grundy: Multifactorial causation of obesity: implications for prevention. The American journal of clinical nutrition **67**,(1998), 563S-72S.
[5]. F. Zurlo, K. Larson, C. Bogardus and E. Ravussin: Skeletal muscle metabolism is a major determinant of resting energy expenditure. The Journal of clinical investigation **86**,(1990), 1423-7.
[6]. S. B. Roberts, J. Savage, W. A. Coward, B. Chew and A. Lucas: Energy expenditure and intake in infants born to lean and overweight mothers. The New England journal of medicine **318**,(1988), 461-6.
[7]. E. Ravussin, S. Lillioja, W. C. Knowler, L. Christin, D. Freymond, W. G. Abbott, V. Boyce, B. V. Howard and C. Bogardus: Reduced rate of energy expenditure as a risk factor for body-weight gain. The New England journal of medicine **318**,(1988), 467-72.
[8]. WHO: "Estimated Overweight & Obesity (BMI ≥ 25 kg/m2) Prevalence, Males, Aged 15+, 2010." (2010) <https://apps.who.int/infobase/Comparisons.aspx?l=&NodeVal=WGIE_BMI_5_cd.0704&DO=1&DDLReg=ALL&DDLSex=1&DDLAgeGrp=15-100&DDLYear=2010&DDLMethod=INTMDCTM&DDLCateNum=6&TxtBxCtmNum=20,35,50,65,80&CBLC1=ON&CBLC3=ON&CBLC4=ON&CBLC6=ON&CBLC8=ON&CBLC10=ON&DDLMapsize=800x480&DDLMapLabels=none&DDLTmpRangBK=0&DDLTmpColor=-3342388> [Accessed 12.apr. 2012].
[9]. WHO: "Estimated Overweight & Obesity (BMI ≥ 25 kg/m2) Prevalence, Female, Aged 15+, 2010." (2010) <https://apps.who.int/infobase/Comparisons.aspx?l=&NodeVal=WGIE_BMI_5_cd.0704&DO=1&DDLReg=ALL&DDLSex=2&DDLAgeGrp=15-100&DDLYear=2010&DDLMethod=INTMDCTM&DDLCateNum=6&TxtBxCtmNum=20,35,50,65,80&CBLC1=ON&CBLC3=ON&CBLC4=ON&CBLC6=ON&CBLC8=ON&CBLC10=ON&DDLMapsize=800x480&DDLMapLabels=none&DDLTmpRangBK=0&DDLTmpColor=-3342388> [Accessed 12.apr. 2012].
[10]. J. Orozco Leonardo, Maria Buchleitner Ana, Gabriel Gimenez-Perez, Marta Roqué i Figuls, Bernd Richter and Didac Mauricio: Exercise or exercise and diet for preventing type 2 diabetes mellitus. Cochrane Database of Systematic Reviews 2008),
[11]. A. Golay and J. Ybarra: Link between obesity and type 2 diabetes. Best Practice & Research Clinical Endocrinology & Metabolism **19**,(2005), 649-663.
[12]. E. A. Richter, B. F. Hansen and S. A. Hansen: Glucose-induced insulin resistance of skeletal-muscle glucose transport and uptake. The Biochemical journal **252**,(1988), 733-7.
[13]. Gerald M. Reaven: THE INSULIN RESISTANCE SYNDROME: Definition and Dietary Approaches to Treatment. Annual Review of Nutrition **25**,(2005), 391-406.
[14]. R. C. Turner, R. R. Holman, D. Matthews, T. D. R. Hockaday and J. Peto: Insulin deficiency and insulin resistance interaction in diabetes: Estimation of their relative

contribution by feedback analysis from basal plasma insulin and glucose concentrations. Metabolism **28**,(1979), 1086-1096.
[15]. Ellen E. Blaak: Metabolic fluxes in skeletal muscle in relation to obesity and insulin resistance. Best Practice & Research Clinical Endocrinology & Metabolism **19**,(2005), 391-403.
[16]. Aaron G. Smith and George E. O. Muscat: Skeletal muscle and nuclear hormone receptors: Implications for cardiovascular and metabolic disease. The International Journal of Biochemistry & Cell Biology **37**,(2005), 2047-2063.
[17]. Alan R. Saltiel and C. Ronald Kahn: Insulin signalling and the regulation of glucose and lipid metabolism. Nature **414**,(2001), 799-806.
[18]. Amira Klip and Michel R Pâquet: Glucose Transport and Glucose Transporters in Muscle and Their Metabolic Regulation. Diabetes Care **13**,(1990), 228-243.
[19]. P M Daniel, E R Love and O E Pratt: Insulin-stimulated entry of glucose into muscle in vivo as a major factor in the regulation of blood glucose. The Journal of Physiology **247**,(1975), 273-288.
[20]. R R Henry, L Abrams, S Nikoulina and T P Ciaraldi: Insulin action and glucose metabolism in nondiabetic control and NIDDM subjects. Comparison using human skeletal muscle cell cultures. Diabetes **44**,(1995), 936-946.
[21]. T Santalucía, M Camps, A Castelló, P Muñoz, A Nuel, X Testar, M Palacin and A Zorzano: Developmental regulation of GLUT-1 (erythroid/Hep G2) and GLUT-4 (muscle/fat) glucose transporter expression in rat heart, skeletal muscle, and brown adipose tissue. Endocrinology **130**,(1992), 837-46.
[22]. Iñaki Azpiazu, Jill Manchester, Alexander V. Skurat, Peter J. Roach and John C. Lawrence: Control of glycogen synthesis is shared between glucose transport and glycogen synthase in skeletal muscle fibers. American Journal of Physiology - Endocrinology And Metabolism **278**,(2000), E234-E243.
[23]. Joachim Nielsen, Hans-Christer Holmberg, Henrik D. Schrøder, Bengt Saltin and Niels Ørtenblad: Human skeletal muscle glycogen utilization in exhaustive exercise: role of subcellular localization and fibre type. The Journal of Physiology **589**,(2011), 2871-2885.
[24]. B. D. Hegarty, S. M. Furler, J. Ye, G. J. Cooney and E. W. Kraegen: The role of intramuscular lipid in insulin resistance. Acta Physiologica Scandinavica **178**,(2003), 373-383.
[25]. L. Storlien: Metabolic flexibility. The Proceedings of the Nutrition Society **63**,(2004), 363.
[26]. Jan Glatz, Joost Luiken and Arend Bonen: Involvement of membrane-associated proteins in the acute regulation of cellular fatty acid uptake. Journal of Molecular Neuroscience **16**,(2001), 123-132.
[27]. A. Bonen, C. R. Benton, S. E. Campbell, A. Chabowski, D. C. Clarke, X. X. Han, J. F. C. Glatz and J. J. F. P. Luiken: Plasmalemmal fatty acid transport is regulated in heart and skeletal muscle by contraction, insulin and leptin, and in obesity and diabetes. Acta Physiologica Scandinavica **178**,(2003), 347-356.
[28]. J. F. C. Glatz, F. G. Schaap, B. Binas, A. Bonen, G. J. Van Der Vusse and J. J. F. P. Luiken: Cytoplasmic fatty acid-binding protein facilitates fatty acid utilization by skeletal muscle. Acta Physiologica Scandinavica **178**,(2003), 367-371.
[29]. David E. Kelley, Bret H. Goodpaster and Len Storlien: MUSCLE TRIGLYCERIDE AND INSULIN RESISTANCE. Annual Review of Nutrition **22**,(2002), 325-346.
[30]. David J. Mangelsdorf, Carl Thummel, Miguel Beato, Peter Herrlich, Günther Schütz, Kazuhiko Umesono, Bruce Blumberg, Philippe Kastner, Manuel Mark, Pierre Chambon and Ronald M. Evans: The nuclear receptor superfamily: The second decade. Cell **83**,(1995), 835-839.

[31]. Sevilla D. Detera-Wadleigh and Thomas G. Fanning: Phylogeny of the Steroid Receptor Superfamily. Molecular Phylogenetics and Evolution **3**,(1994), 192-205.
[32]. Jerrold M. Olefsky: Nuclear Receptor Minireview Series. Journal of Biological Chemistry **276**,(2001), 36863-36864.
[33]. Peter A. Edwards, Heidi R. Kast and Andrew M. Anisfeld: BAREing it all: the adoption of LXR and FXR and their roles in lipid homeostasis. Journal of Lipid Research **43**,(2002), 2-12.
[34]. Tadeja Režen: The impact of cholesterol and its metabolites on drug metabolism. Expert Opinion on Drug Metabolism & Toxicology **7**,(2011), 387-398.
[35]. Maaike H. Oosterveer, Aldo Grefhorst, Albert K. Groen and Folkert Kuipers: The liver X receptor: Control of cellular lipid homeostasis and beyond: Implications for drug design. Progress in Lipid Research **49**,(2010), 343-352.
[36]. B. A. Janowski: An oxysterol signalling pathway mediated by the nuclear receptor LXRα. Nature **383**,(1996), 728.
[37]. P J Willy, K Umesono, E S Ong, R M Evans, R A Heyman and D J Mangelsdorf: LXR, a nuclear receptor that defines a distinct retinoid response pathway. Genes & Development **9**,(1995), 1033-1045.
[38]. Peter A. Edwards, Matthew A. Kennedy and Puiying A. Mak: LXRs;: Oxysterol-activated nuclear receptors that regulate genes controlling lipid homeostasis. Vascular Pharmacology **38**,(2002), 249-256.
[39]. Simon W. Beaven and Peter Tontonoz: Nuclear Receptors in Lipid Metabolism: Targeting the Heart of Dyslipidemia. Annual Review of Medicine **57**,(2006), 313-329.
[40]. Anna C. Calkin and Peter Tontonoz: Liver X Receptor Signaling Pathways and Atherosclerosis. Arteriosclerosis, Thrombosis, and Vascular Biology **30**,(2010), 1513-1518.
[41]. C Song, J M Kokontis, R A Hiipakka and S Liao: Ubiquitous receptor: a receptor that modulates gene activation by retinoic acid and thyroid hormone receptors. Proceedings of the National Academy of Sciences **91**,(1994), 10809-10813.
[42]. D Auboeuf, J Rieusset, L Fajas, P Vallier, V Frering, J P Riou, B Staels, J Auwerx, M Laville and H Vidal: Tissue distribution and quantification of the expression of mRNAs of peroxisome proliferator-activated receptors and liver X receptor-alpha in humans: no alteration in adipose tissue of obese and NIDDM patients. Diabetes **46**,(1997), 1319-1327.
[43]. Shawn Williams, Randy K. Bledsoe, Jon L. Collins, Sharon Boggs, Millard H. Lambert, Ann B. Miller, John Moore, David D. McKee, Linda Moore, Jason Nichols, Derek Parks, Mike Watson, Bruce Wisely and Timothy M. Willson: X-ray Crystal Structure of the Liver X Receptor β Ligand Binding Domain. Journal of Biological Chemistry **278**,(2003), 27138-27143.
[44]. Joshua R. Schultz, Hua Tu, Alvin Luk, Joyce J. Repa, Julio C. Medina, Leping Li, Susan Schwendner, Shelley Wang, Martin Thoolen, David J. Mangelsdorf, Kevin D. Lustig and Bei Shan: Role of LXRs in control of lipogenesis. Genes & Development **14**,(2000), 2831-2838.
[45]. Ji-Young Cha and Joyce J. Repa: The Liver X Receptor (LXR) and Hepatic Lipogenesis. Journal of Biological Chemistry **282**,(2007), 743-751.
[46]. Bethany A. Janowski, Patricia J. Willy, Thota Rama Devi, J. R. Falck and David J. Mangelsdorf: An oxysterol signalling pathway mediated by the nuclear receptor LXR[alpha]. Nature **383**,(1996), 728-731.
[47]. Daniel J. Peet, Stephen D. Turley, Wenzhen Ma, Bethany A. Janowski, Jean-Marc A. Lobaccaro, Robert E. Hammer and David J. Mangelsdorf: Cholesterol and Bile Acid Metabolism Are Impaired in Mice Lacking the Nuclear Oxysterol Receptor LXRα. Cell **93**,(1998), 693-704.
[48]. Knut R. Steffensen and Jan-Åke Gustafsson: Putative Metabolic Effects of the Liver X Receptor (LXR). Diabetes **53**,(2004), S36-S42.

[49]. D. J. Peet, S. D. Turley, W. Ma, B. A. Janowski, J. M. Lobaccaro, R. E. Hammer and D. J. Mangelsdorf: Cholesterol and bile acid metabolism are impaired in mice lacking the nuclear oxysterol receptor LXR alpha. Cell **93**,(1998), 693-704.
[50]. S. Alberti, G. Schuster, P. Parini, D. Feltkamp, U. Diczfalusy, M. Rudling, B. Angelin, I. Bjorkhem, S. Pettersson and J. A. Gustafsson: Hepatic cholesterol metabolism and resistance to dietary cholesterol in LXRbeta-deficient mice. The Journal of clinical investigation **107**,(2001), 565-73.
[51]. Cynthia Hong, Michelle N Bradley, Xin Rong, Xuping Wang, Alan Wagner, Victor Grijalva, Lawrence W. Castellani, Jon Salazar, Susan Realegeno, Rima Boyadjian, Alan M. Fogelman, Brian J. Van Lenten, Srinivasa T. Reddy, Aldons J. Lusis, Rajendra K. Tangirala and Peter Tontonoz: LXRα is uniquely required for maximal reverse cholesterol transport and atheroprotection in ApoE-deficient mice. Journal of Lipid Research 2012),
[52]. Noam Zelcer and Peter Tontonoz: Liver X receptors as integrators of metabolic and inflammatory signaling. The Journal of clinical investigation **116**,(2006), 607-614.
[53]. Tomohiro Yoshikawa, Hitoshi Shimano, Michiyo Amemiya-Kudo, Naoya Yahagi, Alyssa H. Hasty, Takashi Matsuzaka, Hiroaki Okazaki, Yoshiaki Tamura, Yoko Iizuka, Ken Ohashi, Jun-Ichi Osuga, Kenji Harada, Takanari Gotoda, Satoshi Kimura, Shun Ishibashi and Nobuhiro Yamada: Identification of Liver X Receptor-Retinoid X Receptor as an Activator of the Sterol Regulatory Element-Binding Protein 1c Gene Promoter. Molecular and Cellular Biology **21**,(2001), 2991-3000.
[54]. J. J. Repa, G. Liang, J. Ou, Y. Bashmakov, J. M. Lobaccaro, I. Shimomura, B. Shan, M. S. Brown, J. L. Goldstein and D. J. Mangelsdorf: Regulation of mouse sterol regulatory element-binding protein-1c gene (SREBP-1c) by oxysterol receptors, LXRalpha and LXRbeta. Genes Dev **14**,(2000), 2819-30.
[55]. Timothy F. Osborne: Sterol Regulatory Element-binding Proteins (SREBPs): Key Regulators of Nutritional Homeostasis and Insulin Action. Journal of Biological Chemistry **275**,(2000), 32379-32382.
[56]. Tomohiro Yoshikawa, Tomohiro Ide, Hitoshi Shimano, Naoya Yahagi, Michiyo Amemiya-Kudo, Takashi Matsuzaka, Shigeru Yatoh, Tetsuya Kitamine, Hiroaki Okazaki, Yoshiaki Tamura, Motohiro Sekiya, Akimitsu Takahashi, Alyssa H. Hasty, Ryuichiro Sato, Hirohito Sone, Jun-ichi Osuga, Shun Ishibashi and Nobuhiro Yamada: Cross-Talk between Peroxisome Proliferator-Activated Receptor (PPAR) α and Liver X Receptor (LXR) in Nutritional Regulation of Fatty Acid Metabolism. I. PPARs Suppress Sterol Regulatory Element Binding Protein-1c Promoter through Inhibition of LXR Signaling. Molecular Endocrinology **17**,(2003), 1240-1254.
[57]. Haiyan Wang, Pierre Maechler, Peter A. Antinozzi, Laura Herrero, Kerstin A. Hagenfeldt-Johansson, Anneli Björklund and Claes B. Wollheim: The Transcription Factor SREBP-1c Is Instrumental in the Development of β-Cell Dysfunction. Journal of Biological Chemistry **278**,(2003), 16622-16629.
[58]. Renaud Dentin, Jean Girard and Catherine Postic: Carbohydrate responsive element binding protein (ChREBP) and sterol regulatory element binding protein-1c (SREBP-1c): two key regulators of glucose metabolism and lipid synthesis in liver. Biochimie **87**,(2005), 81-86.
[59]. Renaud Dentin, Fadila Benhamed, Isabelle Hainault, Véronique Fauveau, Fabienne Foufelle, Jason R.B. Dyck, Jean Girard and Catherine Postic: Liver-Specific Inhibition of ChREBP Improves Hepatic Steatosis and Insulin Resistance in ob/ob Mice. Diabetes **55**,(2006), 2159-2170.
[60]. T. Y. Chang, C. C. Chang, N. Ohgami and Y. Yamauchi: Cholesterol sensing, trafficking, and esterification. Annual review of cell and developmental biology **22**,(2006), 129-57.

[61]. C. Wang, S. Rajput, K. Watabe, D. F. Liao and D. Cao: Acetyl-CoA carboxylase-a as a novel target for cancer therapy. Frontiers in bioscience (Scholar edition) **2**,(2010), 515-26.
[62]. Yanqiao Zhang, Liya Yin and F. Bradley Hillgartner: Thyroid Hormone Stimulates Acetyl-CoA Carboxylase-α Transcription in Hepatocytes by Modulating the Composition of Nuclear Receptor Complexes Bound to a Thyroid Hormone Response Element. Journal of Biological Chemistry **276**,(2001), 974-983.
[63]. Y. Schutz: Concept of fat balance in human obesity revisited with particular reference to de novo lipogenesis. Int J Obes Relat Metab Disord **28 Suppl 4**,(2004), S3-S11.
[64]. Sean B. Joseph, Bryan A. Laffitte, Parthive H. Patel, Michael A. Watson, Karen E. Matsukuma, Robert Walczak, Jon L. Collins, Timothy F. Osborne and Peter Tontonoz: Direct and Indirect Mechanisms for Regulation of Fatty Acid Synthase Gene Expression by Liver X Receptors. Journal of Biological Chemistry **277**,(2002), 11019-11025.
[65]. D. A. Pan, A. J. Hulbert and L. H. Storlien: Dietary fats, membrane phospholipids and obesity. The Journal of nutrition **124**,(1994), 1555-65.
[66]. James M. Ntambi: Regulation of stearoyl-CoA desaturase by polyunsaturated fatty acids and cholesterol. Journal of Lipid Research **40**,(1999), 1549-1558.
[67]. Kiki Chu, Makoto Miyazaki, Weng Chi Man and James M. Ntambi: Stearoyl-Coenzyme A Desaturase 1 Deficiency Protects against Hypertriglyceridemia and Increases Plasma High-Density Lipoprotein Cholesterol Induced by Liver X Receptor Activation. Molecular and Cellular Biology **26**,(2006), 6786-6798.
[68]. Philippe Costet, Yi Luo, Nan Wang and Alan R. Tall: Sterol-dependent Transactivation of theABC1 Promoter by the Liver X Receptor/Retinoid X Receptor. Journal of Biological Chemistry **275**,(2000), 28240-28245.
[69]. Asha Venkateswaran, Joyce J. Repa, Jean-Marc A. Lobaccaro, Amy Bronson, David J. Mangelsdorf and Peter A. Edwards: Human White/Murine ABC8 mRNA Levels Are Highly Induced in Lipid-loaded Macrophages. Journal of Biological Chemistry **275**,(2000), 14700-14707.
[70]. J. J. Repa, K. E. Berge, C. Pomajzl, J. A. Richardson, H. Hobbs and D. J. Mangelsdorf: Regulation of ATP-binding cassette sterol transporters ABCG5 and ABCG8 by the liver X receptors alpha and beta. The Journal of biological chemistry **277**,(2002), 18793-800.
[71]. Puiying A. Mak, Bryan A. Laffitte, Catherine Desrumaux, Sean B. Joseph, Linda K. Curtiss, David J. Mangelsdorf, Peter Tontonoz and Peter A. Edwards: Regulated Expression of the Apolipoprotein E/C-I/C-IV/C-II Gene Cluster in Murine and Human Macrophages. Journal of Biological Chemistry **277**,(2002), 31900-31908.
[72]. Y. Luo and A. R. Tall: Sterol upregulation of human CETP expression in vitro and in transgenic mice by an LXR element. The Journal of clinical investigation **105**,(2000), 513-20.
[73]. Yuan Zhang, Joyce J. Repa, Karine Gauthier and David J. Mangelsdorf: Regulation of Lipoprotein Lipase by the Oxysterol Receptors, LXRα and LXRβ. Journal of Biological Chemistry **276**,(2001), 43018-43024.
[74]. Bryan A. Laffitte, Lily C. Chao, Jing Li, Robert Walczak, Sarah Hummasti, Sean B. Joseph, Antonio Castrillo, Damien C. Wilpitz, David J. Mangelsdorf, Jon L. Collins, Enrique Saez and Peter Tontonoz: Activation of liver X receptor improves glucose tolerance through coordinate regulation of glucose metabolism in liver and adipose tissue. Proceedings of the National Academy of Sciences **100**,(2003), 5419-5424.
[75]. Lene Malerød, Lene K. Juvet, Audun Hanssen-Bauer, Winnie Eskild and Trond Berg: Oxysterol-activated LXRα/RXR induces hSR-BI-promoter activity in hepatoma cells and preadipocytes. Biochemical and Biophysical Research Communications **299**,(2002), 916-923.
[76]. Jong Bae Seo, Hyang Mi Moon, Woo Sik Kim, Yun Sok Lee, Hyun Woo Jeong, Eung Jae Yoo, Jungyeob Ham, Heonjoong Kang, Myoung-Gyu Park, Knut R. Steffensen, Thomas M. Stulnig, Jan-Åke Gustafsson, Sang Dai Park and Jae Bum Kim: Activated Liver X

Receptors Stimulate Adipocyte Differentiation through Induction of Peroxisome Proliferator-Activated Receptor γ Expression. Molecular and Cellular Biology **24**,(2004), 3430-3444.
[77]. K. T. Dalen, S. M. Ulven, K. Bamberg, J. A. Gustafsson and H. I. Nebb: Expression of the insulin-responsive glucose transporter GLUT4 in adipocytes is dependent on liver X receptor alpha. The Journal of biological chemistry **278**,(2003), 48283-91.
[78]. G. Cao, Y. Liang, C. L. Broderick, B. A. Oldham, T. P. Beyer, R. J. Schmidt, Y. Zhang, K. R. Stayrook, C. Suen, K. A. Otto, A. R. Miller, J. Dai, P. Foxworthy, H. Gao, T. P. Ryan, X. C. Jiang, T. P. Burris, P. I. Eacho and G. J. Etgen: Antidiabetic action of a liver x receptor agonist mediated by inhibition of hepatic gluconeogenesis. The Journal of biological chemistry **278**,(2003), 1131-6.
[79]. Thomas M. Stulnig, Knut R. Steffensen, Hui Gao, Mark Reimers, Karin Dahlman-Wright, Gertrud U. Schuster and Jan-Åke Gustafsson: Novel Roles of Liver X Receptors Exposed by Gene Expression Profiling in Liver and Adipose Tissue. Molecular Pharmacology **62**,(2002), 1299-1305.
[80]. Eili T. Kase, Andreas J. Wensaas, Vigdis Aas, Kurt Højlund, Klaus Levin, G. Hege Thoresen, Henning Beck-Nielsen, Arild C. Rustan and Michael Gaster: Skeletal Muscle Lipid Accumulation in Type 2 Diabetes May Involve the Liver X Receptor Pathway. Diabetes **54**,(2005), 1108-1115.
[81]. Nada Y. Kalaany and David J. Mangelsdorf: LXRS AND FXR: The Yin and Yang of Cholesterol and Fat Metabolism. Annual Review of Physiology **68**,(2006), 159-191.
[82]. M. Loffler, M. Bilban, M. Reimers, W. Waldhausl and T. M. Stulnig: Blood glucose-lowering nuclear receptor agonists only partially normalize hepatic gene expression in db/db mice. The Journal of pharmacology and experimental therapeutics **316**,(2006), 797-804.
[83]. S. E. Ross, R. L. Erickson, I. Gerin, P. M. DeRose, L. Bajnok, K. A. Longo, D. E. Misek, R. Kuick, S. M. Hanash, K. B. Atkins, S. M. Andresen, H. I. Nebb, L. Madsen, K. Kristiansen and O. A. MacDougald: Microarray analyses during adipogenesis: understanding the effects of Wnt signaling on adipogenesis and the roles of liver X receptor alpha in adipocyte metabolism. Mol Cell Biol **22**,(2002), 5989-99.
[84]. Sarah E. Ross, Robin L. Erickson, Isabelle Gerin, Paul M. DeRose, Laszlo Bajnok, Kenneth A. Longo, David E. Misek, Rork Kuick, Samir M. Hanash, Kevin B. Atkins, Sissel M. Andresen, Hilde I. Nebb, Lise Madsen, Karsten Kristiansen and Ormond A. MacDougald: Microarray Analyses during Adipogenesis: Understanding the Effects of Wnt Signaling on Adipogenesis and the Roles of Liver X Receptor α in Adipocyte Metabolism. Molecular and Cellular Biology **22**,(2002), 5989-5999.
[85]. Alexander M. Efanov, Sabine Sewing, Krister Bokvist and Jesper Gromada: Liver X Receptor Activation Stimulates Insulin Secretion via Modulation of Glucose and Lipid Metabolism in Pancreatic Beta-Cells. Diabetes **53**,(2004), S75-S78.
[86]. A. Zanchi, A. Chiolero, M. Maillard, J. Nussberger, H. R. Brunner and M. Burnier: Effects of the peroxisomal proliferator-activated receptor-gamma agonist pioglitazone on renal and hormonal responses to salt in healthy men. The Journal of clinical endocrinology and metabolism **89**,(2004), 1140-5.
[87]. Maaike H. Oosterveer, Theo H. van Dijk, Aldo Grefhorst, Vincent W. Bloks, Rick Havinga, Folkert Kuipers and Dirk-Jan Reijngoud: Lxrα Deficiency Hampers the Hepatic Adaptive Response to Fasting in Mice. Journal of Biological Chemistry **283**,(2008), 25437-25445.
[88]. Aldo Grefhorst, Theo H. van Dijk, Anke Hammer, Fjodor H. van der Sluijs, Rick Havinga, Louis M. Havekes, Johannes A. Romijn, Pieter H. Groot, Dirk-Jan Reijngoud and Folkert Kuipers: Differential effects of pharmacological liver X receptor activation on hepatic and peripheral insulin sensitivity in lean and ob/ob mice. American Journal of Physiology - Endocrinology And Metabolism **289**,(2005), E829-E838.

[89]. Eili Tranheim Kase, Bård Andersen, Hilde I. Nebb, Arild C. Rustan and G. Hege Thoresen: 22-Hydroxycholesterols regulate lipid metabolism differently than T0901317 in human myotubes. Biochimica et Biophysica Acta (BBA) - Molecular and Cell Biology of Lipids **1761**,(2006), 1515-1522.
[90]. Stefan Svensson, Tove Ostberg, Micael Jacobsson, Carina Norstrom, Karin Stefansson, Dan Hallen, Isabel Climent Johansson, Kristina Zachrisson, Derek Ogg and Lena Jendeberg: Crystal structure of the heterodimeric complex of LXR[alpha] and RXR[beta] ligand-binding domains in a fully agonistic conformation. EMBO J **22**,(2003), 4625-4633.
[91]. Bethany A. Janowski, Michael J. Grogan, Stacey A. Jones, G. Bruce Wisely, Steven A. Kliewer, Elias J. Corey and David J. Mangelsdorf: Structural requirements of ligands for the oxysterol liver X receptors LXRα and LXRβ. Proceedings of the National Academy of Sciences **96**,(1999), 266-271.
[92]. Nina Pettersen Hessvik, Siril Skaret Bakke, Robert Smith, Aina Westrheim Ravna, Ingebrigt Sylte, Arild Christian Rustan, G. Hege Thoresen and Eili Tranheim Kase: The liver X receptor modulator 22(S)-hydroxycholesterol exerts cell-type specific effects on lipid and glucose metabolism. The Journal of Steroid Biochemistry and Molecular Biology **128**,(2012), 154-164.
[93]. Xiaolin Li, Vince Yeh and Valentina Molteni: Liver X receptor modulators: a review of recently patented compounds (2007 – 2009). Expert Opinion on Therapeutic Patents **20**,(2010), 535-562.
[94]. Marc W. Andersen, Bernhard Hildebrandt and Reinhard W. Hoffmann: Efficient Stereoselective Total Synthesis of Denticulatins A and B. Angewandte Chemie International Edition in English **30**,(1991), 97-99.
[95]. D. A. Evans, J. Bartroli and T. L. Shih: Enantioselective aldol condensations. 2. Erythro-selective chiral aldol condensations via boron enolates. Journal of the American Chemical Society **103**,(1981), 2127-2129.
[96]. John Xiaoqinag He, Vincent Patrick Rocco, John Mehnert Schaus, Fionna Mitchell Martin, William Martin Owton and David Edward Tupper: Preparation of piperazine derivatives of azepine, oxazepine and thiazepine as dopamine D2 antagonists. WO2005026177A1, 2005.
[97]. Valentina Sepe, Maria Valeria D'Auria, Giuseppe Bifulco, Raffaella Ummarino and Angela Zampella: Concise synthesis of AHMHA unit in perthamide C. Structural and stereochemical revision of perthamide C. Tetrahedron **66**,(2010), 7520-7526.
[98]. Frederick A. Luzzio: The oxidation of alcohols by modified oxochromium(VI)-amine reagents. Org. React. (Hoboken, NJ, U. S.) **53**,(1998), No pp. given.
[99]. Nussbaum Franz von, Sonja Anlauf, Christoph Freiberg, Jordi Benet-Buchholz, Jens Schamberger, Thomas Henkel, Guido Schiffer and Dieter Haebich: Total synthesis and initial structure-activity relationships of longicatenamycin A. ChemMedChem **3**,(2008), 619-626.
[100]. Sun Shine Yuan and Alfred M. Ajami: On the catalytic amidocarbonylation of substituted allylic alcohols. 20. J. Organomet. Chem. **302**,(1986), 255-8.
[101]. Nestor Carballeira, Janice E. Thompson, Eser Ayanoglu and Carl Djerassi: Biosynthetic studies of marine lipids. 5. The biosynthesis of long-chain branched fatty acids in marine sponges. J. Org. Chem. **51**,(1986), 2751-6.
[102]. Maryadele J. O'Neil: The Merck index: an encyclopedia of chemicals, drugs, and biologicals. 2008),
[103]. Gabriel Tojo and Marcos Fernández: Oxidation of alcohols to aldehydes and ketones: a guide to current common practice, Springer, Place, 2006. s.
[104]. Ryosuke Tsutsumi, Takefumi Kuranaga, Jeffrey L. C. Wright, Daniel G. Baden, Emiko Ito, Masayuki Satake and Kazuo Tachibana: An improved synthesis of (−)-brevisamide, a marine monocyclic ether amide of dinoflagellate origin. Tetrahedron **66**,(2010), 6775-6782.

[105]. Nieves Fresno, Ruth Pérez-Fernández, Pilar Goya, Ma Luisa Jimeno, Ibón Alkorta, José Elguero, Laura Menéndez-Taboada and Santiago García-Granda: Oxazolidinone cross-alkylation during Evans' asymmetric alkylation reaction. Tetrahedron **67**,(2011), 9104-9111.
[106]. Zhihua Ma, Yonghua Zhao, Nan Jiang, Xianglin Jin and Jianbo Wang: Stereoselective nucleophilic addition of chiral lithium enolates to (N-tosyl)imines: enantioselective synthesis of β-aryl-β-amino acid derivatives. Tetrahedron Letters **43**,(2002), 3209-3212.
[107]. Kevin Burgess and Michael J. Ohlmeyer: Diastereocontrol in rhodium-catalyzed hydroboration of chiral acyclic allylic alcohol derivatives. Tetrahedron Letters **30**,(1989), 395-398.
[108]. Guy Windey, Karl Seper and John H. Yamamoto: Chemoselective and Stereoselective Reductions with Modified Borohydride Reagents. ChemInform **34**,(2003), no-no.
[109]. Kenso Soai and Atsuhiro Ookawa: Mixed solvents containing methanol as useful reaction media for unique chemoselective reductions within lithium borohydride. The Journal of Organic Chemistry **51**,(1986), 4000-4005.
[110]. Michael T. Crimmins, Kyle A. Emmitte and Jason D. Katz: Diastereoselective Alkylations of Oxazolidinone Glycolates: A Useful Extension of the Evans Asymmetric Alkylation. Organic Letters **2**,(2000), 2165-2167.
[111]. Jean-Yves Le Brazidec, Charles A. Gilson and Marcus F. Boehm: Stereoselective Synthesis of the C1−C13 Fragment of 2,3-Dihydrodorrigocin A. The Journal of Organic Chemistry **70**,(2005), 8212-8215.
[112]. Jie Jack Li: Name Reactions: A Collection of Detailed Reaction Mechanisms, Springer-Verlag Berlin Heidelberg, Place, 2006. s. 10-11.
[113]. Maria Carla Marcotullio, Valerio Campagna, Silvia Sternativo, Ferdinando Costantino and Massimo Curini: A New, Simple Synthesis of N-Tosyl Pyrrolidines and Piperidines. Synthesis **2006**,(2006), 2760,2766.
[114]. Stephen Caddick, Jonathan D. Wilden and Duncan B. Judd: Direct Synthesis of Sulfonamides and Activated Sulfonate Esters from Sulfonic Acids. Journal of the American Chemical Society **126**,(2004), 1024-1025.
[115]. Michael B. Smith and Jerry March: March's advanced organic chemistry: reactions, mechanisms, and structure, Wiley, Place, 2001. s. 576-577.
[116]. Robert M. Silverstein, Francis X. Webster and David J. Kiemle: Spectrometric identification of organic compounds, Wiley, Place, 2005. s.

A. Spectra of Starting Material

A.1 ^{1}H NMR-spectrum of (R)-4-benzyl-3-propionyloxazolidin-2-one

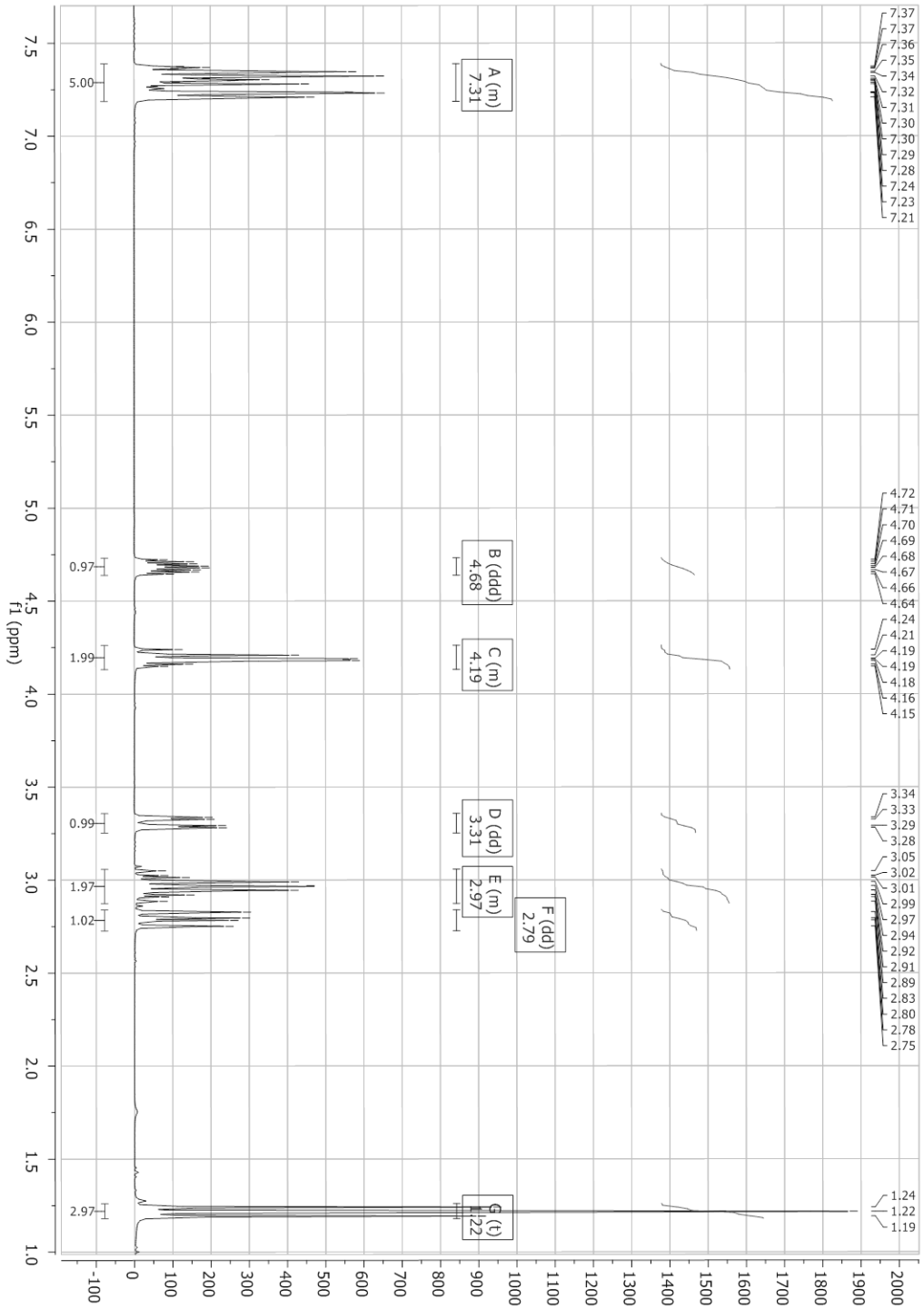

A.2 ^{13}C NMR-spectrum of (R)-4-benzyl-3-propionyloxazolidin-2-one

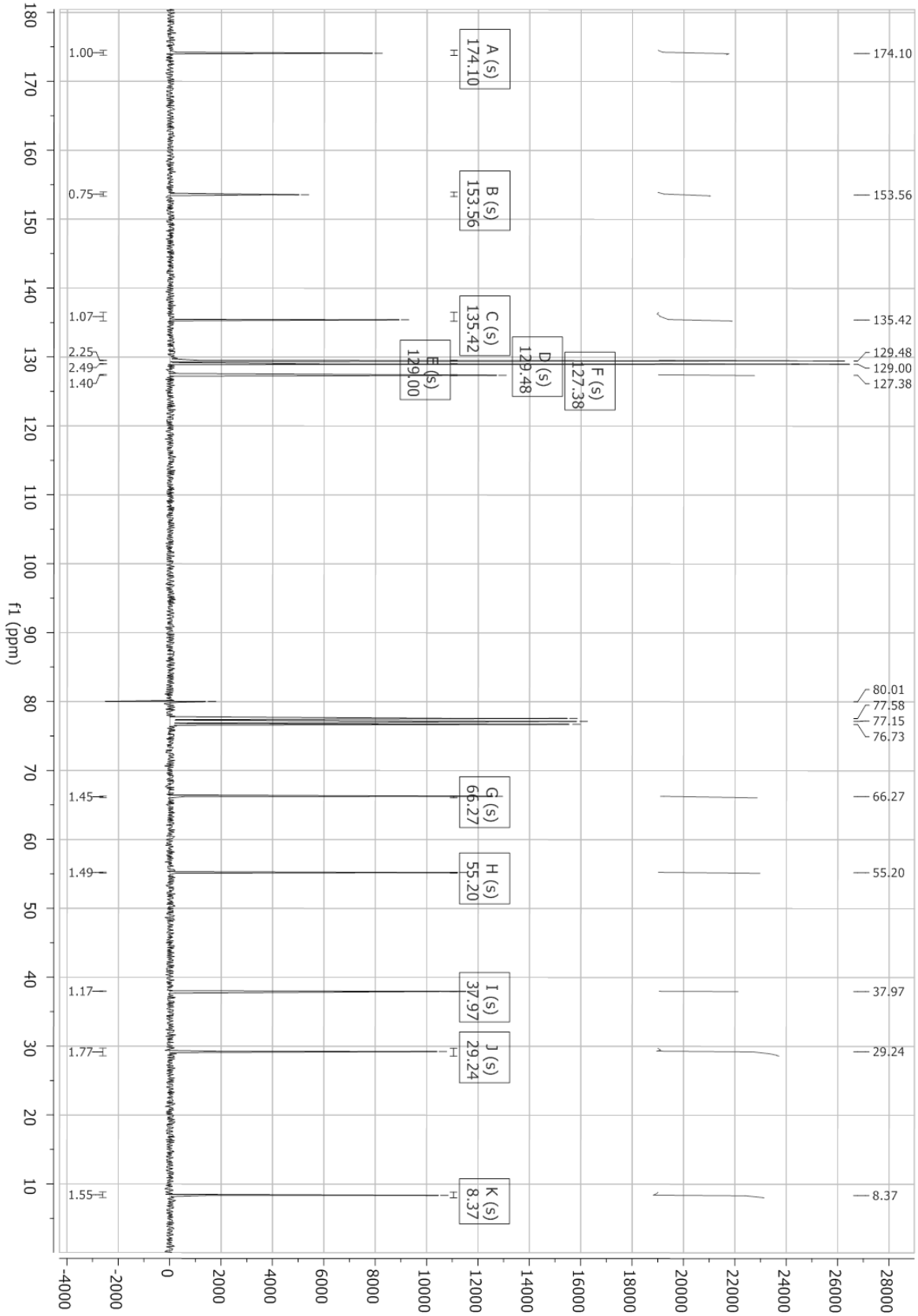

A.3 ^{1}H NMR-spectrum of (6-((tert-butyldimethylsilyl)oxy)naphthalen-2-yl)methanol

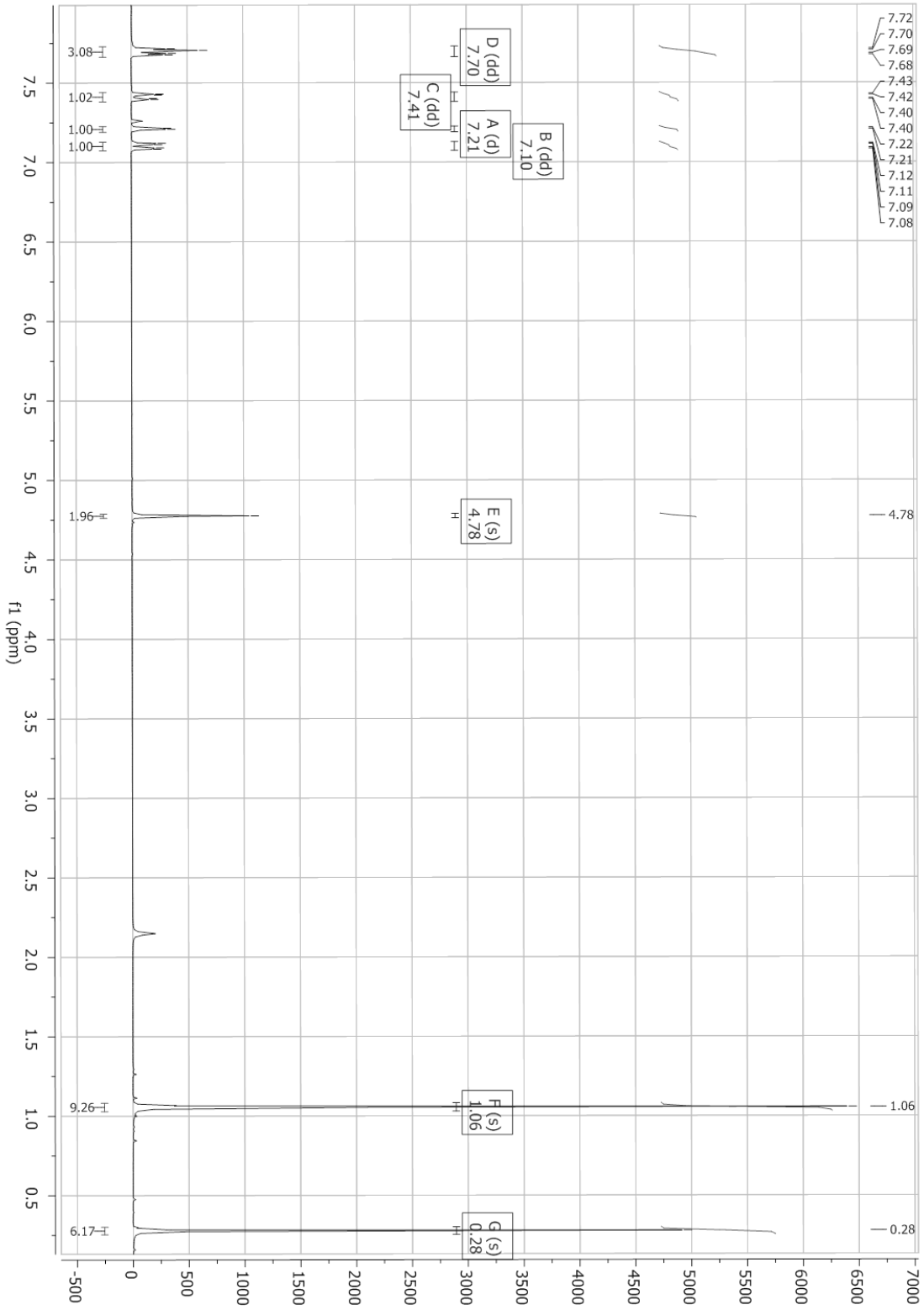

A.4 ^{13}C NMR-spectrum of (6-((tert-butyldimethylsilyl)oxy)naphthalen-2-yl)methanol

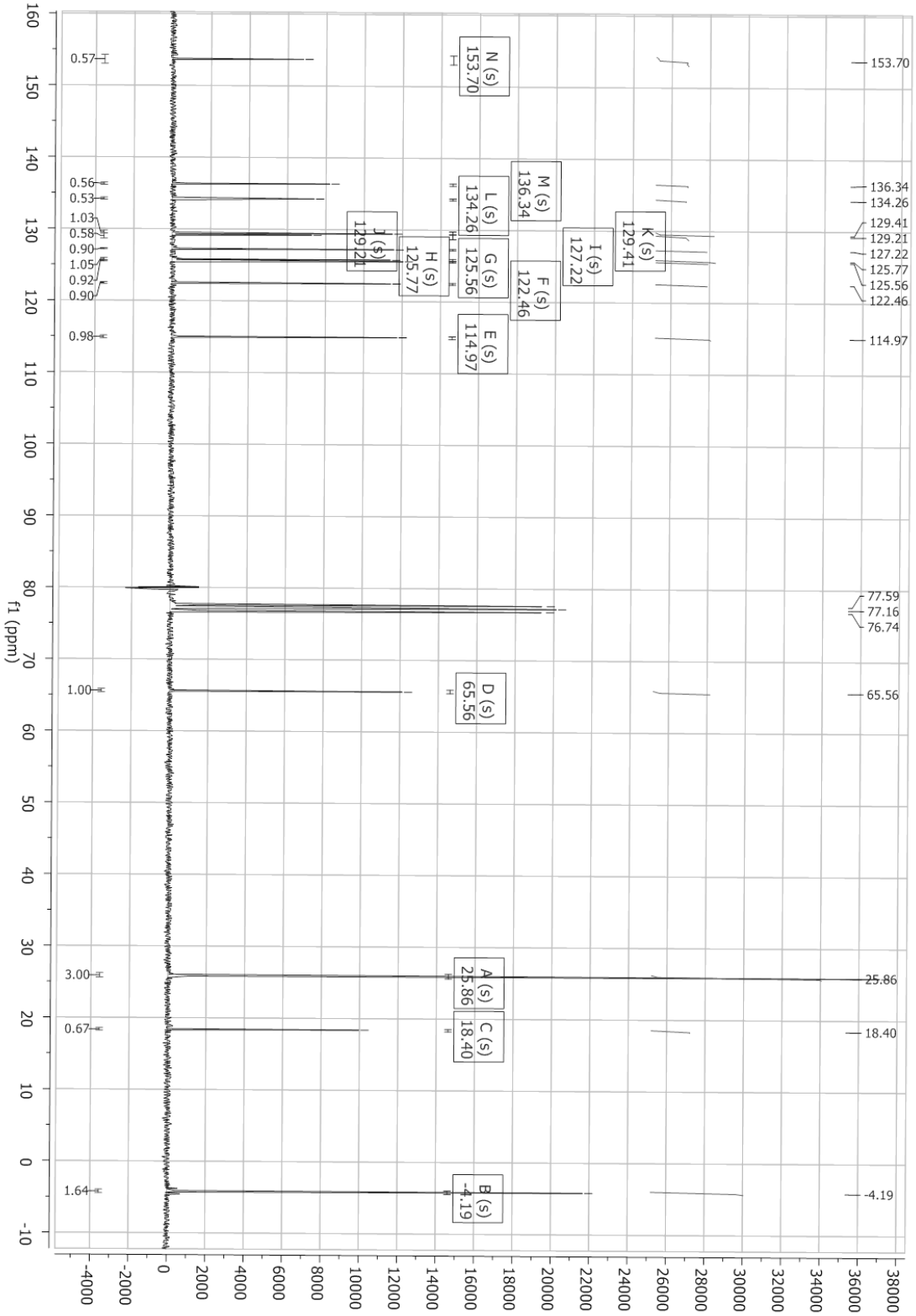

B. Spectra of Compounds

B.1 ^{1}H NMR-spectrum of 4-methylpentanal (I)

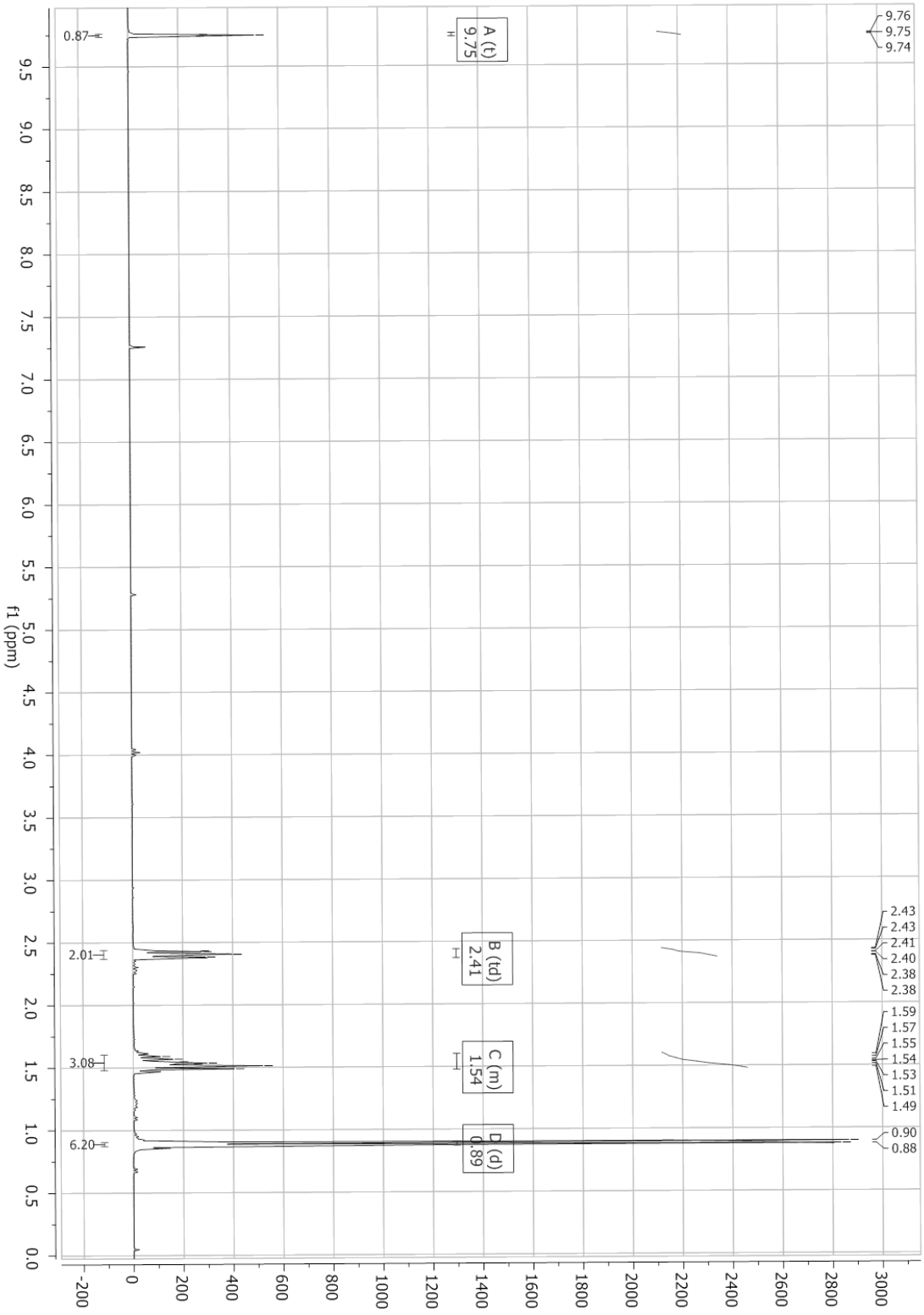

B.2 ^{1}H NMR-spectrum of 4-methylpentanal (I) after 6 weeks in freezer

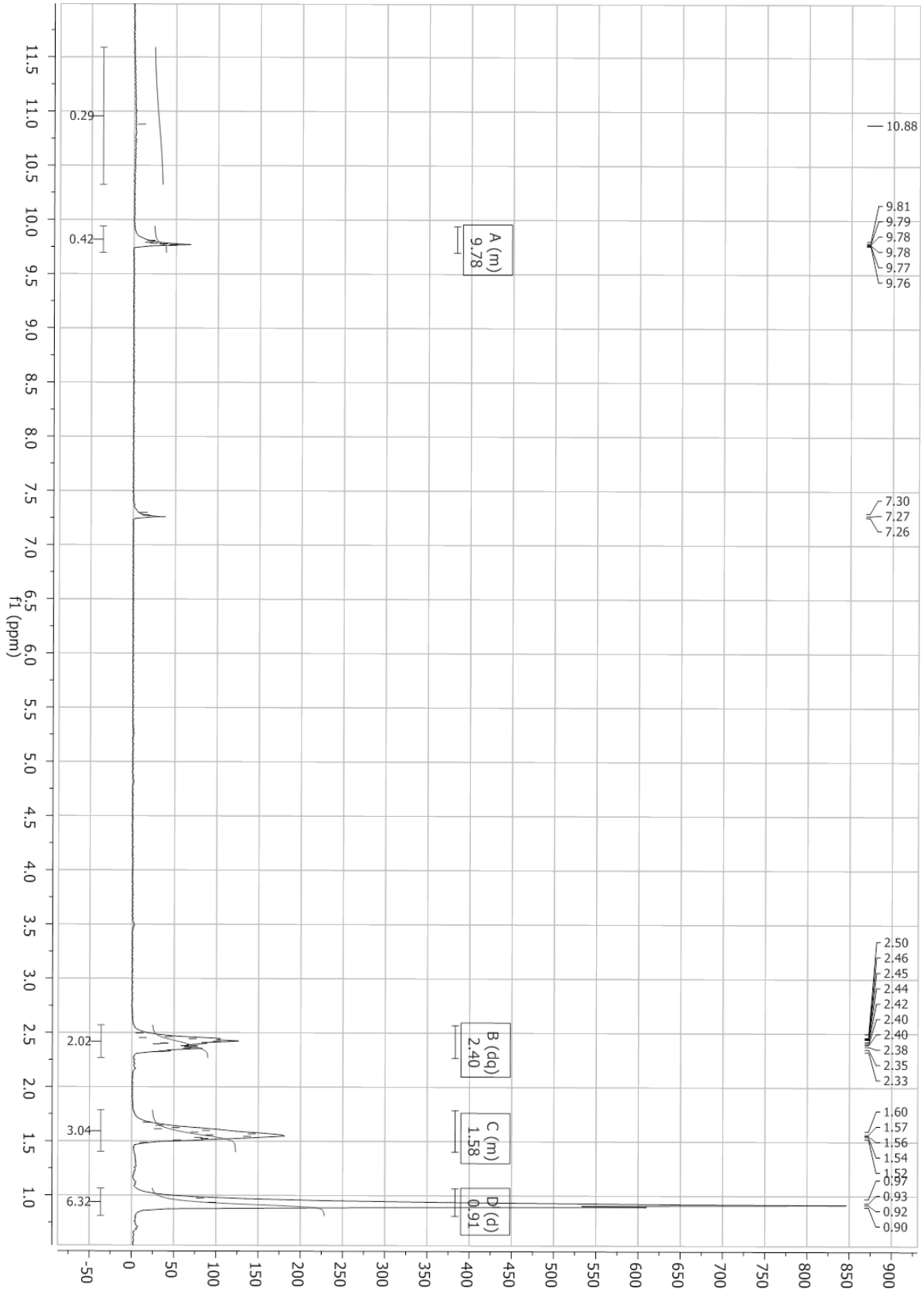

B.3 ^{1}H NMR-spectrum of 4-(R)-Benzyl-3-(3-(S)-hydroxy-2(S),6-dimethyl-heptanoyl)-oxazolidin-2-one (II)

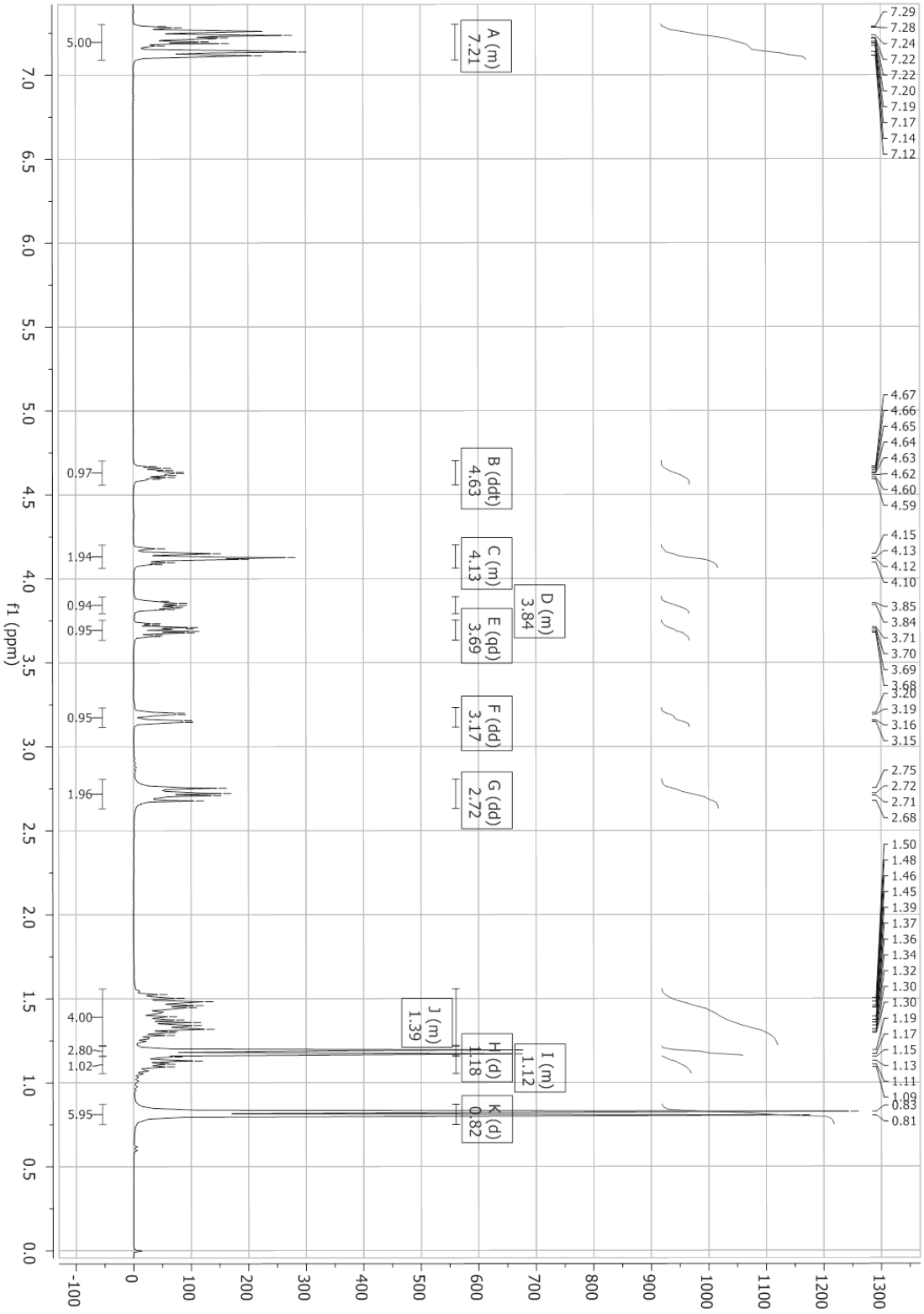

B.4 ^{13}C NMR-spectrum of 4-(R)-Benzyl-3-(3-(S)-hydroxy-2(S),6-dimethyl-heptanoyl)-oxazolidin-2-one (II)

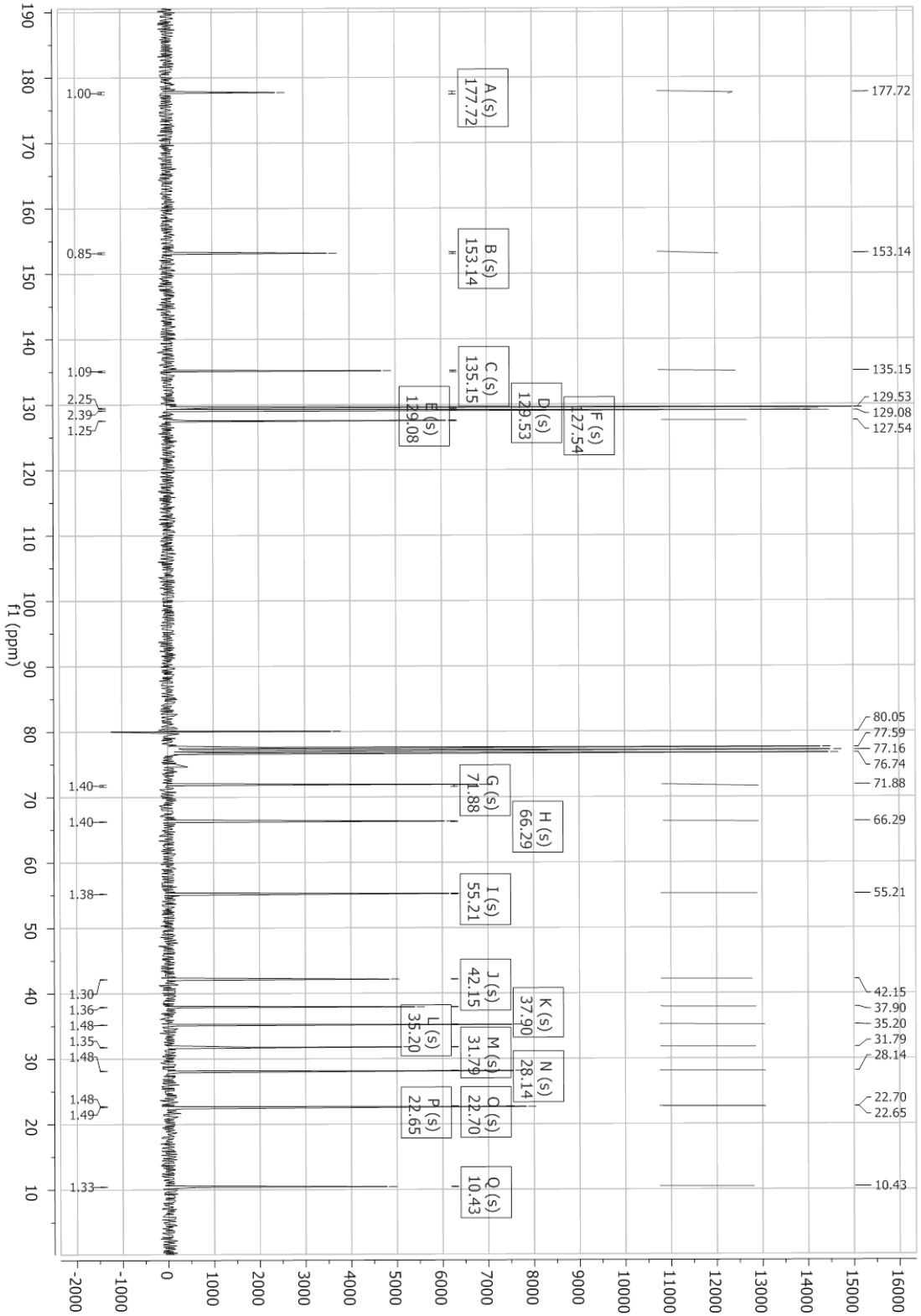

B.5 COSY NMR-spectrum of 4-(R)-Benzyl-3-(3-(S)-hydroxy-2(S),6-dimethyl-heptanoyl)-oxazolidin-2-one (II)

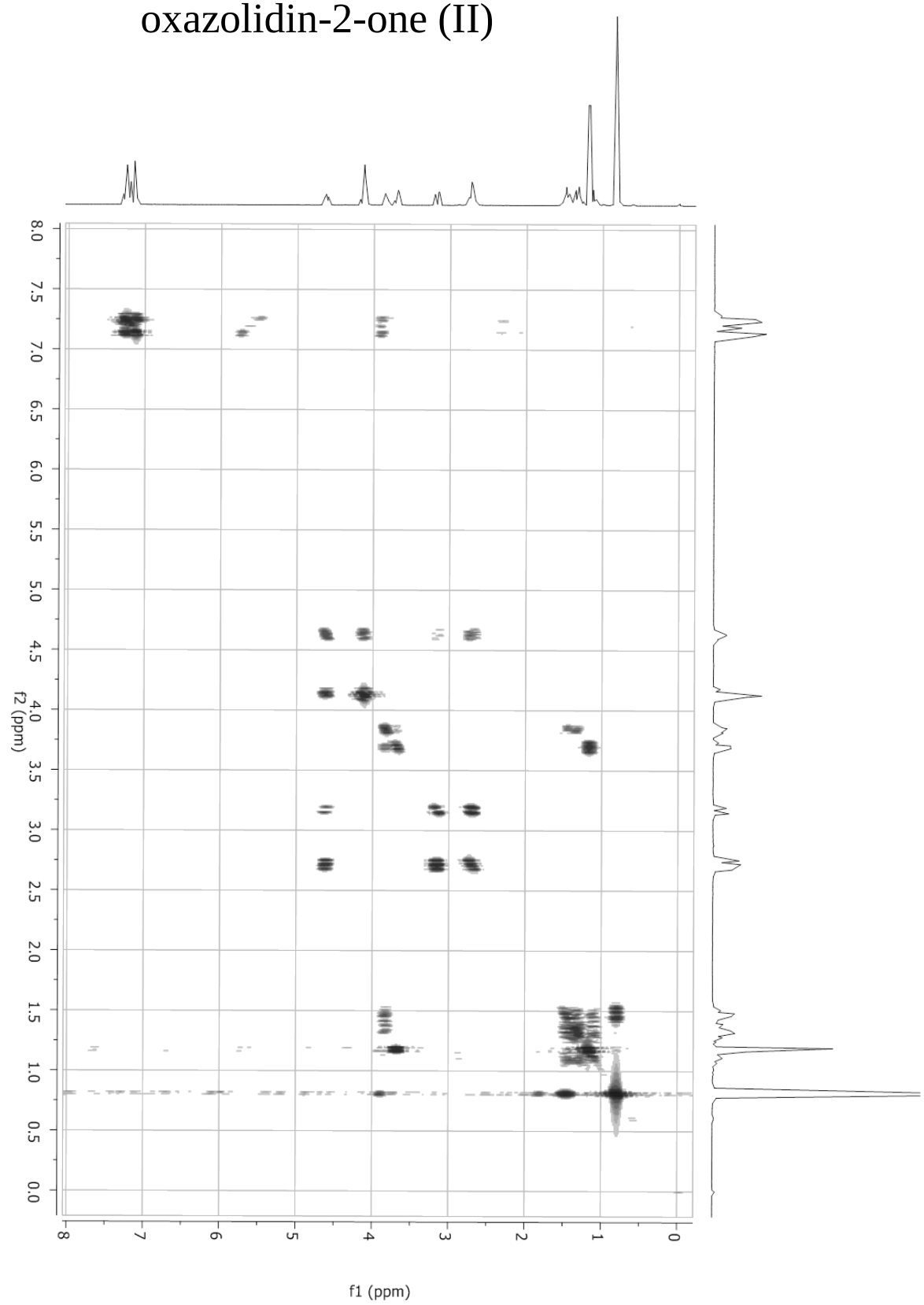

B.6 ^{1}H NMR-spectrum of (2S,3S)-2,6-dimethylheptane-1,3-diol (III)

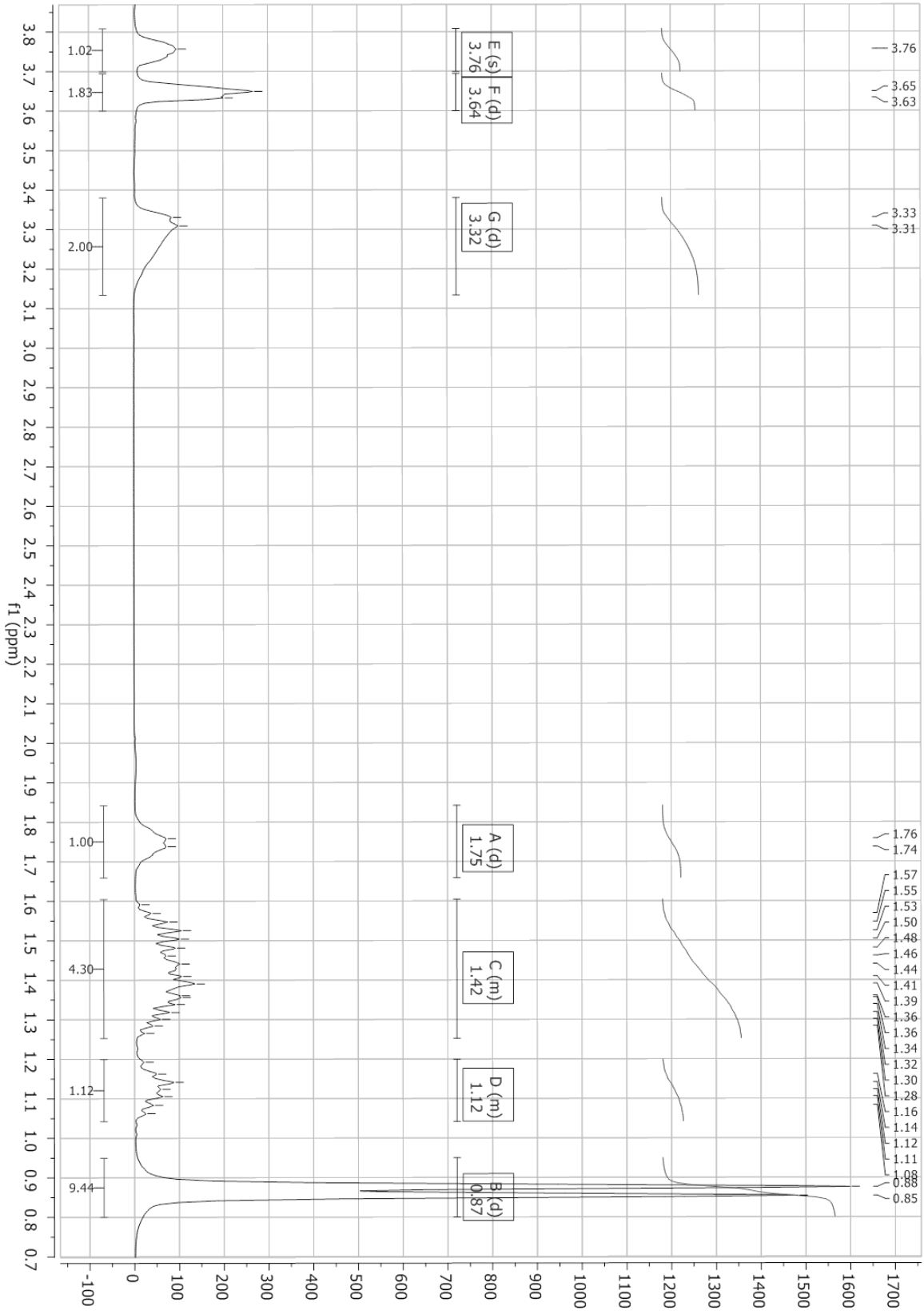

B.7 ^{13}C NMR-spectrum of (2S,3S)-2,6-dimethylheptane-1,3-diol (III)

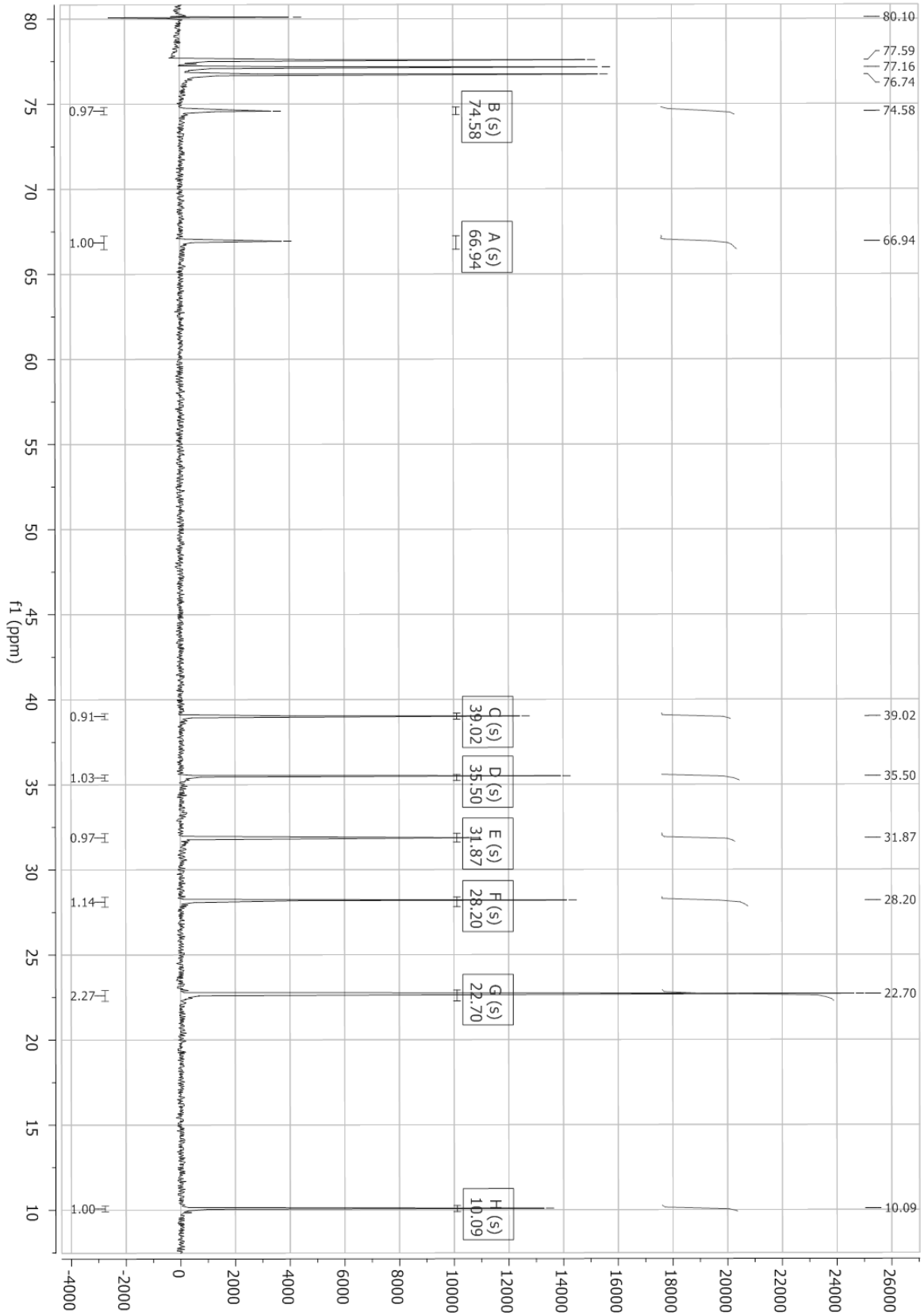

B.8 COSY NMR-spectrum of (2S,3S)-2,6-dimethylheptane-1,3-diol (III)

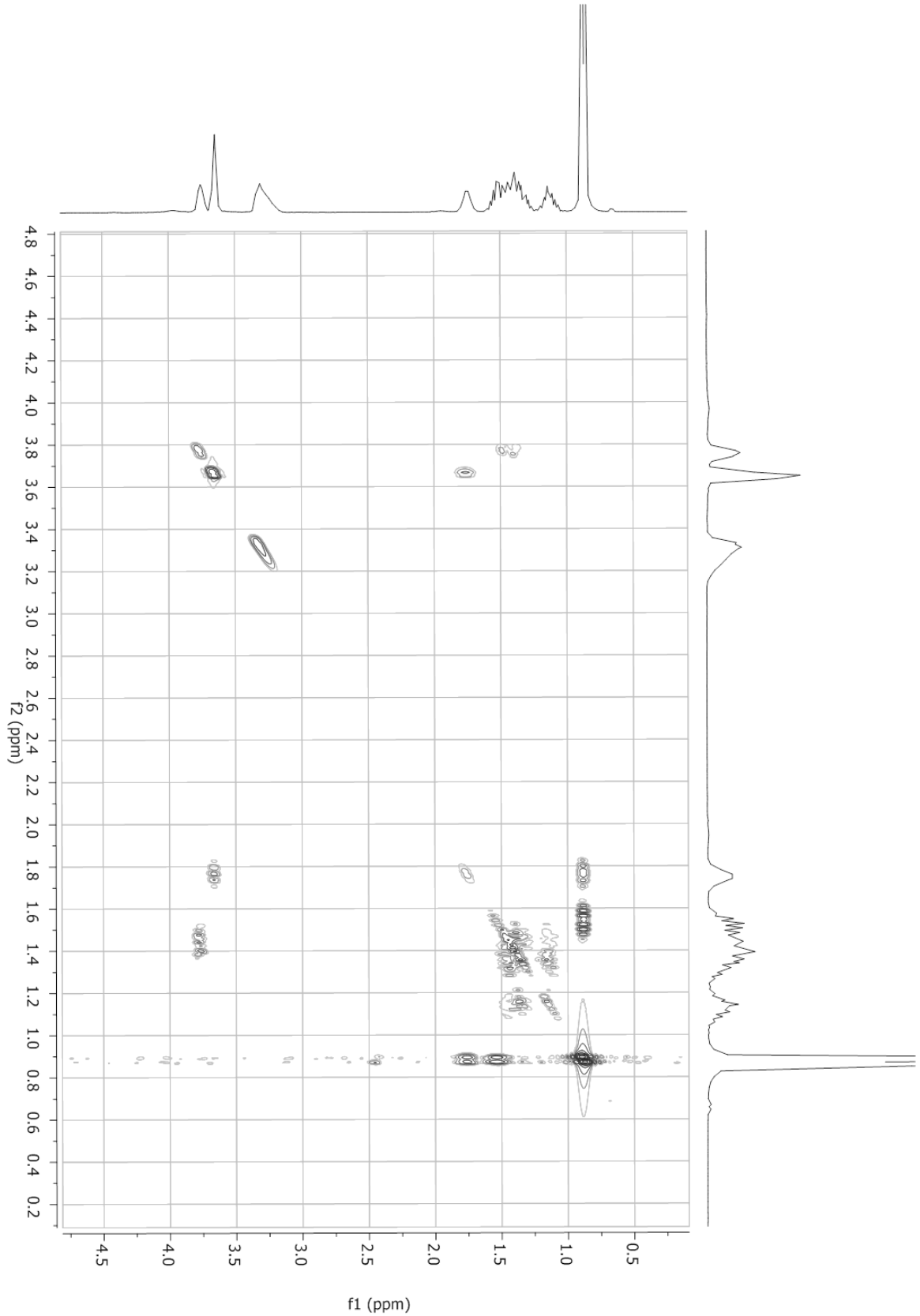

B.9 ^{1}H NMR-spectrum of ((6-(bromomethyl)naphthalen-2-yl)oxy)(tert-butyl)dimethylsilane (IVa)

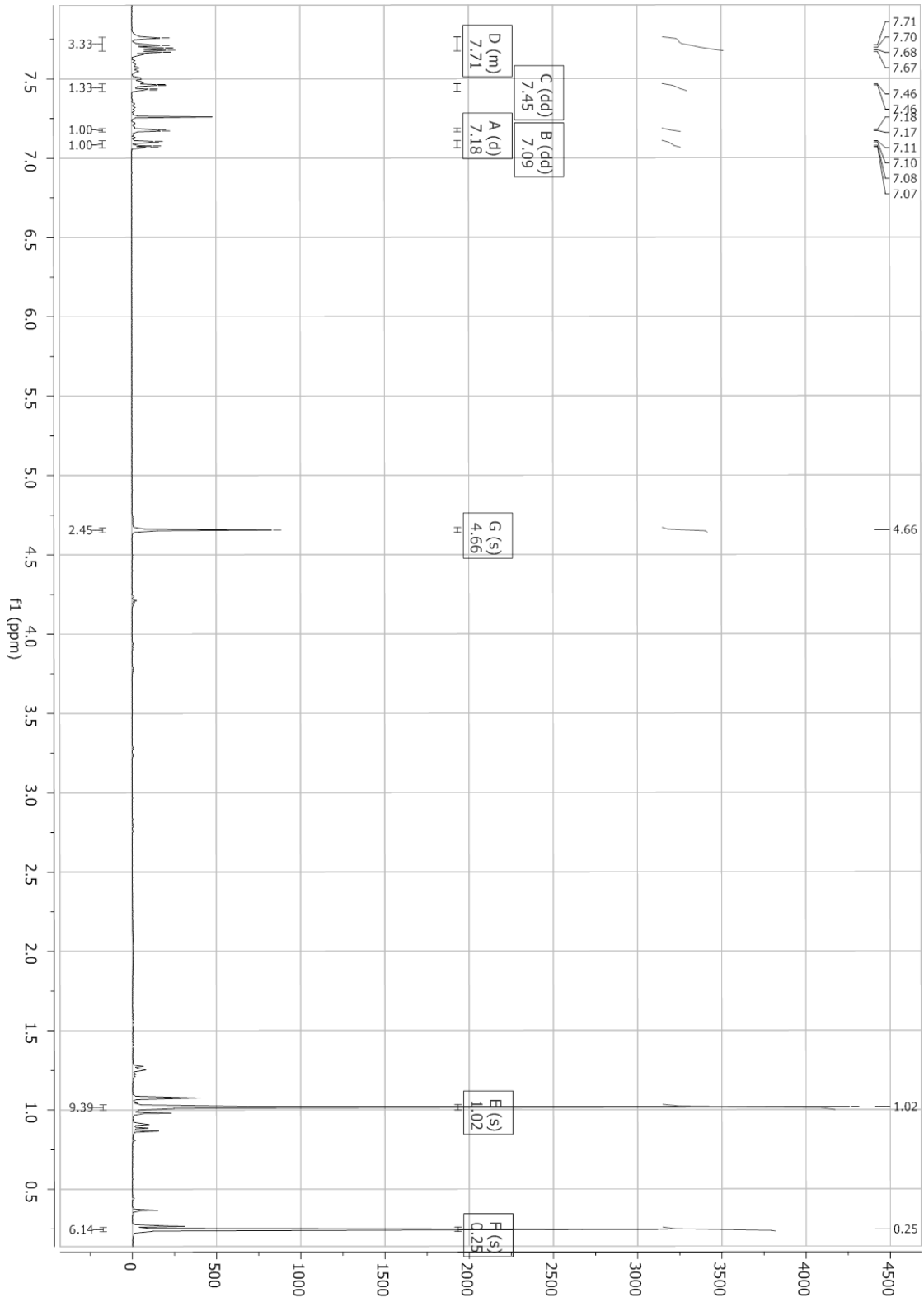

B.10 ^{13}C NMR-spectrum of ((6-(bromomethyl)naphthalen-2-yl)oxy)(tert-butyl)dimethylsilane (IVa)

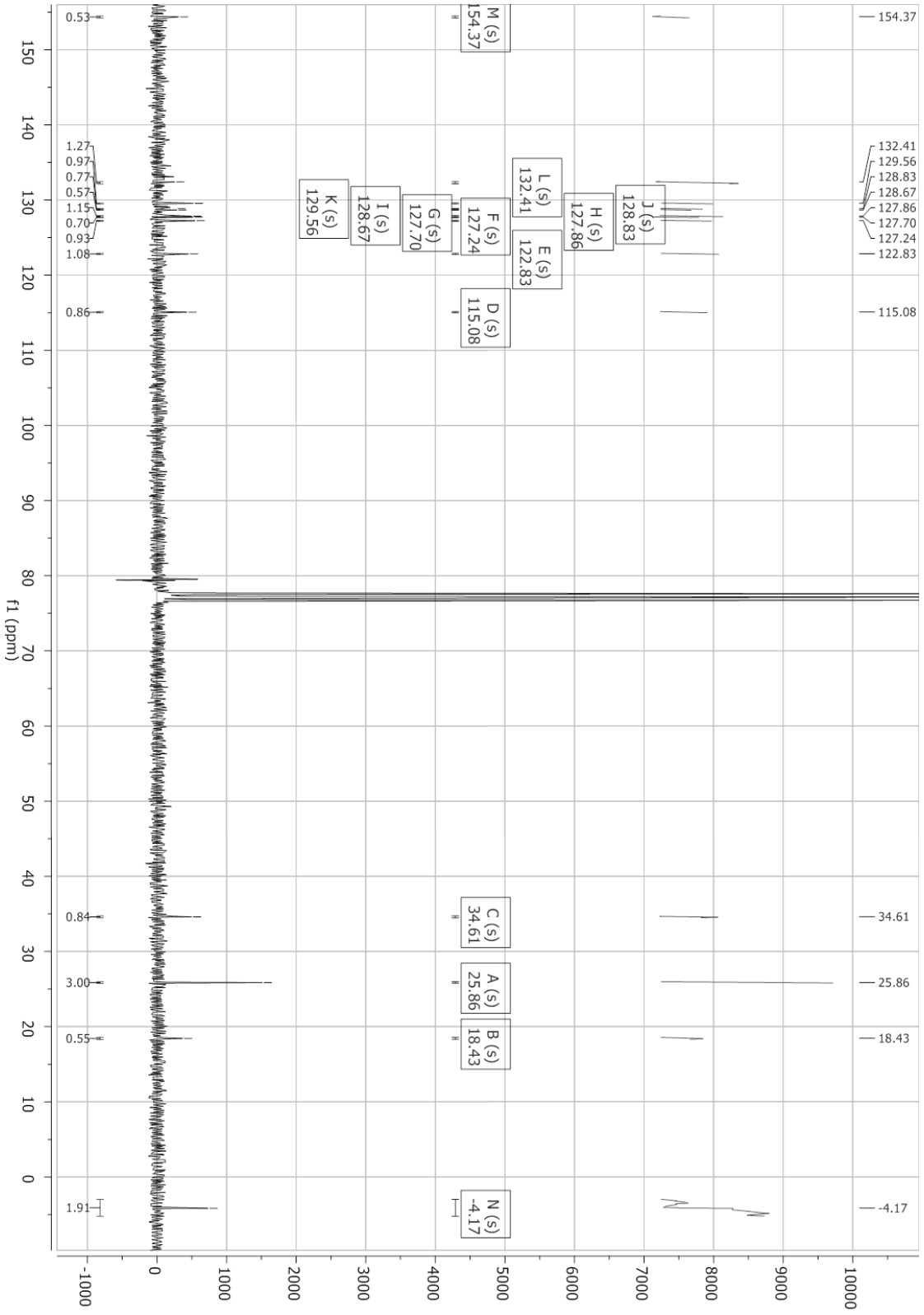

B.11 ^{1}H NMR-spectrum of (6-((tert-butyldimethylsilyl)oxy)naphthalen-2-yl)methyl methanesulfonate (IVb) in DMSO

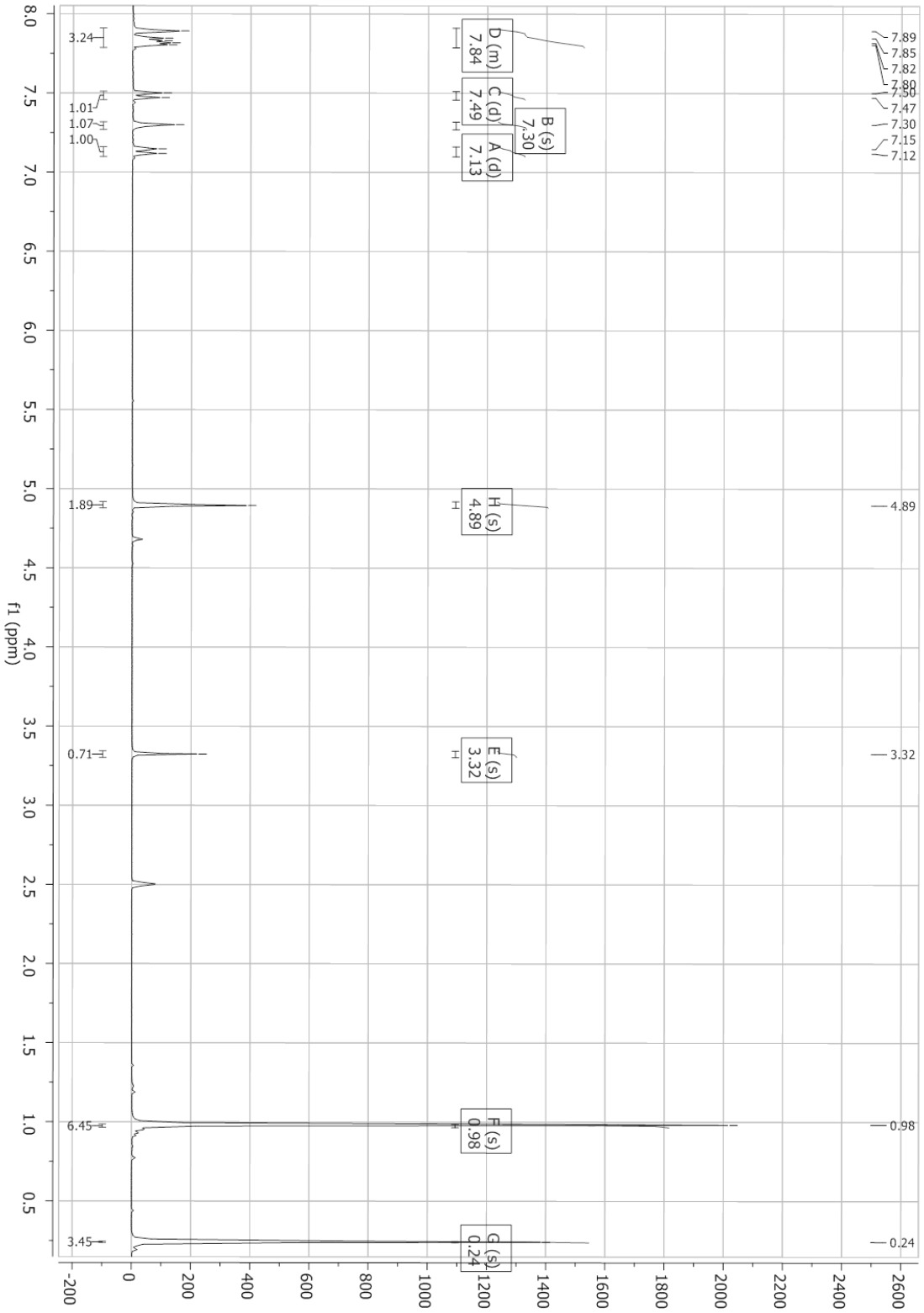

B.12 ^{1}H NMR-spectrum of (6-((tert-butyldimethylsilyl)oxy)naphthalen-2-yl)methyl methanesulfonate (IVb) in $CDCl_3$

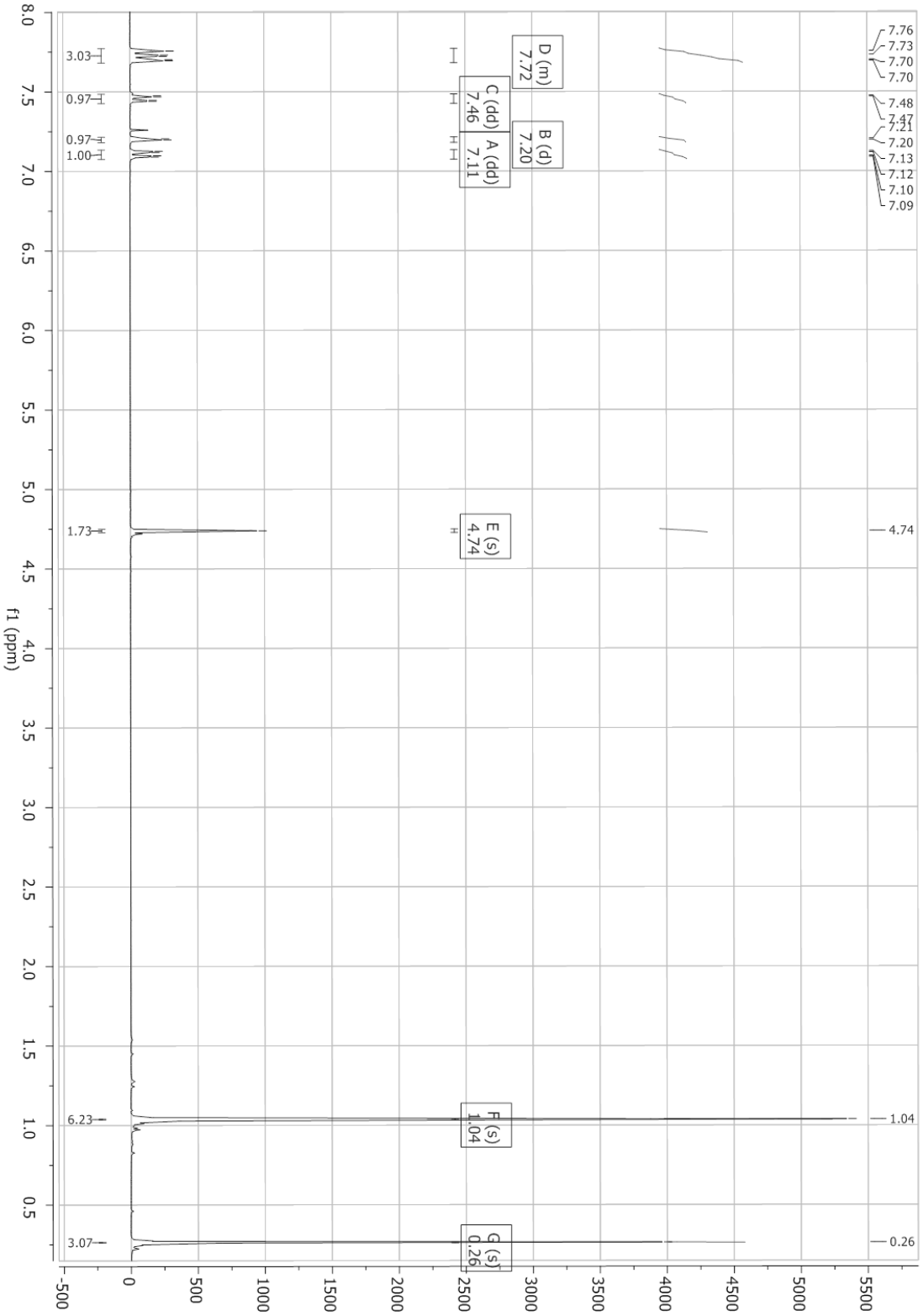

B.13 ^{13}C NMR-spectrum of (6-((tert-butyldimethylsilyl)oxy)naphthalen-2-yl)methyl methanesulfonate(IVb)in DMSO

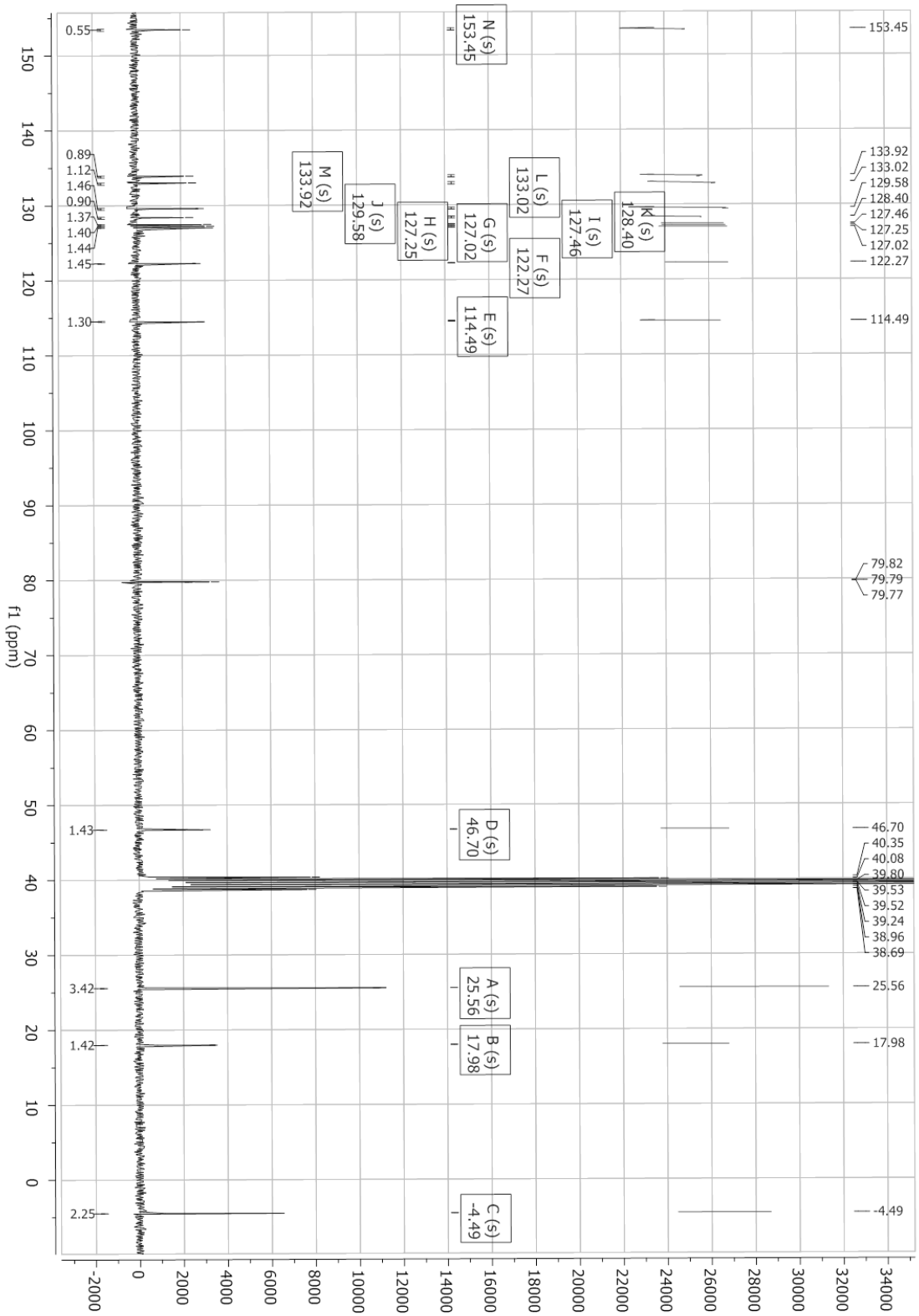

B.14 ^{13}C NMR-spectrum of (6-((tert-butyldimethylsilyl)oxy)naphthalen-2-yl)methyl methanesulfonate in (IVb) $CDCl_3$

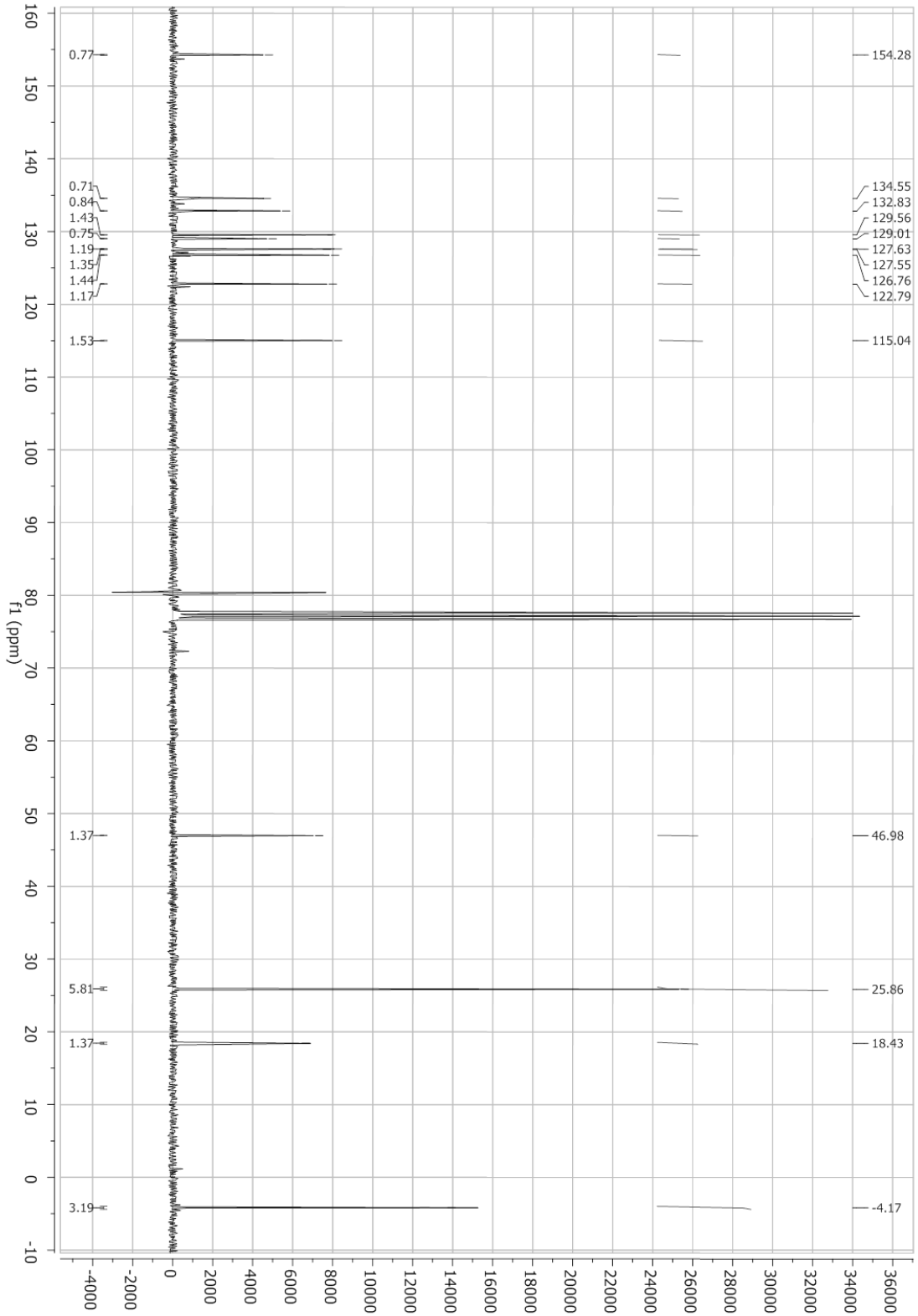

B.15 ^{1}H NMR-spectrum of product after attempting to synthesize 22(S)-HC analogue **V**

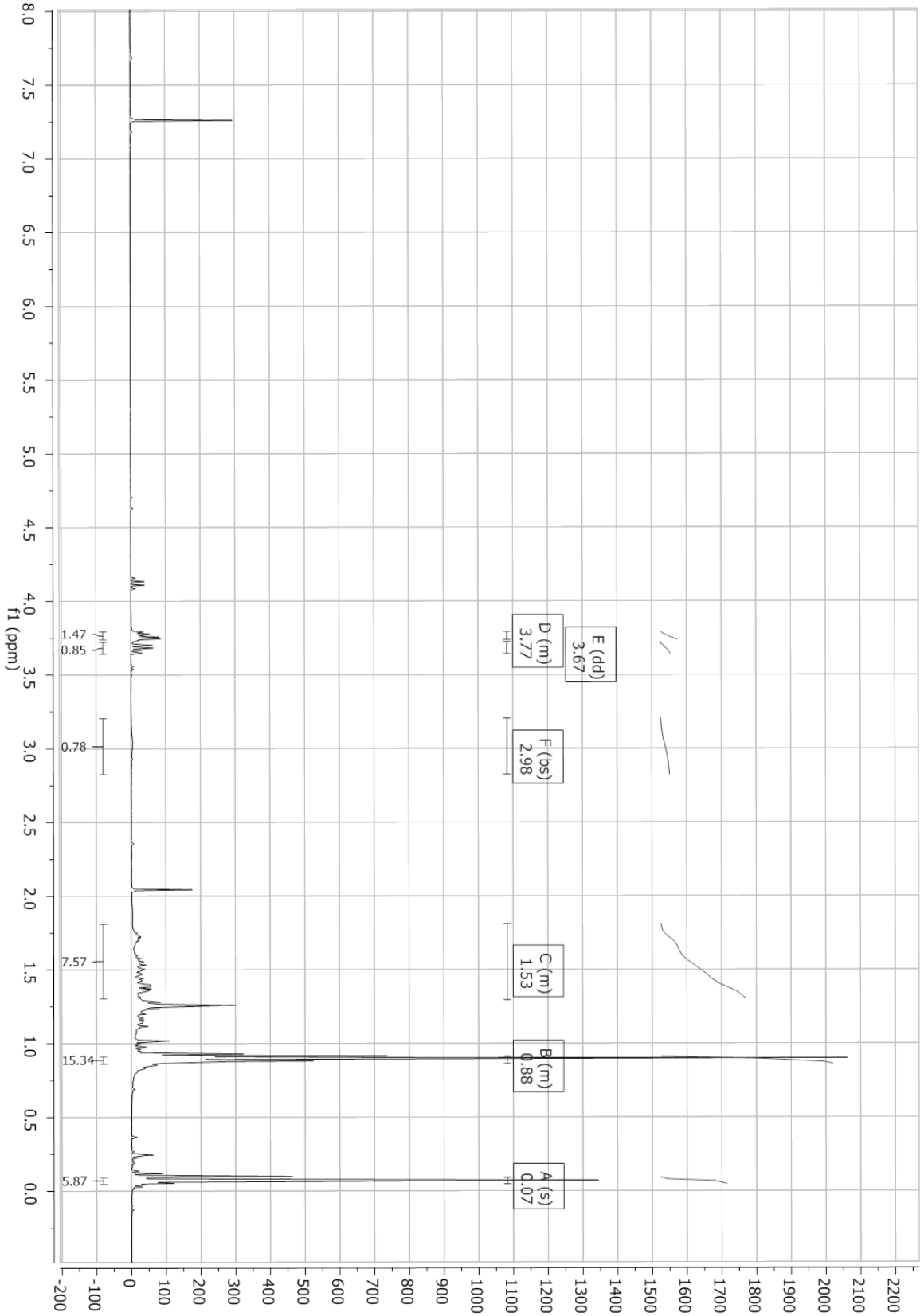

B.16 ^{13}C NMR-spectrum of product after attempting to synthesize 22(S)-HC analogue **V**

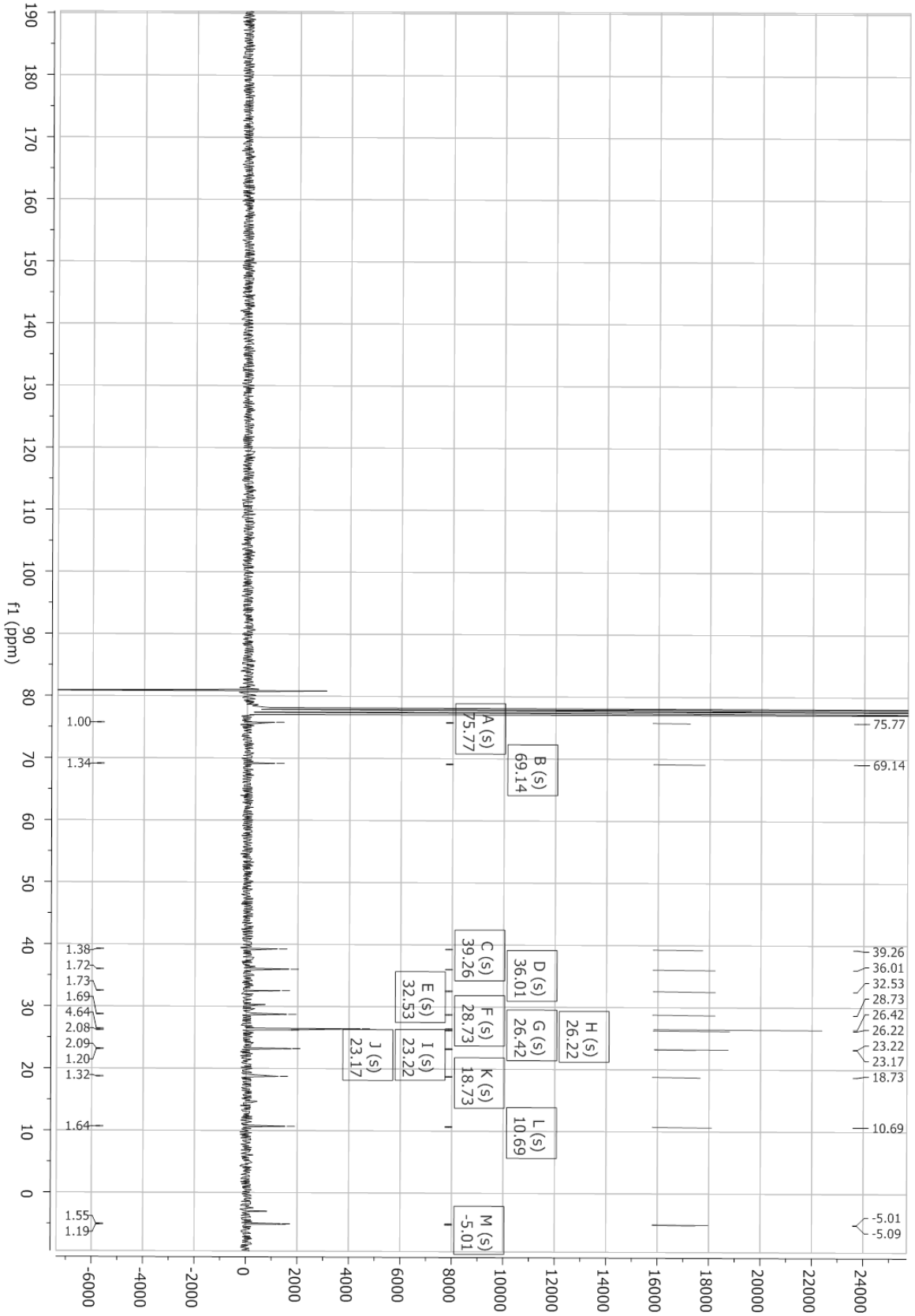

B.17 ^{1}H NMR-spectrum of product after attempting to synthesize 22(S)-HC analogue **VI**

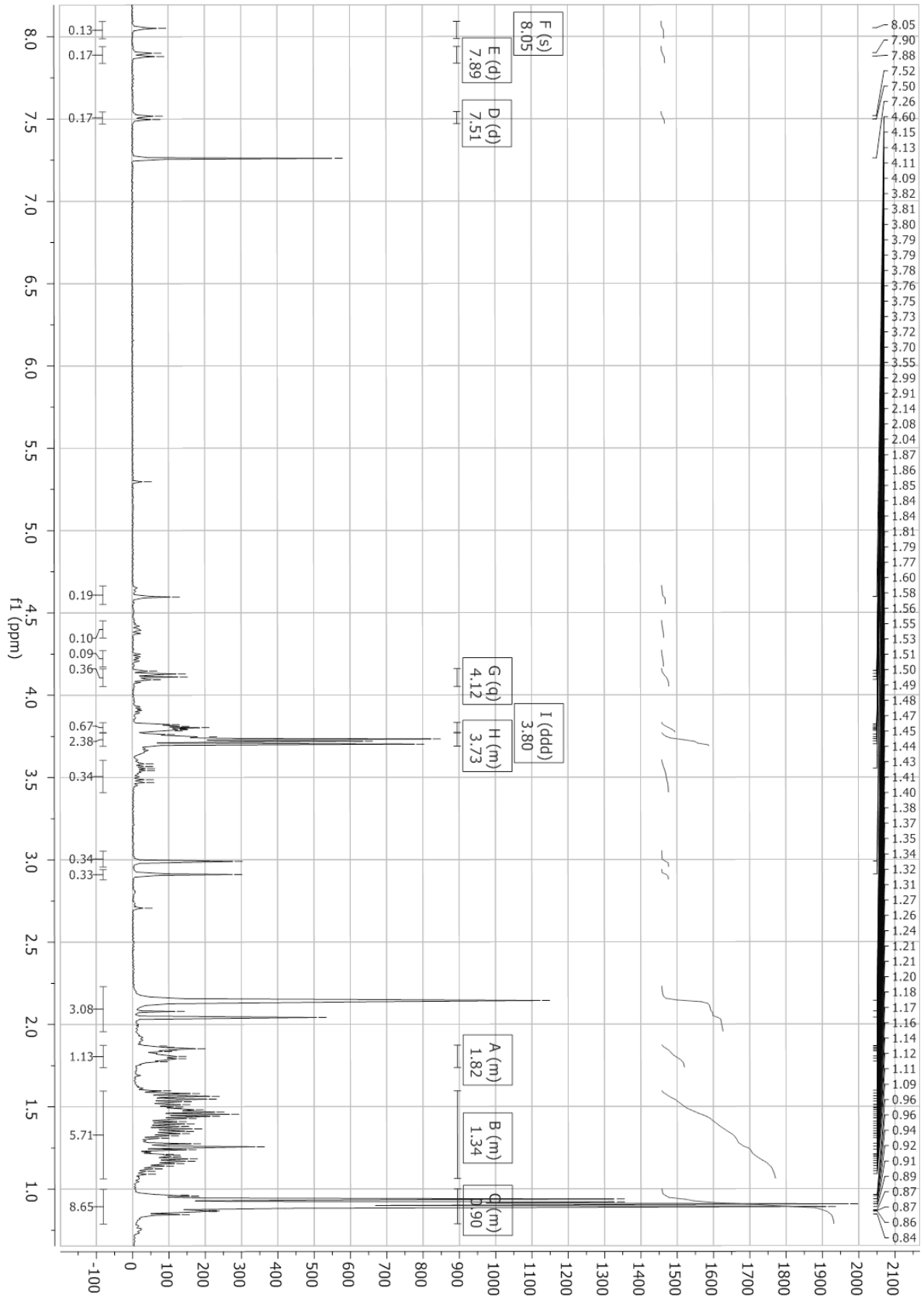

B.18 ^{13}C NMR-spectrum product after attempting to synthesize 22(S)-HC analogue **VI**